1. Report No.	2. Government Accession No.	3. Recipient's Catalog No.
CA15-1648 FHWA-TPF-5(166)		

4. Title and Subtitle	5. Report Date
Application of Three-Dimensional Laser Scanning for the Identification, Evaluation, and Management of Unstable Highway Slopes	March 2015
	6. Performing Organization Code

7. Author	8. Performing Organization Report No.
John M. Kemeny, Ph.D	

9. Performing Organization Name and Address	10. Work Unit No.
University of Arizona 1235 E. James E. Rogers Way, Room 229 Tucson, AZ 85721-0012	11. Contract or Grant No. TPF-5(166)

12. Sponsoring Agency Name and Address	13.Type of Report & Period Covered
Arizona Department of Transportation 206 S. 17th Avenue Phoenix, Arizona 85007	FINAL (12/08 – 12/11)
	14. Sponsoring Agency Code

15. Supplementary Notes

Project performed in cooperation with the Federal Highway Administration.

16. Abstract

Ground-based LIDAR (Light Detection and Ranging) is a new technology for capturing and visualizing three-dimensional (3D) data. The output of a LIDAR scan is a “point cloud” consisting of millions of points that represent the 3D surface that was scanned. Measurements and calculations can be made from the point cloud itself, or from a triangulated surface produced from the point cloud. This report describes the results of a Transportation Pooled Fund project to investigate the use of ground-based LIDAR for highway geotechnical applications. The eight states in the project are Arizona, California, Colorado, New Hampshire, New York, Pennsylvania, Tennessee, and Texas. As part of the pooled fund project, LIDAR scanning was conducted in each of these states, and the point clouds were analyzed for rock mass characterization, rockfall, rockfall hazard ratings, slope stability, and change detection. This report describes the scanning and point cloud processing that was conducted, and the final results of the analysis, for each of the eight states. This report also discusses best practices that were developed for ground-based LIDAR scanning and point cloud processing, and some new techniques that were developed to analyze overhangs, joint persistence, and joint friction angle. Some specific guidelines are given for estimating the time required for scanning and point cloud processing, as well as some issues to be aware of when using ground-based LIDAR for highway geotechnical applications. Overall, it is shown that ground-based LIDAR is an efficient and accurate way to collect field information for highway geotechnical analysis.

17. Key Words	18. Distribution Statement	23. Registrant's Seal
Ground-based LIDAR, point cloud processing, rock mass characterization slope stability, rockfall, overhangs, rockfall hazard ratings, change detection	Document is available to the U.S. Public through the National Technical Information Service, Springfield, Virginia, 22161	

19. Security Classification	20. Security Classification	21. No. of Pages	22. Price
Unclassified	Unclassified	140	

DISCLAIMER/DISCLOSURE STATEMENT

This report was funded in part through grants from the Federal Highway Administration, U.S. Department of Transportation. The contents of this report reflect the views of the authors, who are responsible for the facts and the accuracy of the data, and for the use or adaptation of previously published material, presented herein. The contents do not necessarily reflect the official views or policies of the Arizona Department of Transportation or the Federal Highway Administration, U.S. Department of Transportation. This report does not constitute a standard, specification, or regulation. Trade or manufacturers' names that may appear herein are cited only because they are considered essential to the objectives of the report. The U.S. government and the State of Arizona do not endorse products or manufacturers.

Application of Three-Dimensional Laser Scanning for the Identification, Evaluation, and Management of Unstable Highway Slopes

Pooled Fund Study
Final Report TPF-5(166)
March 2015

Prepared by:
John M. Kemeny, Ph.D.
Dept. of Mining and Geological Engineering
University of Arizona
1235 E. James E. Rogers Way, Room 229
Tucson, AZ 85721-0012

Published by:
Arizona Department of Transportation
206 S. 17th Avenue
Phoenix, AZ 85007
in cooperation with
U.S. Department of Transportation
Federal Highway Administration

SI* (MODERN METRIC) CONVERSION FACTORS

APPROXIMATE CONVERSIONS TO SI UNITS

Symbol	When You Know	Multiply By	To Find	Symbol
		LENGTH		
in	inches	25.4	millimeters	mm
ft	feet	0.305	meters	m
yd	yards	0.914	meters	m
mi	miles	1.61	kilometers	km
		AREA		
in^2	square inches	645.2	square millimeters	mm^2
ft^2	square feet	0.093	square meters	m^2
yd^2	square yard	0.836	square meters	m^2
ac	acres	0.405	hectares	ha
mi^2	square miles	2.59	square kilometers	km^2
		VOLUME		
fl oz	fluid ounces	29.57	milliliters	mL
gal	gallons	3.785	liters	L
ft^3	cubic feet	0.028	cubic meters	m^3
yd^3	cubic yards	0.765	cubic meters	m^3
		NOTE: volumes greater than 1000 L shall be shown in m^3		
		MASS		
oz	ounces	28.35	grams	g
lb	pounds	0.454	kilograms	kg
T	short tons (2000 lb)	0.907	megagrams (or "metric ton")	Mg (or "t")
		TEMPERATURE (exact degrees)		
°F	Fahrenheit	5 (F-32)/9 or (F-32)/1.8	Celsius	°C
		ILLUMINATION		
fc	foot-candles	10.76	lux	lx
fl	foot-Lamberts	3.426	$candela/m^2$	cd/m^2
		FORCE and PRESSURE or STRESS		
lbf	poundforce	4.45	newtons	N
lbf/in^2	poundforce per square inch	6.89	kilopascals	kPa

APPROXIMATE CONVERSIONS FROM SI UNITS

Symbol	When You Know	Multiply By	To Find	Symbol
		LENGTH		
mm	millimeters	0.039	inches	in
m	meters	3.28	feet	ft
m	meters	1.09	yards	yd
km	kilometers	0.621	miles	mi
		AREA		
mm^2	square millimeters	0.0016	square inches	in^2
m^2	square meters	10.764	square feet	ft^2
m^2	square meters	1.195	square yards	yd^2
ha	hectares	2.47	acres	ac
km^2	square kilometers	0.386	square miles	mi^2
		VOLUME		
mL	milliliters	0.034	fluid ounces	fl oz
L	liters	0.264	gallons	gal
m^3	cubic meters	35.314	cubic feet	ft^3
m^3	cubic meters	1.307	cubic yards	yd^3
		MASS		
g	grams	0.035	ounces	oz
kg	kilograms	2.202	pounds	lb
Mg (or "t")	megagrams (or "metric ton")	1.103	short tons (2000 lb)	T
		TEMPERATURE (exact degrees)		
°C	Celsius	1.8C+32	Fahrenheit	°F
		ILLUMINATION		
lx	lux	0.0929	foot-candles	fc
cd/m^2	$candela/m^2$	0.2919	foot-Lamberts	fl
		FORCE and PRESSURE or STRESS		
N	newtons	0.225	poundforce	lbf
kPa	kilopascals	0.145	poundforce per square inch	lbf/in^2

*SI is the symbol for the International System of Units. Appropriate rounding should be made to comply with Section 4 of ASTM E380.
(Revised March 2003)

CONTENTS

LIST OF FIGURES

LIST OF TABLES

ACRONYM LIST

ADOT	Arizona Department of Transportation
ADT	average daily traffic
CAD	computer-aided design
Caltrans	California Department of Transportation
CDOT	Colorado Department of Transportation
CFLH	Central Federal Lands Highway Division
DOT	department of transportation
FHWA	Federal Highway Administration
LIDAR	Light Detection and Ranging
MYA	million years ago
NHI	National Highway Institute
NHSDOT	New Hampshire State Department of Transportation
NTIS	National Technical Information Service
NYSDOT	New York State Department of Transportation
OHF	overhang factor
PennDOT	Pennsylvania Department of Transportation
RHRS	Rockfall Hazard Rating System
SR	state route
SRCC	Southern Regional Climate Center
TAC	technical advisory committee
TDG	Tennessee Division of Geology
TDOT	Tennessee Department of Transportation
WRCC	Western Regional Climate Center

ACKNOWLEDGMENTS

I would like to thank the members of the Technical Advisory Committee for their commitment to this project, which included at various times Christ Dimitroplos, Frank Darmiento, Virgil Coxon, Bill Webster, Ty Ortiz, Bob Group, Krystle Pelham, Doug Hadjin, Brad Foltz, Lori McDowell, Len Oliver, Vanessa Bateman, John Delphia, Tony Lujan, Mark McClelland, Marcus Galvan, Keith Turner, and Justin Henwood. I want to especially thank Nick Priznar for his continued efforts and support on this project. He was a true friend and will be missed.

EXECUTIVE SUMMARY

Ground-based LIDAR (Light Detection and Ranging) is a new technology for capturing and visualizing three-dimensional (3D) data. The output of a LIDAR scan is a "point cloud" consisting of millions of points that represent the 3D surface that was scanned. Ground-based LIDAR is ideal for many geotechnical applications, including surface and underground rock mass characterization, surface slope stability, underground ground control, rockfall and displacement monitoring, and change detection. LIDAR scanning collects data from a distance, and thus increases the safety associated with data collection in unstable ground conditions. LIDAR scanning can collect data from areas where normal access would be difficult or impossible. LIDAR data are of high-resolution and using LIDAR scans eliminates many of the human bias and low-resolution issues with hand-collected data. Finally, LIDAR scanning and point cloud processing are fast and allow for characterization of a site in a timely fashion.

This final report presents results from Transportation Pooled Fund Project TPF-5(166), titled "Application of Three-Dimensional Laser Scanning for the Identification, Evaluation, and Management of Unstable Highway Slopes." Participants in the pooled fund study include Arizona, California, Colorado, New Hampshire, New York, Pennsylvania, Tennessee, and Texas. As part of the pooled fund project, LIDAR scanning was conducted in each of these states, and the resulting point clouds were analyzed to look at rock mass characterization, rockfall, slope stability, and change detection. The purpose of the pooled fund project was to demonstrate geotechnical applications of ground-based LIDAR for highway slopes, and to train state departments of transportation (DOTs) on the use of point cloud processing software.

Specific outcomes and accomplishments of the LIDAR pooled fund project include:

- Completion of ground-based LIDAR scanning, and analysis of the resulting point clouds, in each of the eight states
- Development of best practices for field LIDAR scanning
- Development of efficient and repeatable ways to process LIDAR data for highway geotechnical applications
- Development some new analysis techniques to analyze overhangs, joint persistence, and joint friction angle
- Continual discussions over the three-year project period with highway geotechnical personnel from each of the eight state DOTs
- Training of DOT geotechnical personnel on LIDAR scanning and point cloud processing
- Distribution of the Split-FX point cloud processing software to each of the eight states
- Several published papers and invited talks covering the results of the LIDAR pooled fund project

Based on the results of the three-year LIDAR pooled fund project, it is recommended that ground-based LIDAR be used for highway geotechnical applications.

1. INTRODUCTION

Terrestrial LIDAR (Light Detection and Ranging), also referred to as Terrestrial Laser Scanning and Ground-Based LIDAR, is a new technology for capturing and visualizing three-dimensional (3D) data. The output of a LIDAR scan is a "point cloud" consisting of millions of points that represent the 3D surface that was scanned. Measurements and calculations can be made from the point cloud itself, or from a triangulated surface produced from the point cloud. Point cloud processing software refers to software specifically designed to process point clouds from LIDAR scans. LIDAR scanning and point cloud processing software are now routinely used in a number of engineering and architectural fields.

Terrestrial LIDAR is ideal for many geotechnical applications, including surface and underground rock mass characterization, surface slope stability, underground ground control, rockfall and displacement monitoring, and change detection. LIDAR scanning collects data from a distance, and thus increases the safety associated with data collection in unstable ground conditions. LIDAR scanning can collect data from areas where normal access would be difficult or impossible. LIDAR data are of high-resolution and using LIDAR scans eliminates many of the human bias and low-resolution issues with hand-collected data. Finally, LIDAR scanning and point cloud processing is very fast and allows for the characterization of a site in a timely fashion. Details on the use of terrestrial LIDAR for geotechnical applications are described in Kemeny and Turner (2008).

Transportation Pooled Fund project TPF-5(166), "Application of Three-Dimensional Laser Scanning for the Identification, Evaluation, and Management of Unstable Highway Slopes," was established to investigate the use of ground-based LIDAR for highway geotechnical applications. Pooled Fund Study TPF-5(166) explored the uses of terrestrial LIDAR for geotechnical applications by state departments of transportation (DOTs) and in particular addressed the following issues:

- Transportation agencies are not familiar with LIDAR technology and the range of its possible uses.
- There are a limited number of case studies illustrating the uses of terrestrial LIDAR for specific geotechnical applications.
- There is a lack of documented and fully qualified procedures for data acquisition to ensure accuracy and "fitness for purpose" of terrestrial LIDAR data.
- Transportation agencies do not have expertise with point cloud processing software. Terrestrial LIDAR produces very large 3D point clouds that are visually interesting but not immediately analyzable by traditional software products.

Eight states have participated in Transportation Pooled Fund Project TPF-5(166): Arizona, California, Colorado, New Hampshire, New York, Pennsylvania, Tennessee, and Texas. Arizona is the lead state DOT.

This is the final report on Transportation Pooled Fund Project TPF-5(166). The outline for this report is as follows. Chapter 2 gives an overview of ground-based LIDAR, point cloud processing software, and the types of geotechnical studies that can be conducted using ground-based LIDAR. Chapter 3 gives an overview of the sites that were selected for field case studies and the types of analysis that were conducted for each state. In general, one site was selected in each of

the eight states participating in the pooled fund project, with the exception of Colorado, which selected two sites. Chapters 4 through 11 provide details on the scanning, point cloud processing, and results from each of the field test sites in each state. These chapters are based on the individual state reports that were submitted as part of the pooled fund study and they represent the bulk of this final report. Finally, Chapter 12 provides discussions and conclusions from the LIDAR pooled fund study.

It should be noted that the content of this final report assumes some knowledge of geotechnical concepts as they apply to transportation projects. This includes topics such as rock discontinuities, rock mass characterization, stereographic projection, joint friction angle, slope stability, rockfall, and other topics. Readers are encouraged to explore the many good books, reports, and papers on these subjects, including Goodman (1993), Hoek (2007), Hudson and Harrison (2000), FHWA (1989), and NTIS (1994).

2. GROUND-BASED LIDAR AND POINT CLOUD PROCESSING

GROUND-BASED LIDAR

LIDAR is the acronym for Light Detection and Ranging. LIDAR is a technology that uses light to image objects, such as buildings, highways, and rock outcrops, in three dimensions. LIDAR can use ultraviolet, visible, or near-infrared light. A typical LIDAR unit contains a laser along with rotating mirrors or pan-tilt devices. In time-of-flight LIDAR, pulses of light are emitted, reflected off an object, and received; the distance between the scanner and the reflected point is accurately calculated using the time of flight and the speed of light. The position (x,y,z) of the reflected point is then determined by using this distance along with an accurate measurement of the orientation of the pulse. In phase-shift LIDAR, a sinusoidally modulated pulse is emitted and reflected off an object. The time of flight is then determined from the phase shift and the modulation frequency.

The output from a LIDAR scan is a point cloud, which is produced by repeating the process of laser pulse emission and reception millions of times across the object of interest. The distance between points in a point cloud is referred to as the point cloud spacing and is one of the most important parameters of a point cloud. Smaller point cloud spacing provides additional topographic detail, but at the cost of additional scan times and larger file sizes. Figure 1a shows a point cloud of a 25-meter-high highway rock outcrop. It has a point spacing that varies from about 1.1 cm (.43 inch) at the bottom to about 2.6 cm (1 inch) at the top, with a total of 1.6 million points. In addition to the position (x,y,z) of each point, the intensity of the reflection of each point is also recorded, resulting in a data file that contains columns of x, y, z, and intensity information. Objects closer to the scanner will produce a higher intensity, and light-colored objects have a higher intensity than darker-colored objects. The reflected intensity also depends on the angle of incidence and the roughness of the surface. For example, in Figure 1a, high intensity values can be seen in the blast hole half-casts because of their smooth surface.

Point clouds can be combined with high-resolution digital camera images to produce color point clouds. To produce a color point cloud, LIDAR and digital camera images are accurately aligned, and the color information from the digital camera is then mapped or draped onto the point cloud, resulting in a data file that contains columns of x, y, z, red, green, and blue information. In some cases the color camera and LIDAR are combined into a single unit, and a color point cloud is automatically created. In other cases the camera is mounted on a separate tripod or on top of the scanner, in which case the color point cloud is created using separate alignment and draping software. Figure 1b shows a color point cloud created by draping a color image onto the intensity point cloud shown in Figure 1a. In general, color point clouds are preferred due to the additional details that they provide. However, color point clouds are subject to sun shadows and camera exposure problems. Sun shadows can be seen in the color point cloud in Figure 1b.

Figure 1. Scans from a highway rock slope in New Hampshire, from left, a) an intensity point cloud and b) a color point cloud.

LIDAR scans can be captured from stationary tripods, moving vehicles on the ground or water, low-flying aircraft, and high-altitude aircraft. Ground-based or terrestrial LIDAR refers to LIDAR units mounted on a stationary tripod, as well as to the stop-and-scan technique, in which a truck or van containing a LIDAR unit will stop, take a scan, and then move to the next scanning position. Mobile LIDAR refers to scanning from moving trucks, vans, and boats; airborne LIDAR refers to scanning done from aircraft. In mobile and airborne LIDAR, GPS and motion sensing equipment are used to track the position of the scanner and to compensate for vehicle and aircraft vibrations and rotations. In general, the highest accuracies are available from ground-based LIDAR. Only ground-based LIDAR is considered in the LIDAR pooled fund project described in this report.

The specifications for four typical ground-based LIDAR units – the Optech ILRIS-HD, the ISITE 8800, the Leica C10, and the FARO Focus3D 120 – are shown in Table 1. The first three shown are time-of-flight scanners with data capture rates from 8800 to 50,000 points per second (pps) and range accuracies of 4-10 mm at a distance of 50-100 m (.16 to .39 inches at a distance of 164 to 328 feet). These can be compared to the FARO Focus3D phase shift scanner, which has a data capture rate as high as 976,000 pps and a range accuracy from 1-2 mm (at a distance of 25 m). The Optech and ISITE scanners are long-range scanners with maximum ranges of 1250–1400 m (4100 to 4592 feet) at 80 percent reflectivity. For reference, rock outcrops and, in particular, dark-colored rocks will usually have reflectivity values lower than 80 percent.

Table 1. Specifications of Four Ground-Based LIDAR Scanners

				
	Optech ILRIS-HD	**I-SITE 8800**	**Leica C10**	**FARO Focus3D 120**
Type	Time-of-flight	Time-of-flight	Time-of-flight	Phase-shift
Wavelength	1550 nm (5084 nft)	Near-infrared	532 nm (1745 nft)	905 nm (2968 nft)
Min. range	3 m (9.84 ft)	2.5 m (8.2 ft)	0.1 m (.33 ft)	0.6 m (1.97 ft)
Max. range	1250 m (4100 ft)at 80% reflectivity	1400 m (4592 ft) at 80% reflectivity	300 m (984 ft) at 90% reflectivity	120 m (394 ft)
Max. data rate	10,000 pps	8800 pps	50,000 pps	976,000 pps
Range accuracy	7 mm at 100 m (.27 inch at 328 ft)	10 mm (.39 inch) (distance not given)	4–6 mm (.16 to .23 inch) at 50 m (164 ft)	0.95–2.2 mm (.037 to .086 inch) at 25 m (82 ft)
Scanner weight	14 kg (30.9 lbs) without battery	14 kg (30.9 lbs) without battery	13 kg (28.6 lbs) without batteries	5.0 kg (119 lbs) with internal battery
Reference	http://www.optech.com	http://www.maptek.com	http://www.leica-geosystems.com	http://www.faro.com

POINT CLOUD PROCESSING

Point cloud processing software is designed specifically for viewing and manipulating LIDAR point clouds. Most of the LIDAR manufacturers have developed their own point cloud processing software, and in addition, many third-party point cloud processing software packages now exist. Certain features, such as point cloud viewing, editing, registration, and measurement, are common to all of the software packages. Some of the software packages also contain computer-aided design (CAD) features such as surface reconstruction and solid modeling.

The LIDAR pooled fund project used the Split-FX point cloud processing software (Split Engineering 2010). The Split-FX software is designed specifically for geotechnical analysis from point clouds, including the delineation of rock discontinuities, stereographic projection, cross sections, and change detection. Some examples of the types of geotechnical analyses that can be conducted using the Split-FX point cloud processing software are described below.

Fracture Delineation and Stereographic Projection

Because fractures are most often flat or planar, fracture surfaces can be automatically identified in a point cloud by searching for flat objects. In the Split-FX program, the triangulated mesh of the surface derived from the point cloud is used to search for fractures. Figure 2a shows a triangulated mesh and Figure 2b shows the fractures that have been automatically delineated using the Split-FX software. Once the fracture surfaces have been identified, the fracture orientations can be plotted on a stereonet (mapping that projects three-dimensional data onto a plane [Goodman 1993]). The fracture area of each delineated fracture surface is also calculated. Stereonet interpretation is improved when fracture areas are represented on the stereonet by varying sizes of plotting icon (bigger icon for bigger fracture areas). In Figure 2c, larger delineated fracture surfaces are plotted as larger circles, resulting in a stereonet that clearly reflects the geologic structure at the site.

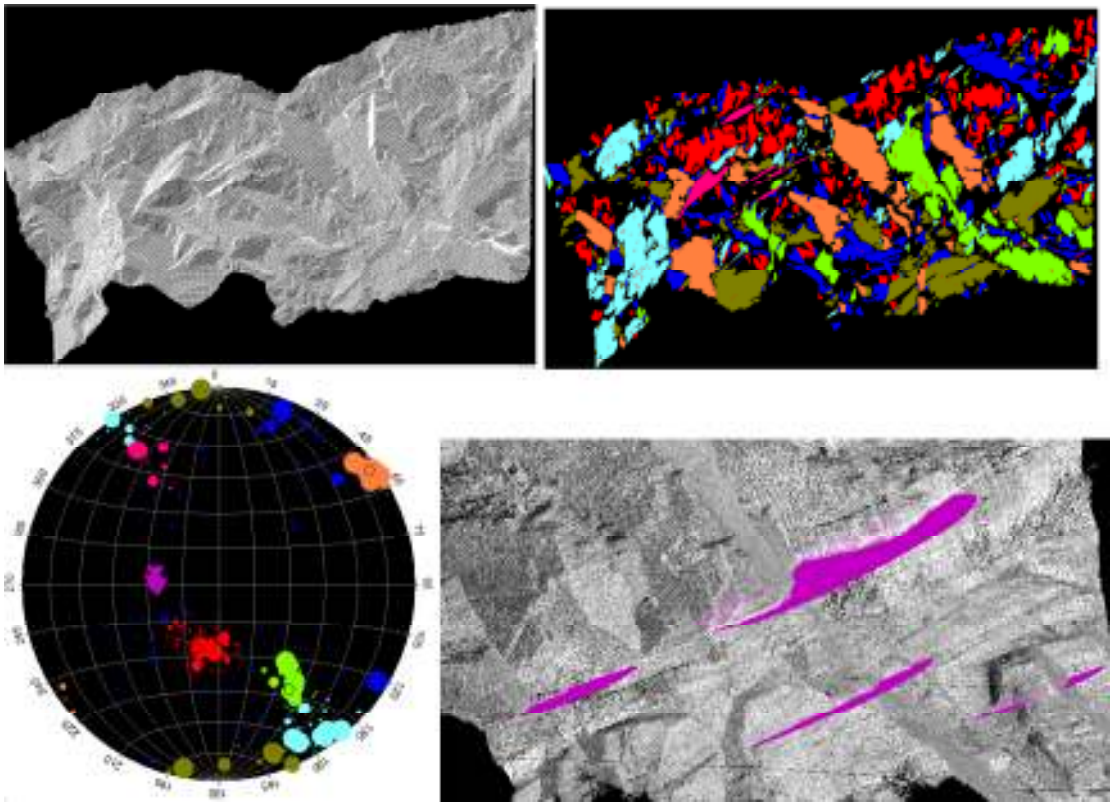

Figure 2. Fracture delineation using the Split-FX point cloud processing software showing, top left, a) triangulated mesh; top right, b) automated fracture surface delineation; bottom left, c) lower hemisphere stereonet (circles represent surfaces, triangles represent traces), and, bottom right, d) fracture trace delineation.

Fracture surfaces are not necessarily identified for all fractures in a scanned rock outcrop. For example, fracture surfaces that dip away from the scanner will not be visible in the point cloud. Also, because fracture surfaces only occur where the rock mass has broken along the fractures, fracture surfaces are often not visible in smooth blasted walls. Fractures can also be delineated

using fracture traces. In the Split-FX program, fracture traces can be manually delineated in the point cloud and the orientation is determined by fitting a best-fit plane through the 3D points of the trace. Figure 2d shows an example of delineating fracture traces in a portion of the point cloud where fracture surfaces do not occur. The orientations of the fractures have been plotted as triangles in Figure 2c. Most if not all of the important geologic structure in a rock outcrop can be captured using fracture surface and fracture trace delineation.

Cross Sections

Ground-based LIDAR is particularly useful for making detailed cross sections that can aid in many types of geotechnical analyses. Unlike airborne LIDAR, ground-based LIDAR provides significant detail in vertical cross sections that can be used to look for overhanging rock slabs or to determine rockfall trajectories. Figure 3a shows a vertical cross section through the point cloud in Figure 2. It shows where the cross section intersected the triangulated mesh (white) as well as where it intersected delineated fracture surfaces (colored). Cross sections can also be used to provide information on surface roughness. Figure 3c shows a cross section through one of the orange fractures in Figure 2b.

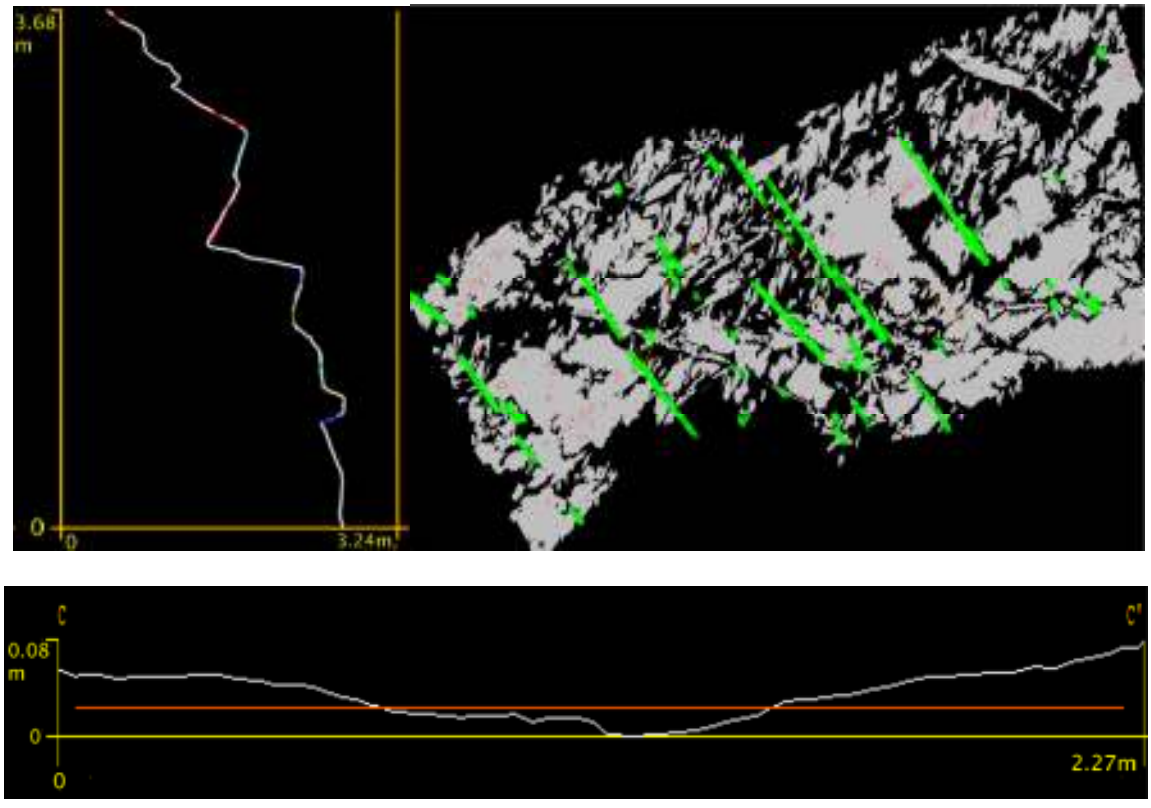

Figure 3. Upper left shows a) a vertical cross section through point cloud in Figure 2, upper right shows b) a method for measuring fracture spacing (orange set from Figure 2 highlighted in green), and bottom is c) a profile of one of the orange fractures in Figure 2 (red line is the average orientation of the fracture).

Length and Volume Measurements

Length and volume measurements are useful for determining fracture spacing, block volume, fracture persistence, and other rock mass parameters. One way to measure the true fracture spacing for a particular joint set is to highlight the joint set by selecting the fractures on the stereonet, and then orienting the point cloud perpendicular to those fractures, as shown in Figure 3b for the orange set in Figures 2b and 2c. Spacing measurements can then be made using standard measurement tools in the point cloud processing software.

Exporting Data for Slope Stability and Rockfall Hazard Rating Systems

Data from point cloud processing software can be exported to various programs to analyze slope stability or to be used in rockfall hazard rating systems. Exporting options include the export of the point cloud, triangulated mesh, delineated fractures, cross sections, and length and volume measurements. The study team has found with both the Utah and Tennessee rockfall hazard rating systems that most of the parameters can be determined from point cloud processing software (see Chapter 10: Tennessee). In many of the commercial slope and underground stability programs (e.g., Rocscience Dips, Swedge, and Unwedge), the slope stability information from the point cloud processing can be used directly.

Change Detection

LIDAR point clouds are very useful for measuring ground movements and detecting where rockfall events have taken place. LIDAR change detection involves taking the point clouds from "before" and "after" scans and creating a "difference" point cloud. The difference cloud is created by subtracting the *after* cloud from the *before* cloud. Before the subtraction takes place, the two point clouds must be accurately aligned. This is a two-step process. In the first step, markers are manually inserted in the *before* and *after* clouds to give a crude alignment. This step is not necessary if the scanner is not moved between the before and after scans. In the second step, the clouds are accurately aligned using an Iterative Closest Point (ICP) algorithm (Pomerleau et al. 2013). Once the difference cloud is created, it can be visualized in different ways. Normally, change that involves movement away from the scanner (such as a missing rock on the slope) is given one color (red in this case), change that involves movement towards the scanner (such as new rock in a ditch) is given another color (blue in this case) and movement less than the noise level is given a third color (gray in this case).

Figure 4a shows a difference point cloud produced from two scans taken at the site shown in Figure 2. The scans were taken about five years apart. Blue indicates movement toward the scanner and, in this case, many plants that have grown in size show up as blue. Red indicates movement away from the scanner, and the large red object in the center right indicates a rock block that fell from the slope. Figures 4b and 4c show before and after portions of the point cloud near the red object, and the missing rock in Figure 4c is apparent. The volume and shape of the rock block can be determined from the difference point cloud and also from the before and after clouds.

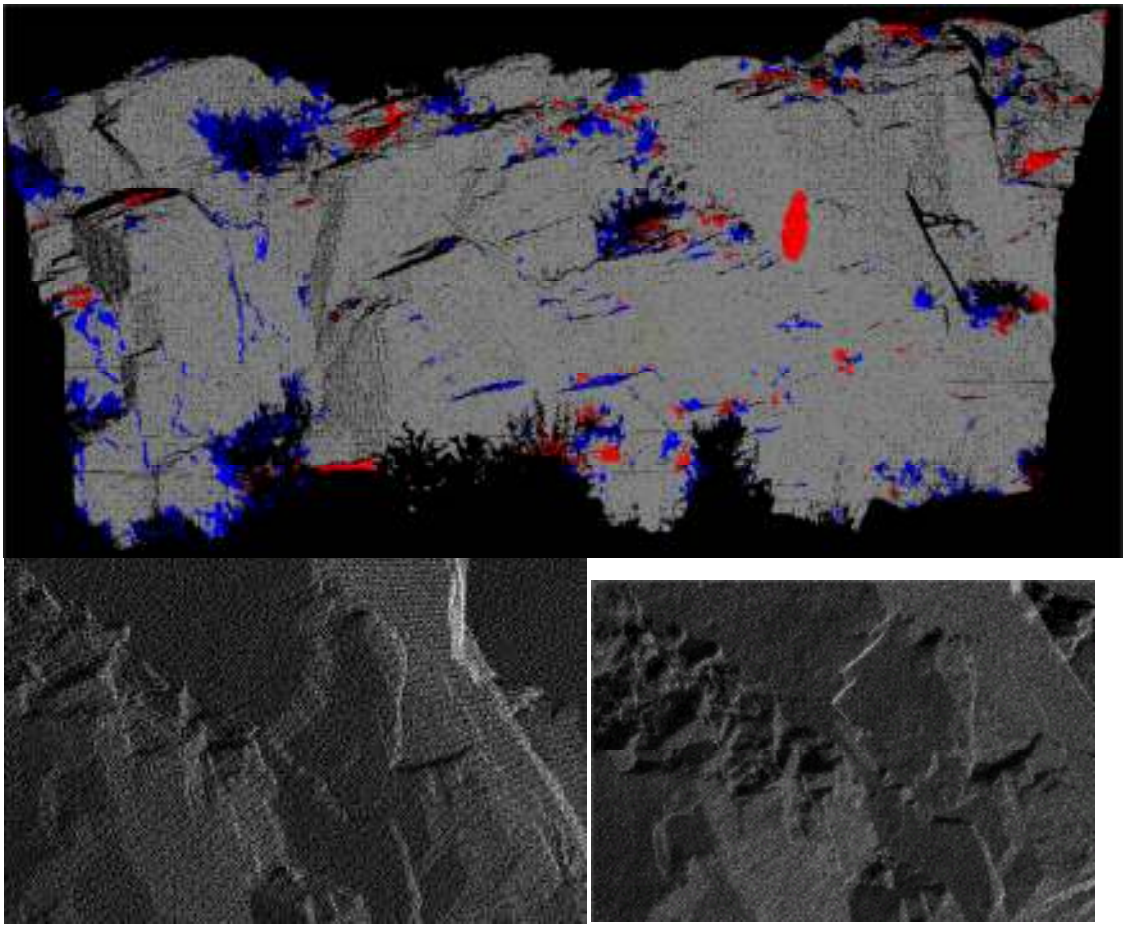

Figure 4. Change detection using LIDAR point clouds at the same site as shown in Figure 2. Top image (a) shows a difference point cloud produced from two scans showing missing rock block in red. Lower left image (b) shows the "before" point cloud in the vicinity of missing rock block, and lower right image (c) shows the "after" cloud in the same vicinity.

3. FIELD SITE SELECTION AND TYPES OF ANALYSIS CONDUCTED

FIELD SITE SELECTION

One of the primary tasks in the first six months of the LIDAR pooled fund project was to determine the specific scanning activity that would be conducted in each state. A Technical Advisory Committee (TAC) was established for Transportation Pooled Fund project TPF-5(166), consisting of a primary geotechnical contact person for each participating state, as well as the PI from the University of Arizona and the ADOT administrator of the pooled fund project. The members of the TAC are shown in Table 2. Monthly phone meetings were held with the TAC throughout the duration of the project.

Table 2. Members of the TAC for TPF-5(166)

ADOT Administrator: Christ Dimitroplos (originally Frank Darmiento)
PI: John Kemeny, University of Arizona
AZ: Nick Priznar and Virgil Coxon
CA: Bill Webster
CO: Ty Ortiz and Bob Group
NH: Krystle Pelham
NY: Doug Hadjin
PA: Brad Foltz
TN: Lori McDowell and Len Oliver (originally Vanessa Bateman)
TX: John Delphia and Tony Lujan (originally Mark McClelland and Marcus Galvan)

Based on discussions with the TAC members, nine field sites were established in the eight states, consisting of two sites in Colorado and one site in each of the other seven states. Descriptions of the nine sites are given in Table 3, and pictures of the nine sites are shown in Figure 5.

Table 3. Nine Sites Selected for the LIDAR Pooled Fund Study

State	Location	Geology	Geotechnical Issue at Site
AZ	I-40 near Flagstaff	Basalt flows and breccia	Rockfall
CA	299 near Weaverville	Meta-sediments	Rockfall, wedge and toppling
CO	US 285 near Indian Hills	Boulders in sandy matrix	Boulders detach
CO	CDOT lot near Empire	Jersey and plastic barriers	Change detection test
NH	I-93, near Woodstock	Gneiss and foliated schistose	Plane and wedge failures
NY	Route 5 near Schenectady	Horizontally bedded limestone	Rockfall, overhangs
PA	SR 11/15 New Buffalo	strained clastic sedimentary	Rockfall and slope stability
TN	I-24 near Monteagle	Limestone, shale, sandstone	Rockfall, overhangs
TX	Loop 375 near El Paso	Marble, limestone, rhyolite	Rockfall and slope stability

Figure 5. Nine sites were selected for the LIDAR pooled fund study. Top row, left to right: Arizona, California, and Colorado Site 1. Middle row: Colorado Site 2 (an artificial rock surface), New Hampshire, and New York. Bottom row: Pennsylvania, Tennessee, and Texas.

Table 3 and Figure 5 show that eight of the nine sites are highway rock slopes, and one site is an artificial "slope" consisting of jersey and plastic barriers. The eight rock slopes cover a wide variety of rock types and slope conditions. In general, the rock slopes were selected because of geotechnical issues. Some of these issues are apparent in the photos in Figure 5. For example, the New Hampshire site shows wedge and plane failures that have occurred, and the Tennessee site shows overhanging sandstone slabs posing a hazard to the interstate highway below. The Colorado site is an ancient landslide deposit and the large boulders are prone to toppling, as shown in Figure 6a.

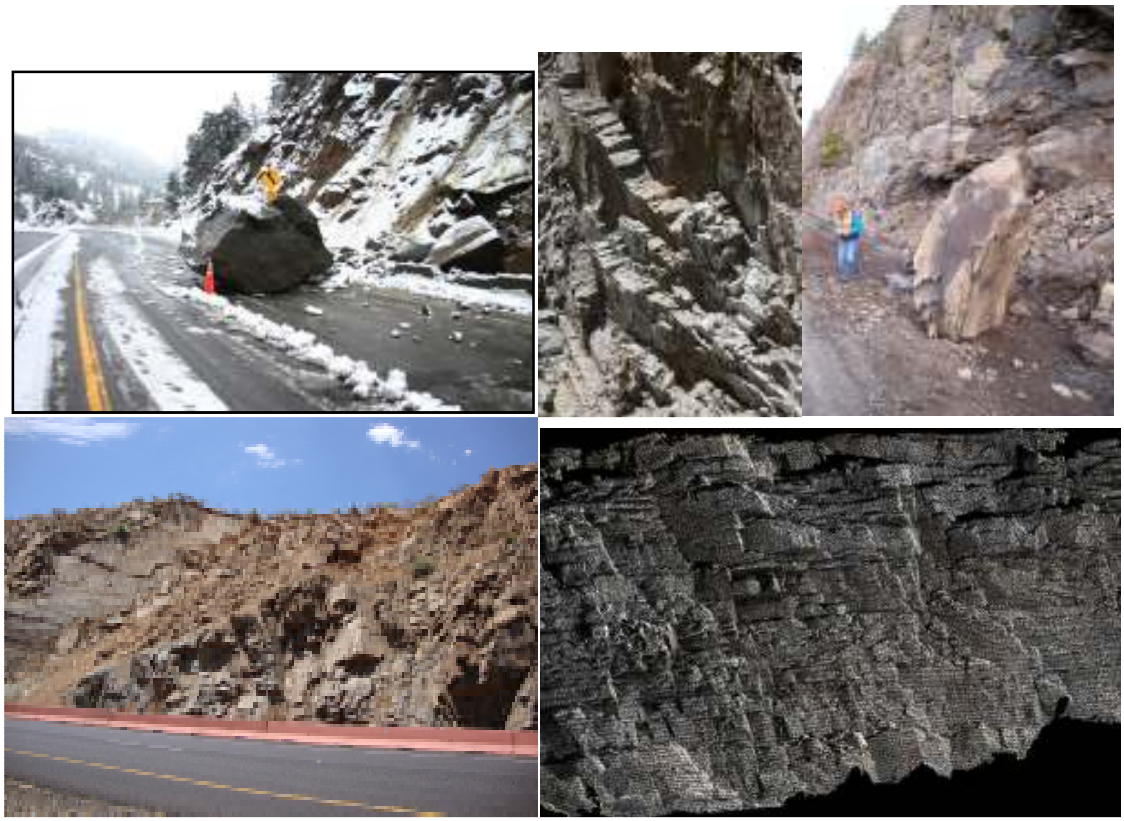

Figure 6. Images showing geotechnical issues associated with some of the pooled fund sites: top row, left to right, rockfall at one Colorado site, toppling at the California site, and rockfall at the Arizona site. Bottom left shows wedge failure at the Texas site, and bottom right shows overhangs at the New York site (Photos courtesy of CDOT).

TYPES OF ANALYSIS CONDUCTED

Following field site selection, the LIDAR scanning methods and the types of analysis that would be conducted for each field site were determined. As described above, the types of geotechnical issues at the sites included slope stability (plane, wedge, and toppling), rockfall, and overall slope maintenance. It was decided that the LIDAR scanning should support the investigations of these geotechnical issues as well as explore new ways to use and process LIDAR data. The following types of analysis were considered:

1. Rock mass characterization
    a. LIDAR characterization of joint orientation from fracture surfaces and traces
    b. LIDAR measurements of joint spacing and joint persistence
    c. LIDAR measurements of joint roughness and joint friction angle estimation
2. Slope stability
    a. Analysis of plane, wedge, and toppling failure from the LIDAR data
    b. Comparison of the predicted slope stability with actual field conditions
3. Rockfall
    a. Generation of vertical cross sections from the LIDAR point clouds

b. Analysis of overhangs from the cross sections
c. Analysis of rockfall trajectories from the cross sections
d. Determination of rockfall hazard ratings from the LIDAR data

4. Change detection
    a. Rescanning at one or more sites to generate before and after point clouds
    b. Analysis of rockfall and ground movement from the point clouds
    c. Field experiments to determine accuracy of change detection

It was not possible to conduct all the types of analysis mentioned above at all the sites. Based on discussions with members of the TAC, different analyses were conducted in each state. These analyses are listed in Table 4, which shows that basic rock mass characterization, slope stability, and rockfall studies were conducted in all states except Colorado. Colorado took the lead in change detection studies, Tennessee took the lead in looking at rockfall hazard ratings, and California took the lead in looking at fracture roughness and fracture persistence.

Table 4. Types of Analysis Conducted in Each State

State	Rock Mass Characterization			Slope Stability		Rockfall				Change Detection		
	1a	1b	1c	2a	2b	3a	3b	3c	3d	4a	4b	4c
AZ	X	X		X	X	X	X	X		X		
CA	X	X	X	X	X	X						
CO 1										X	X	
CO 2										X		X
NH	X	X		X	X	X	X	X				
NY	X	X		X	X	X	X	X				
PA	X	X		X	X	X	X	X				
TN	X	X		X	X	X	X	X	X			
TX	X	X		X	X	X	X	X				

The next eight chapters discuss specific project details and results, one chapter for each of the eight states in the pooled fund project.

4. ARIZONA

This chapter discusses scanning that took place in Arizona as part of the LIDAR pooled fund project, as well as the results of analyzing the Arizona scans.

OVERVIEW OF THE ARIZONA SITE

The Arizona site is a rock slope next to the westbound lane of Interstate 40 at milepost 180.1. The site is about 11 miles west of Flagstaff, Arizona, and about 18 miles east of Williams, Arizona. A picture of the site is shown in Figure 7.

Figure 7. The Arizona site, showing the Leica scanner used to conduct scans.

I-40 is a divided rural interstate that runs east-west and consists of two 12-ft lanes with 4-ft inside shoulders and 10-ft outside shoulders in both directions. The alignment in this area is along a curve with a 75 mph speed limit. The rock slopes were excavated approximately (0.75: 1) to (0.5:1) and range 80 ft or more in height. The entire cut is approximately 1200 ft long. Approximately 8,500 vehicles pass this cut every day. The sight distance is approximately 800 ft under good conditions. The normal annual precipitation in the area is approximately 25 inches per year. The average elevation is approximately 7,200 ft above sea level.

The high roadway cut slopes were constructed in extrusive basalt flows and breccias to accommodate the interstate highway alignment. The as-built plans indicate the cut was originally excavated with controlled blasting techniques. However, the slope may have also been damaged by blasting during this process. The existing cut produces a significant volume of rockfall and requires maintenance forces to clear out the cut ditch several times a year. The

adverse orientation of some of the joint planes tends to form wedges and planes that become unstable in times of increased precipitation and ice development. A significant rockfall event took place in February 2005, during a period of time when a number of heavy rainfall and snow events occurred. Water appears to be infiltrating in rock discontinuities and may be accelerating deterioration of the slope. Large boulders up to 6 feet in diameter have fallen onto travel lanes despite the existing catchment ditch. The major focus of rockfall is near the east end of the cut section, coincident with a highly fractured zone in the face. The intent is to use LIDAR to identify the major structural geologic discontinuities that control rockfall and also identify the structural trends that will permit redesign of the existing cut to increase slope stability or define rockfall mitigation measures for the entire cut.

The geology of the site is mapped as series of extrusive and pryoclastic lithologies associated with the San Francisco Volcanic Field, ranging in age from Holocene to Pliocene (0.1 to 5.3 million years ago [MYA]). In general, they are composed of basalts, andesite, dacite, rhyodacite, and rhyolite flows and domes. A series of moderately eroded cinder cones and associated pryoclastic deposits are regionally present. Underlying these deposits is an erosional unconformity on top of the Permian Kaibab Formation (286 MYA). This contact is recognized as a former topographic surface, which consisted of low hills and low gradient streams and pediments that were formed on the Kaibab Formation and are now concealed by volcanic deposits.

Numerous curvilinear and undulating to near-vertical cooling joints in the cut face form wedges and boulders. In places, multiple flows and basalt breccias result in a highly fractured rock mass. Some of the joint plane dips adversely into the roadway and are potentially hazardous to the traveling public.

LIDAR SCANNING AT THE ARIZONA SITE

Scanning was conducted in November 2009 by ADOT personnel using a Leica Scanstation time-of-flight scanner. ADOT personnel produced a registered color point cloud of the entire slope, and this point cloud was then broken up into five sections for analysis with the Split-FX point cloud processing software. Table 5 gives details on the five point clouds. Scan 1 covers the easternmost part of the slope and Scan 5 covers the westernmost part of the slope. There are several reasons for breaking the slope into five sections. First, since the point cloud of the entire slope contains over 15 million points, breaking it into sections creates manageable subsets of point cloud data. Second, the geologic structure varies along the length of the slope, and this allows geotechnical analysis of subsections of the slope.

For example, the approximate location of Scan 2 is shown in Figure 8a, and the color point cloud of Scan 2 is shown in Figure 8b. The length of this point cloud is about 503 ft, the height ranges from 60 to over 100 ft, and the point cloud contains about 4 million points. The average dip of the rock slope in Scan 2 is 65.5 degrees and the average dip direction is 208.1 degrees. The delineated fracture surfaces and traces from this point cloud are shown in Figure 8c.

Table 5. Summary of Point Cloud Information from the Arizona Site

Scan	Number of Points	Average Slope information			
		Length (ft)	Height (ft)	Dip	Dip Direction
Scan 1	1,753,908	311	73	52	192.4
Scan 2	4,023,555	503	102	65.5	208.1
Scan 3	3,590,494	501	112	64.8	210.8
Scan 4	4,962,057	493	112	64	210.7
Scan 5	3,175,289	546	102	59.4	211.9
Total	16,505,303	Avg 470.8	Avg 100.2	Avg 61.1	Avg 206.8

Figure 8a. Approximate location of the Scan 2 point cloud (between the red lines).

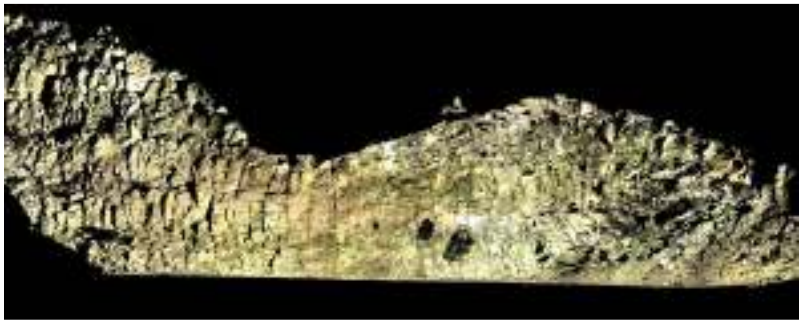

Figure 8b. The point cloud of Scan 2.

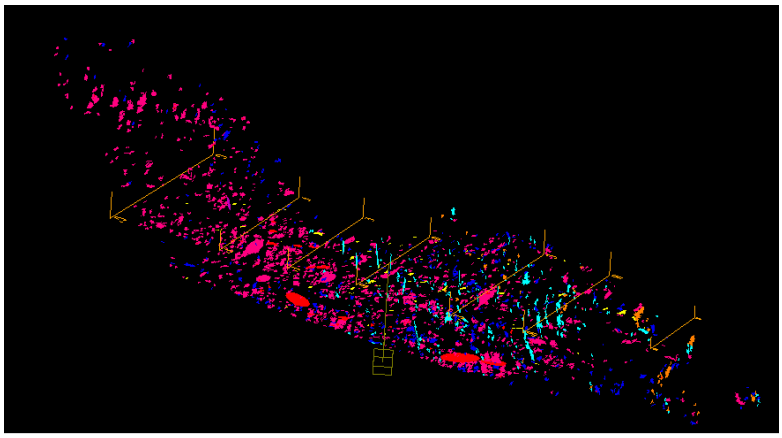

Figure 8c. The delineated fractures in Scan 2.

POINT CLOUD PROCESSING OF THE SCANS FROM THE ARIZONA SITE

For the Arizona site, point cloud processing was conducted for three main types of analysis, as described below.

Rock Mass Characterization

Important attributes of the geologic structure were extracted from the point clouds, including discontinuity orientation and spacing. The orientation results were plotted on a stereonet and the primary joint sets were determined.

The stereonet results from Scans 1-5 have been combined into a single stereonet and are shown in Figures 9a and 9b. In Figure 9a, the icons in the stereonet are differentiated by scan number (1-5). It shows that some of the geologic structure shows up only in one or two of the scans, while other structure shows up across the entire slope. In Figure 9b, the icons in the stereonet are differentiated by set number (1-8). Eight primary joint sets have been determined from the combined data, and the mean orientation and the Fisher constant for each set are given in Table 6. In addition to these eight sets, there are a number of fractures that are not assigned to any set (gray triangles in Figure 9b). Most of these are blasting fractures that are sub-parallel to the slope. The average orientation of the highway is also shown in Figures 9a and 9b. Figure 10 shows how the blasting fractures emanate from the blast hole half-casts, and also how the blasting fractures interact with natural fractures in the rock mass. The results in Figure 9 show that the geologic structure is complex and contains several sets of subvertical cooling joints, as well as subhorizontal discontinuities and several sets of discontinuities that dip adversely and may be prone to plane and wedge sliding. This is discussed further in the section on slope stability.

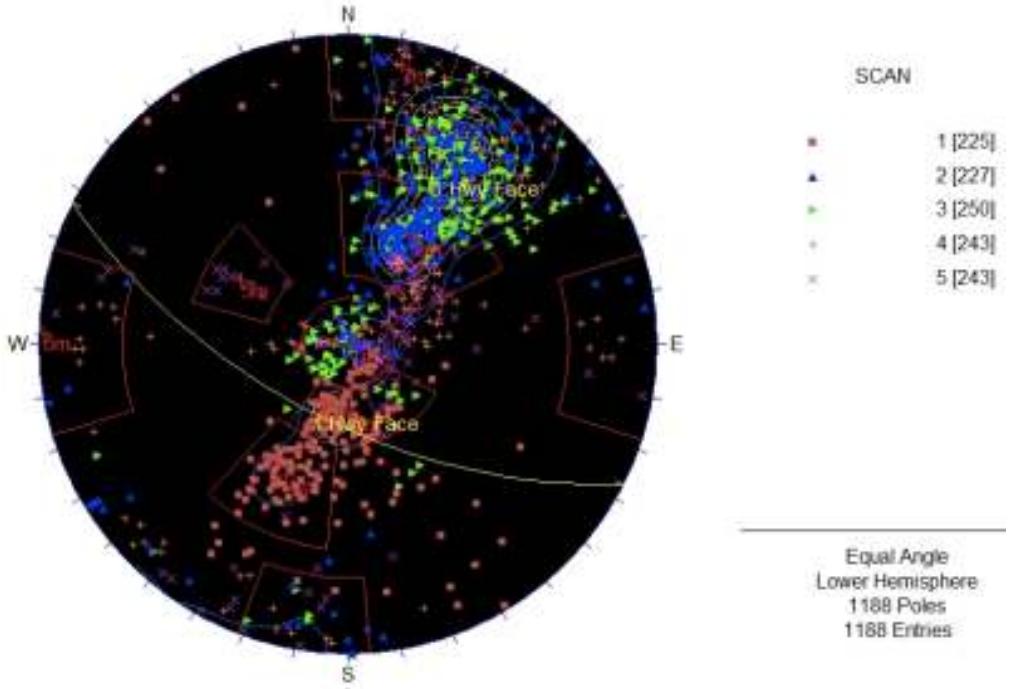

Figure 9a. Combined fractures from Scans 1-5, separated by scan.

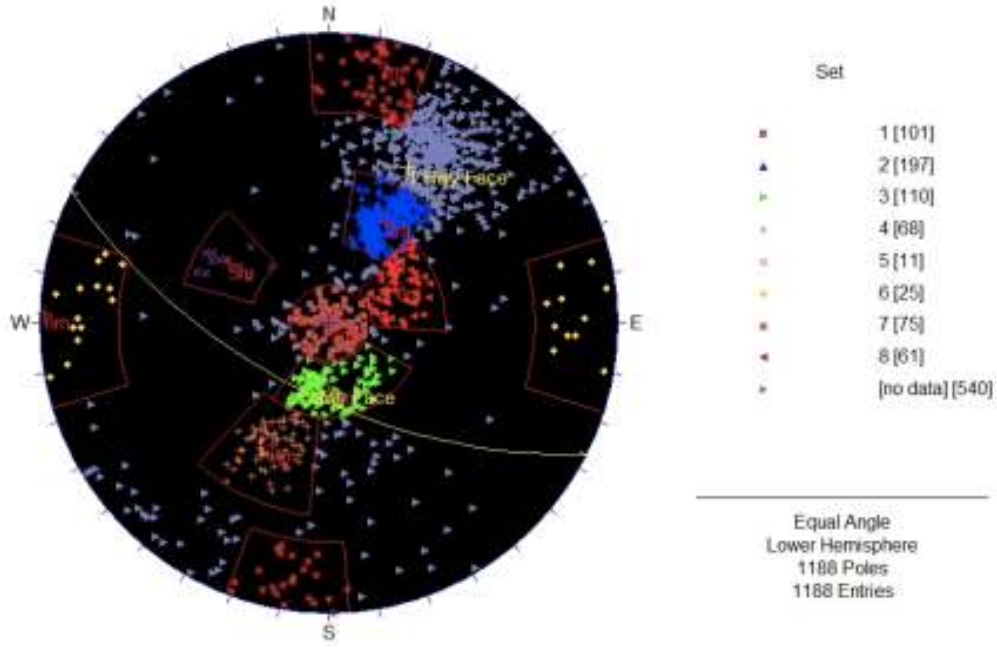

Figure 9b. Combined fractures from Scans 1-5, separated by set.

Figure 10. Rock slope in Scan 2 showing pre-split half-casts, blasting fractures, and natural fractures.

Table 6. Major Fracture Sets from the Arizona Site

Set	Average Dip	Average Dip Direction	Fisher Constant
1	1	321	68
2	44	209	92
3	25	360	55
4	50	25	80
5	44	121	89
6	89	92	35
7	85	191	52
8	30	240	66

Slope Stability

For the Arizona site, a kinematic analysis of plane failure and a probabilistic analysis of wedge failure were conducted. The plane sliding analysis was conducted using the Rocscience Dips program, and the wedge sliding analysis was conducted using the Rocscience Swedge program (Rocscience 2010).

The kinematic analysis for plane failure is shown in Figure 11. The analysis follows the procedure described in Rocscience (2010). All fracture poles from scans 1-5 have been included. The

stereonet in Figure 11 shows a friction circle (centered about the center of the stereonet) and a daylighting envelope. The friction circle was drawn assuming a friction angle of 35 degrees. Fracture poles that are outside the friction circle and inside the daylighting envelope are susceptible to plane sliding. The plane sliding analysis in Figure 11 clearly identifies set 2 and the steeply dipping portion of set 8 as those susceptible to plane sliding. Figure 11 also shows that set 2 appears throughout the highway cut while the steeply dipping portion of set 8 appears only in scans 4 and 5 (west end of the highway cut).

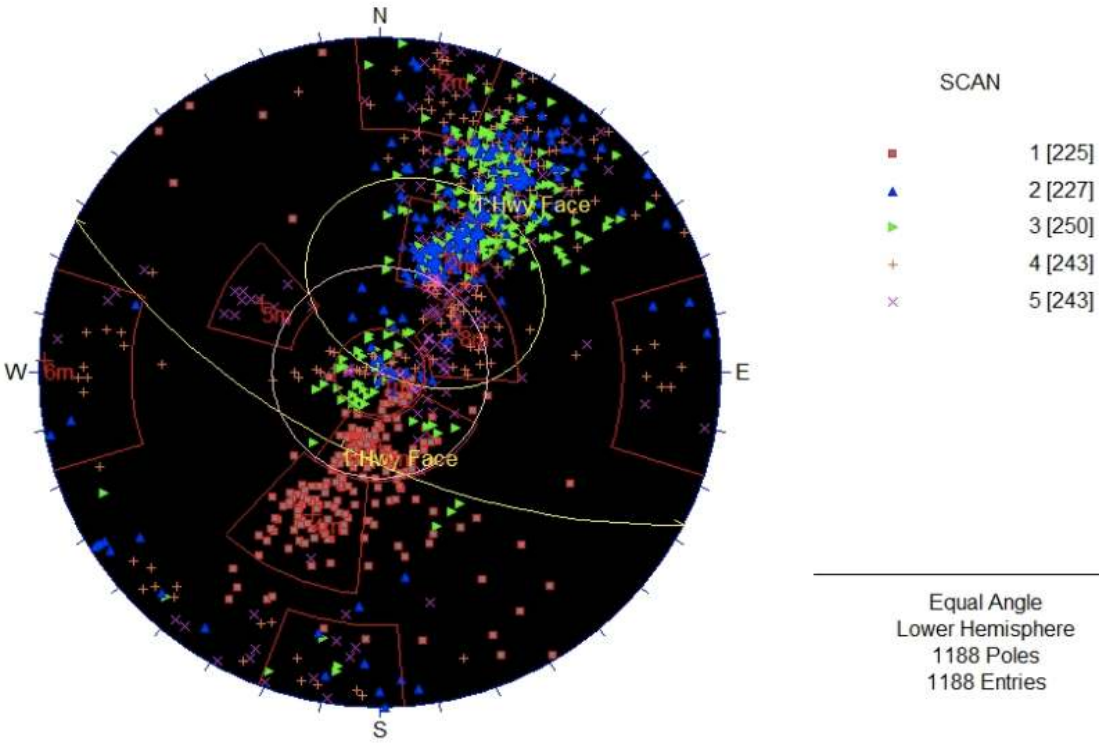

Figure 11. Plane sliding analysis. Fracture poles outside the friction circle (centered about the center of the stereonet) and inside the daylighting circle are susceptible to plane sliding.

The probabilistic analysis for wedge failure is shown in Table 7. The wedge failure analysis used the information listed in Tables 5 and 6 (average dip and dip direction for each set, Fisher constant for each set, and average highway cut orientation). Every possible combination of joint set pairs was analyzed for possible wedge failure. For the eight joint sets, there are 28 possible joint set pairs. The probability of failure for each joint set pair was calculated by making 10,000 picks from a Fisher distribution for orientation of each fracture making up the joint set pair. The percent of the picks that results in wedge failure is the probability of failure. For each joint set pair, the probability of wedge failure was calculated once assuming dry (no water pressure) and once assuming wet (fractures filled with water) conditions. In Table 7, dry conditions are shown in red and wet conditions are shown in blue. A friction angle of 35 degrees and zero joint cohesion were assumed.

Probabilities of failure can range from 0 to 100 percent, and a probability of failure greater than 20 or 30 percent indicates likelihood for wedge failure to occur. Table 7 shows that the highest

probabilities of failure are almost always associated with Joint Set 2. This includes wedges formed from sets 2/3, 2/5, 2/6, and 2/7. Joint Set 2 occurs in many of the scans but some of the other sets occur in only one or two of the scans. Joint Set 5, for example, only occurs in Scan 5 (west end of slope). Note that Joint Set 2 is also the primary structure associated with plane failure at the Arizona site.

Table 7. Probabilities of Failure for Wedge Sliding

Arizona Swedge Slope Stability Analysis ϕ=35°								
Prob of Fail (Dry/Wet)								
Joint Set	1	2	3	4	5	6	7	8
1		14.96%	2.62%	4.63%	0.01%	2.00%	4.48%	2.52%
2	11.03%		23.56%	11.07%	93.62%	86.33%	48.13%	67.13%
3	0.00%	20.44%		2.09%	4.51%	0.00%	7.26%	10.91%
4	0.00%	9.74%	0.66%		18.92%	0.00%	0.51%	2.60%
5	0.00%	43.30%	3.86%	16.14%		24.04%	0.06%	8.50%
6	0.00%	50.65%	0.00%	0.00%	0.32%		0.20%	4.66%
7	0.00%	44.64%	0.00%	0.00%	0.04%	0.20%		64.70%
8	0.21%	61.91%	0.90%	0.18%	0.21%	0.32%	12.33%	

Analysis of Rockfall from Cross Sections

A number of cross sections were made in each of the five scans, as shown in Figure 12. Two types of analysis were made from the cross sections: an analysis of overhangs and an analysis of the trajectories of possible rockfall.

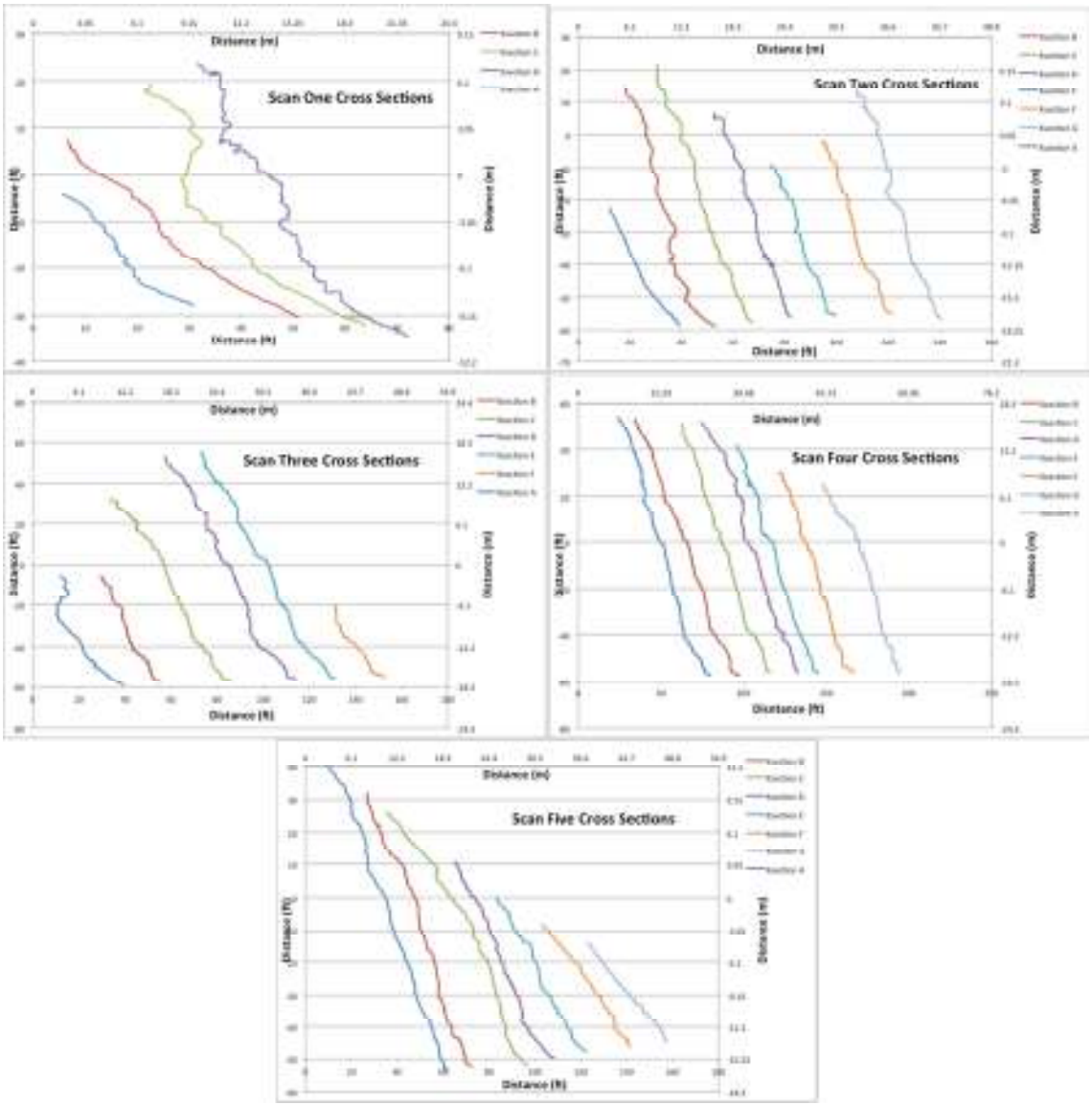

Figure 12. Slope profiles for Scans 1-5.

Rockfall along steep highway slopes is often associated with weathering of the slope, which causes rock blocks to loosen and displace under the influence of gravity and tension, as opposed to gravity and frictional sliding in the cases of plane and wedge failure. As a result, slopes become rough and irregular over time and contain overhanging blocks that are likely to produce rockfall. Rockfall rating systems such as the ones used in Utah and other states use information on slope roughness and overhangs as part of their rockfall hazard evaluations.

One way to evaluate slope roughness and overhangs from LIDAR point clouds is to analyze vertical cross sections. The Overhang Factor (OHF), a parameter that relates to rockfall potential, has been extracted from these cross sections. OHF is calculated by determining the percent of slope segments that consists of overhanging slopes. A slope segment size of about 1 foot was used in this analysis, and along a cross section, each segment was evaluated for overhang and

given an overhang rating. As shown in Figure 13, the overhang ratings for individual segments range from 0 for no overhang to 10 for severe overhang. The OHF was calculated by summing up the individual ratings along a cross section and normalizing them by the maximum rating possible. An OHF above 4 or 5 percent indicates the possibility of rockfall issues. Table 8 gives the OHFs for the cross sections shown in Figure 12. Almost all of the cross sections with overhang ratings greater than 4 percent are located on the eastern part of the highway cut in Scans 1 and 2. This agrees with rockfall problems with the highway cut, which mostly occur in the eastern part of the scanned area.

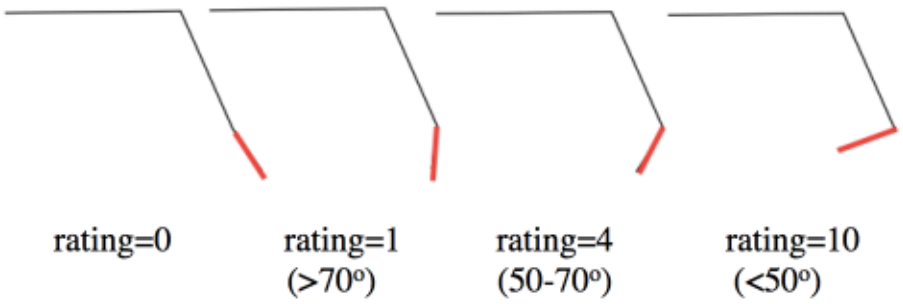

Figure 13. Overhang rating system for segments of a slope profile from LIDAR point clouds.

Table 8. OHFs for the Cross Sections Shown in Figure 12

Section	Overhang Factor (OHF)				
	Scan 1	Scan 2	Scan 3	Scan 4	Scan 5
A-A’	0.89	1.25	1.24	2.16	0.47
B-B’	0.44	10.51	1.69	2.03	2.45
C-C’	12.5	4.93	2.31	1.80	2.38
D-D’	10.21	3.33	2.57	4.92	1.43
E-E’		3.27	2.62	6.45	1.37
F-F’		1.96	1.57	3.34	0.78
G-G’		6.00		2.24	0

Cross sections associated with potential rockfall can be identified by using the OHF. Using these cross sections, a trajectory analysis can then be conducted to determine if rockfall will be confined to the ditch or if a rockfall hazard exists. As an example, Figure 14 shows the rockfall trajectories calculated using the Rocscience RocFall program. A small block size was used to simulate loose rock crumbling along cross section B-B’ of Scan 2, which has one of the highest OHFs. Impact and rebound properties of a weathered rock were used, with a talus cover at the bottom of the slope. A small ditch was also added between the slope and the highway. Based on these input parameters, 100 trials were simulated. The results indicate that of the 100 trials, over 10 of them ended up in the highway, indicating that a rockfall hazard does exist in the eastern part of the Arizona site.

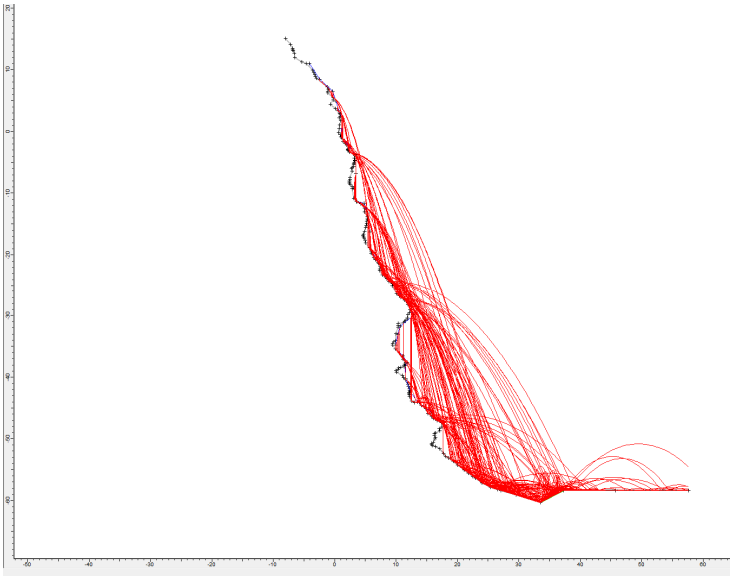

Figure 14. Trajectories of cross section B-B’ in Scan 2.

5. CALIFORNIA

This chapter discusses scanning that took place in California as part of the LIDAR pooled fund project, as well as the results of analyzing the California scans.

OVERVIEW OF THE CALIFORNIA SITE

The California site for the pooled fund study is a rock slope along California State Route 299's westbound lane at milepost 37.5. The northeast striking rock slope is approximately 300 ft in length along the highway with an approximate maximum height of 80 ft and an average dip of approximately 70 degrees to the southeast. Rocks at the site are pre-cretaceous metavolcanic accreted terranes. The rock mass is intercepted by five joint sets, which create a highly fractured rock mass structure. The most prominent joint set dips steeply toward and often overhangs the highway, contributing to the instability of the rock mass with potential toppling failures. A shallower highway dipping joint set combines with two sets that dip northeast and southwest to form potential wedge failures. A picture of the highway with the slope is shown in Figure 15.

The climate at the site can be inferred from two nearby data stations, which are located at Big Bar and Weaverville. Based on these two stations, winter averages show precipitation ranging from maximum average monthly amounts of 6.81 to 7.27 inches, minimum temperatures from 27.5 to 33.1 °F, and maximum temperatures from 46.6 to 47.8 °F. Winter season also holds the record daily rainfall amount of 5.50 inches for Weaverville and 7.27 inches for Big Bar. The average annual snowfall ranges from 6.7 inches in Big Bar to 22.3 inches in Weaverville. The rainy season, defined here as months during which the average rainfall is greater than 2 inches, extends from October through April; this is when the probability for slope failure is highest, especially when combined with the winter freeze-thaw cycles (WRCC 2011).

Figure 15. Westbound view of the California SR 299 highway cut.

As part of the pooled fund project, LIDAR scanning and point cloud processing of the California site was conducted. CALTRANS hopes to learn several things from the scanning and analysis of the results. They plan to re-align the highway into the existing cut and use a new slope ratio of

0.1:1 (H:V). As a portion of the study, CALTRANS would like to analyze the site utilizing LIDAR and Split-FX to determine if the structure of the meta-volcanic rock will induce rockfall at this site with the proposed slope ratio. They are interested in quantifiable parameters that can be extracted from LIDAR scanning to evaluate geologic structure (i.e., stereonets) and the likelihood for slope failure and rockfall.

LIDAR SCANNING AT THE CALIFORNIA SITE

A team from the Department of Mining and Geological Engineering at the University of Arizona performed LIDAR scanning of the California site on June 10, 2011 , using an Optech ILRIS3D time-of-flight scanner. Seven scans were taken, referred to as NFCurve1 through NFCurve7; details of these scans are given in Table 9 and their locations are shown in Figure 16. Unregistered point clouds were produced for each of the seven scans, ranging from 944,958–1,690,430 million points. Discontinuity identification was conducted on each scan individually. Analysis was conducted for the entire highway cut on one stereonet, which plotted the poles of all fracture planes and traces for NFCurve2 through NFCurve7 (NFCurve1 was not included due to a registration problem with that scan). Scan times ranged from about 15 min to about 19 min, and in total about four hours were spent at the site. The point spacing in the scans ranges from about 1.0–4.8 cm. The wide range of point spacing was a result of the scans having to be taken at close distances to the slope face. As seen in Figure 16, the short distance required oblique angle scans of the slope that resulted in variable point density due to the large distance variability in each scan. In addition to the scans, a high-resolution digital image was taken at each of the seven locations using a Nikon D90 12 MP digital camera. These digital images were then draped over the point clouds to produce color point clouds. Figure 17 shows the color point cloud from NFCurve7. The point clouds were registered using readings taken from a Brunton compass for the scanner orientation (see Table 10). The compass was used to measure the scanner's up-down and left-right tilts as well as its bearing. The Brunton compass was adjusted for local magnetic declination prior to taking measurements.

Table 9. Scan Information for the California Site

Scan	Number of Points	Scan Time (approximate)	Average Slope Information			
			Length (m)	Height (m)	Dip	Dip Direction
NFCurve1	1,409,814	17 minutes	21.6	13.5	21.8	113.6
NFCurve2	1,707,888	18 minutes	36.8	19.3	65.3	113.8
NFCurve3	1,475,370	17 minutes	30.3	18.8	78.1	120.2
NFCurve4	1,521,520	18 minutes	23.4	14.1	60.8	136.1
NFCurve5	1,370,616	17 minutes	38.2	15.5	74.8	124.3
NFCurve6	1,690,430	19 minutes	65.4	19.8	76.7	128.6
NFCurve7	944,958	15 minutes	87.3	18.3	73.9	126.0
Total	10,120,596	2 hours				

Table 10. Scanner Orientations

Scan	NFCurve1	NFCurve2	NFCurve3	NFCurve4	NFCurve5	NFCurve6	NFCurve7
Azimuth	253	238	357.5	265.5	245	15	10
Tilt (for/aft)	29.5 back	11 back	19.5 back	24 back	12.5 back	6.5 back	10.5 back
Tilt (side)	2 right	0.5 left	1.5 left	4 left	2.5 left	4.5 right	2.0 left
Height (in)	38.5	43.1	41.3	44	39.5	43.5	36.8

Figure 16. Approximate locations of scans NFCurve1 to NFCurve7.

Figure 17. Color point cloud of the NFCurve7 LIDAR scan.

POINT CLOUD PROCESSING OF SCANS FROM THE CALIFORNIA SITE

For the California site, point cloud processing was conducted for three main types of analysis, as described below.

Rock Mass Characterization

Important attributes of the geologic structure, including discontinuity orientation and spacing, were extracted from the point clouds. The orientation results were plotted on a stereonet and the primary joint sets are determined.

The combined fracture results for LIDAR scans NFCurve2 through NFCurve7 are shown in Figure 18 and Table 11. Figure 18a through 18f show the fracture surfaces that were delineated in each of the point clouds. Figure 18g is a stereonet pole plot, where the different scans are represented with different icons. This figure shows that the geologic structure is similar between the different scans, indicating that a single structural analysis can be conducted of the slope. Figure 18h is a stereonet pole plot, where the different joint sets are represented by different icons. Six prominent joint sets can be seen in the stereonet in Figure 18h indicating possible plane, wedge, toppling, and overhang failure modes relative to the overall orientation of the slope. The overall slope has an average dip of 70 degrees and dip direction of about 115, as shown in Table 10. The orange set strikes parallel to the slope and daylights, with an average dip of about 56 degrees. Plane sliding is possible on this joint set. The teal set also strikes parallel to the slope and has an average dip of about 88 degrees. The average dip is not overhanging but, as shown in the stereonet, many of the joints within this set do overhang and toppling is possible on the overhanging blocks. Based on the orientations of the purple and magenta sets, wedge failure could be associated with these sets. Finally, the red set is subhorizontal and overhangs could be associated with this set that could pose a rockfall hazard. A detailed slope stability analysis with these different modes of failure is given later in this chapter.

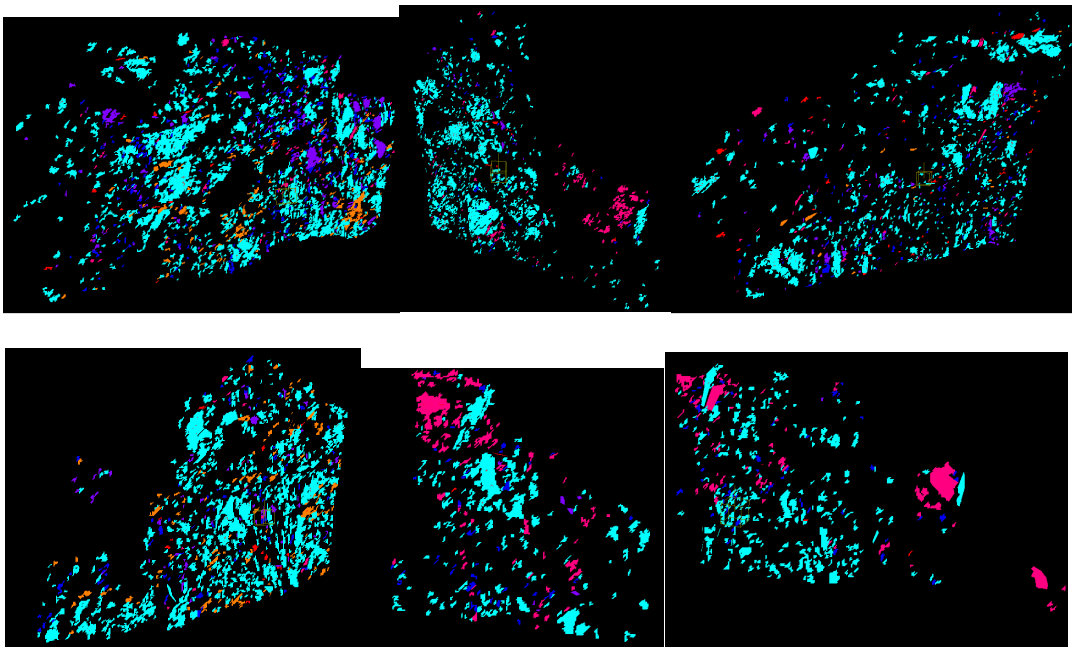

Figure 18a-f. Top row, from left to right, a through c, and bottom row, left to right, d through f, show LIDAR point clouds with fracture patches in scans NFCurve2 through NFCurve7, respectively.

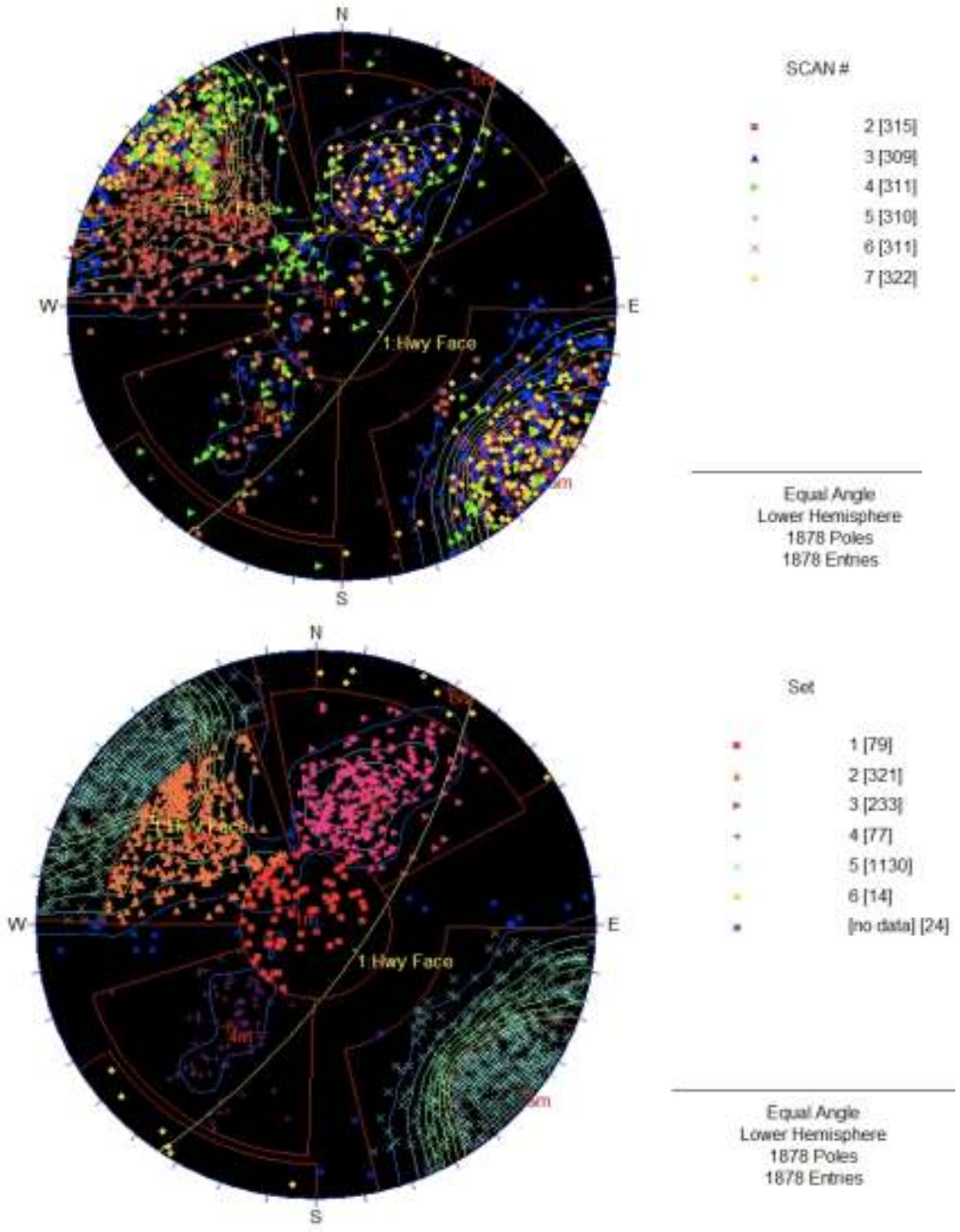

Figure 18g-h. Top to bottom, images are (g) lower hemisphere stereonet plot for the combined discontinuity orientations extracted from LIDAR NFCurve2 through NFCurve7, separated by scan, and (h) combined results of NFCurve2-NFCurve7, separated by set.

Table 11. NFCurve2 – NFCurve7 Average Results for All Joint Sets

Set	Average Dip	Ave. Dip Direction	Fisher Constant	Ave. Joint Spacing (m)
1 (red)	11	126	19	1.47
2 (orange)	59	128	21	0.58
3 (magenta)	53	201	23	1.1
4 (purple)	52	40	23	1.31
5 (teal)	88	309	21	0.43
6 (yellow)	89	209	20	0.43

Roughness and Persistence

As part of the analysis of the data from the California site, some mew methods for extracting joint friction angle and persistence from LIDAR point clouds were investigated. Since direct shear tests of the fractures at this site were not conducted, the friction angles for the different discontinuity sets were established by first determining a likely base friction angle based on the rock type at the site, and then determining the additional friction angle due to large-scale roughness. Large-scale roughness can be determined from the LIDAR point clouds in a very straightforward manner, as discussed in Kemeny and Turner (2008). Roughness can be determined by either analyzing two-dimensional profiles through the fractures, or by determining average dilation angles from triangulated meshes of exposed fracture surfaces. The dilation angle approach was used, and details of this approach are described in Mansfield and Kemeny (2009). For joint sets 1 through 5, a representative fracture surface was selected and meshed in the Split-FX program (this procedure was not done for Joint Set 6). The dip and dip direction of the mesh triangles were then imported into a statistical analysis program (Rocscience Dips), and for each representative fracture, the Fisher constant K was determined that represents the scatter in the triangle orientations. The average dilation angle, θ_{50}, was then calculated with the following formula (Mansfield and Kemeny 2009):

$$\theta_{50} = \frac{67.5}{\sqrt{\ }}.$$

Average dilation angles for each of the five joint sets are shown in Table 12. The dilation angles ranged from 7.5 (purple and teal sets) to 12.2 degrees (red set). Assuming that no weak discontinuity fill existed, the base friction angle was determined from direct shear tests on sawcut samples. For the metavolcanic rocks at the site, a base friction angle of 32 degrees was chosen based on Jaeger et al. (1979). The total friction angle for each joint set is then the sum of the base and dilation angles, as shown in Table 12. These friction angles, ranging from 39.5 to 44 degrees, could be used in the slope stability calculations for the site. Since this procedure for determining joint friction angles is new and has not been validated with laboratory tests, the study team has chosen not to use these values in the slope stability calculations presented in the Analysis of Slope Stability section of this chapter. Rather, the slope stability calculations were made with a friction angle of 35 degrees to be consistent with the analyses for the other states in the LIDAR pooled fund project.

Table 12. Dilation Angles and Joint Friction Angles for Joint Sets 1-5 (Base Friction Angle of 32 Degrees Assumed)

Joint Set	Fisher Constant	Dilation Angle	Friction Angle
Set 1 (red)	30.66	12.19	44.19
Set 2 (orange)	63.44	8.46	40.46
Set 3 (magenta)	70.05	8.06	40.06
Set 4 (purple)	80.91	7.5	39.5
Set 5 (teal)	81.39	7.48	39.48

Persistence is the spatial extent of discontinuities in a rock mass. Persistence is very important for rock engineering design, yet very difficult to measure in practice. One problem is that fractures can appear to be very persistent based on trace lengths (bedding planes for example), but their actual persistence in practice can be much smaller due to numerous small rock bridges that occur along the fractures. There are several ways that LIDAR point clouds can be used to estimate joint persistence. One method is to measure trace lengths from color point clouds. Another method that takes into account the problem with rock bridges is to measure the size of the exposed portion of discontinuities. These sizes are often less than the trace length but represent the actual sizes that can contribute to slope failure. This second approach is used to estimate persistence for each of the five joint sets at the California site.

For each of the five joint sets, persistence was defined as the maximum existing joint length found from fracture patches delineated by the Split-FX point cloud processing software. To determine the maximum joint length, the largest fractures for each joint set were removed from the point cloud and measured using measurement tools in the point cloud processing software. The maximum joint persistence for each set is shown below in Table 13. The results ranged from 0.92 m (3.02 ft) for Joint Set 1 to 6.35 m (20.8 ft) for Joint Set 3. Joint persistence can also be estimated by compiling the maximum joint length for every delineated fracture patch, plotting the distribution of lengths for each joint set, and then using an aspect of the distribution, such as the mean length, as the persistence for that joint set. Because the Split-FX program is currently unable to easily compile this information, this approach was not used in the LIDAR Pooled Fund project.

Table 13. Persistence for Joint Sets in NFCurve Scans

Joint Set	Max. Persistence (m)
Set 1 (red)	0.92
Set 2 (orange)	6.10
Set 3 (magenta)	6.35
Set 4 (purple)	2.28
Set 5 (teal)	3.24

Analysis of Slope Stability

Rockfall refers to individual blocks of rock dislodging from the slope. Slope stability refers to larger masses of rock undergoing unstable wedge and plane frictional sliding. A slope stability analysis for the California site was conducted using the discontinuity orientation information obtained from the point clouds and discussed previously (see Figure 18 and Tables 11, 12, and 13). The slope stability analysis was conducted based on discontinuity kinematics using the stereonet , using the Rocscience Dips program for wedge, planar, and toppling failures.

The result of a wedge failure analysis utilizing stereographic projection in the Dips program is shown in Figure 19. In this analysis, a friction angle of 35 degrees was used, along with the average orientation of the slope and the average dip and dip direction of joint sets 1-5. The analysis follows the procedure described in Rocscience (2010) and elsewhere. Any joint intersections that occur within the yellow zone in Figure 19 have the potential for wedge failure. This analysis does not take into account joint cohesion or water. Also, this analysis only uses the average orientations for each joint set and does not take into account the scatter about the mean orientations.

The kinematic analysis shows that wedges formed by the two joint combinations, 2/3 and 2/4, have the potential for wedge failure. Also, Figure 19 indicates that the joint combination 4/5 is very close to the yellow zone, and considering scattering in orientations, some wedges with this combination probably also have the potential for wedge failure. Numerous examples from the field site supporting these conclusions are shown in Figure 20. These examples are from both the point clouds and from pictures taken at the site. The existing topography at the site, as shown in Figure 20, may represent previous wedge failures, some of which may have had substantial size and mass. The persistence values found in Table 13 show that a wedge formed by Joint Sets 2 and 3 could have a length of at least 6 m (19.7 ft).

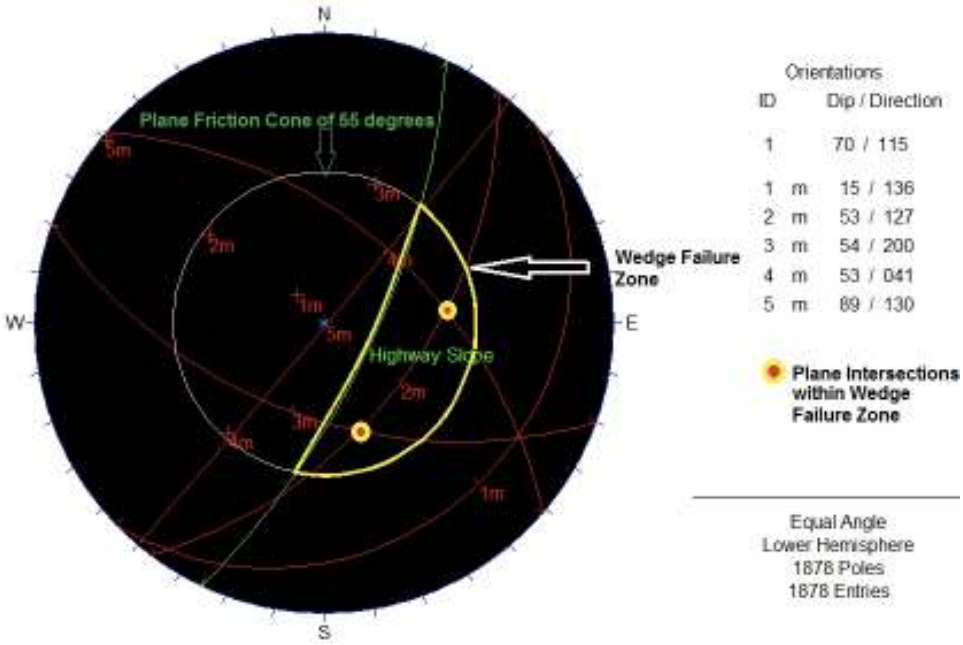

Figure 19. Rocscience Dips wedge failure kinematic analysis for the California site.

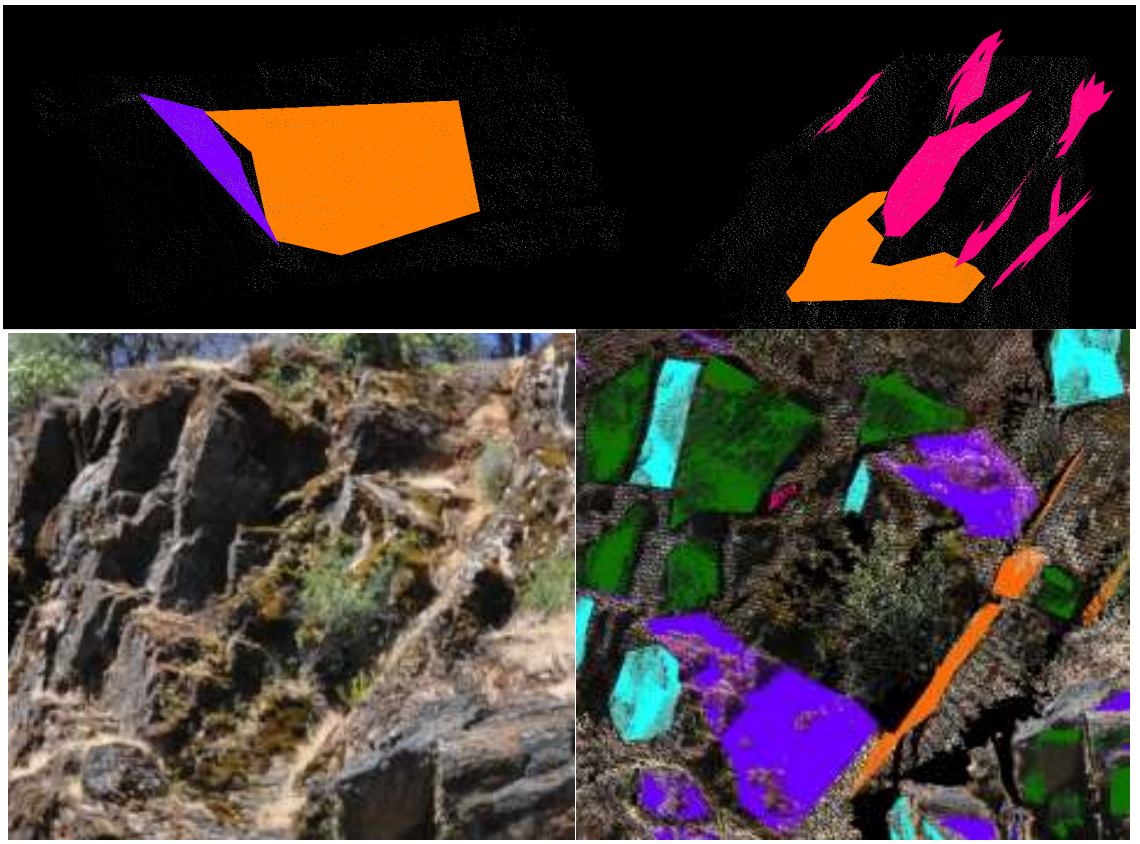

Figure 20. Clockwise from upper left are a wedge formation from Joint Set 4 (purple) and Joint Set 2 (orange); a wedge formation from Joint Set 3 (magenta) and Joint Set 2 (orange); a point cloud image of the a large existing wedge slide with orange and purple patches for sets 2 and 4 respectively; and a photo of that wedge slide, which was formed by joints 2 and 4.

A kinematic analysis for plane failure is shown in Figure 21. The analysis follows the procedure described in Rocscience (2010) and elsewhere. Any joint pole that occurs within the red zone in Figure 21 has the potential for plane failure. This analysis assumes a friction angle of 35 degrees and the average orientation of the slope. It considers all fracture poles at the site. The planar failure analysis shown in Figure 21 clearly identifies Joint Set 2 as the one susceptible to plane failure based on the average road cut slope with a dip of 70 degrees and a dip direction of 115 degrees. Although this set of rock fractures was present in all sections of the slope, scans NFCurve2, NFCurve4, and NFCurve5 held most of the measurable fracture surfaces with this orientation. Figure 22 shows how this mid-angle fracture set intersects the slope surface.

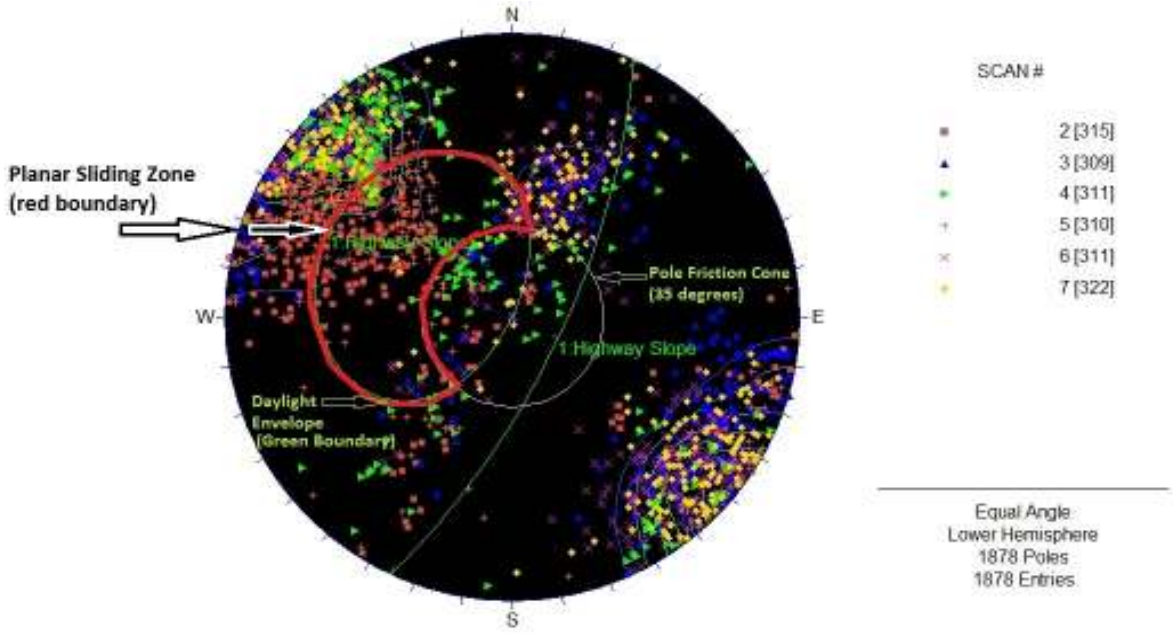

Figure 21. Rocscience Dips planar failure kinematic analysis for the California site.

Figure 22. Left is an image of possible planar failure surfaces of approximately 50-degree dipping Joint Set 2 (light orange) with respect to the general rock face, while right shows a side view of Split-FX image of Joint Set 2 (orange) as compared to the main slope surface (teal).

A kinematic analysis for toppling failure is shown in Figure 23. The analysis follows the procedure described in Rocscience (2010) and elsewhere. Any joint pole that occurs within the red zone in Figure 23 has the potential for toppling failure. This analysis assumes a friction angle of 35 degrees and the average orientation of the slope. It considers all fracture poles at the site. Figure 23 shows that the joints that are susceptible to toppling are the subset of Joint Set 5 (teal) that overhang, and there are a significant number of these fractures. Rockfall due to this mode of failure is considered a significant risk at the site, based on the large number of

overhanging joints, the weathering of the rock mass that is taking place, and the limited ditch width at this site. Figure 24 shows a photo of the overhanging fractures with small joint spacings and the narrow ditch. Figure 24 also shows the Split-FX point cloud image of some overhanging fractures of Joint Set 5. With the number of overhanging fractures, a narrow ditch width, and a climate with a long rainy season and winter freeze-thaw cycles (WRCC 2011), the rockfall hazard at this site is predicted to be relatively high.

Rockfall due to the tension failure of overhanging slabs is another type of slope failure that must be considered. In many cases, sub-vertical joints are involved, since these will produce the most severe overhang. Overhanging of sub-vertical joints is a major rockfall hazard on many rock slopes, such as horizontally bedded sandstone, limestone, and shale. At the California site, the sub-horizontal set is Joint Set 1 (red). Overhanging on this set is not considered to be a hazard because of the limited number of sub-horizontal joints, the average joint set spacing of 1.5 m (4.92 ft)(see Table 11), and the maximum persistence of less than 1 m (3.28 ft) (see Table 13).

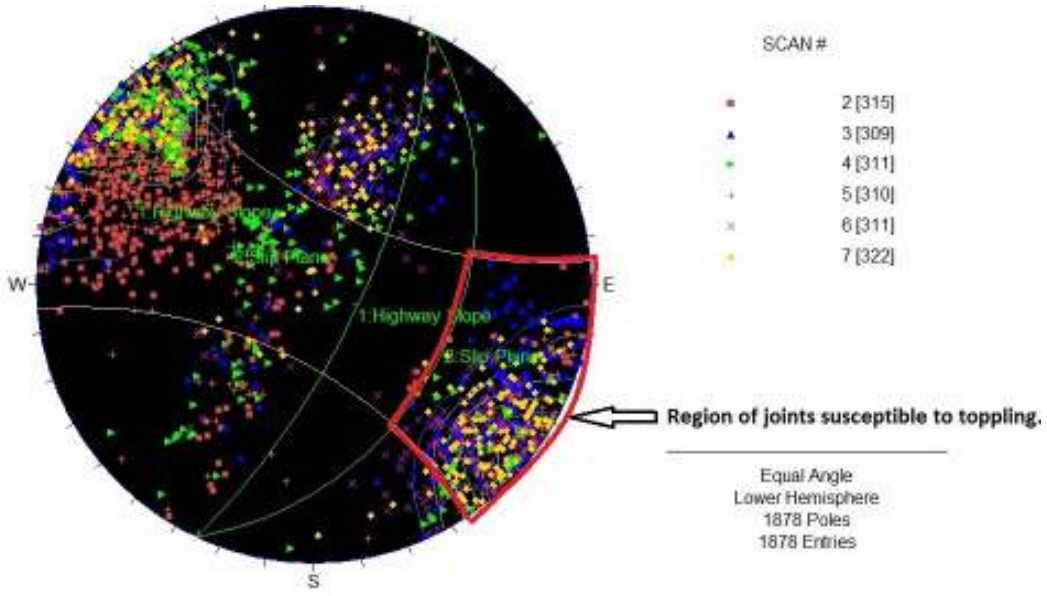

Figure 23. Rocscience Dips analysis for toppling failure at the California site.

Figure 24. Left to right, a digital image of overhanging fractures of Joint Set 5 (teal) with minimal ditch width, and an image of color point cloud showing overhanging fractures of Joint Set 5 (teal).

6. COLORADO

This chapter discusses scanning that took place in Colorado as part of the LIDAR pooled fund project, as well as the results of analyzing the Colorado scans.

OVERVIEW OF LIDAR SCANNING IN COLORADO

The use of ground-based LIDAR for monitoring rock movement and rockfall was investigated at two sites in Colorado for the pooled fund project, as described below.

Site 1: Along U.S. Route 285

The first site is along U.S. Route 285 at mile marker 246.7, approximately 20 miles from downtown Denver, Colorado. This is a divided four-lane highway with an average annual daily traffic count of about 27,000. The speed limit through this section of highway is 35 miles per hour. The cut slope is approximately 420 ft in length and a maximum height of no more than about 60 ft. The average grade of the cut slope is 60 degrees. The ditch width varies between 9 and 12 ft and concrete barriers have been installed along the edge of the ditch. Pictures of the site are shown in Figure 25.

Figure 25. Colorado Site 1 along with the scanner used, an Optech ILRIS3D.

The rock slope at this site consists of angular boulders dispersed within a fine matrix. This slope was created by a historic landslide. Weathering over time causes the angular boulders to protrude from the slope, loosen, and finally roll down the slope. The ditch and jersey barriers contain most of the rockfall, but in the past few years several large boulders have rolled onto the west-bound lanes of U.S. 285, as in the 2007 event shown in Figure 26.

Figure 26. Large rockfall along U.S. 285 in Colorado that occurred in April 2007 (Photo courtesy of CDOT).

Original LIDAR scans of the slope were taken September 9, 2009, and rescanning of the same slope was made on June 15, 2010. Details of the scans are given in Table 14. In the time period between the scans several boulders did become dislodged from the slope and were captured by the LIDAR change detection analysis, as discussed later.

Site 2: Near Empire, Colorado

The second site is located in the Colorado Department of Transportation's (CDOT) storage facility near Empire, Colorado. The test site is a manmade wall consisting of jersey barriers, plastic barriers, some thin cement sheets, and some round concrete blocks. Pictures of the site are shown in Figures 27a – 27b. The site is meant to simulate a rock slope. Small displacements were made to the plastic barriers, cement sheets, and the concrete blocks, and "before" and "after" LIDAR scans were made to determine if these small displacements could be detected.

Figure 27a. At Site 2 in Colorado, an image of the jersey and plastic barriers.

Figure 27b. At Site 2, (top) the Optech scanning of the site from the distance of 286 meters (938 ft), and (bottom) the Optech and ISITE scanners, also at the 286-meter distance.

Baseline scans were initially made at distances of about 110 and 286 m (361 and 938 ft) from the wall. Movements in the range of 0.3 – 4 inch were then made in the barriers, sheets and blocks, and rescans were made at both distances. A second set of movements were made, and rescanning was again conducted. Scanning was conducted using two scanners, an Optech ILRIS3D and an ISITE 8800. In addition, two other technologies were used at the site: fiber-optic strain gauges supplied by Applied Geomechanics Incorporated, and rf transmitted accelerometers supplied by Silent Solutions Security. Details of the scans are shown in Table 14. This report describes only the analysis of results from one set of ISITE scans (110 m, or 361 ft, distance, before and after Movement 1) even though scanning with the ISITE 8800 scanner was conducted at two other locations.

Table 14. Details of Scans Made for the Pooled Fund Project

Site	Location	Date	Scanner	Event	# Points (after cropping)
Site 1- U.S. 285, mile marker 246.7	Right side of slope	Sept. 9, 2009	ILRIS-3D	Before scan	1,779,339
	Left side of slope	Sept. 9, 2009	ILRIS-3D	Before scan	1,316,635
	Right side of slope	June 15, 2010	ILRIS-3D	After scan	2,393,937
	Left side of slope	June 15, 2010	ILRIS-3D	After scan	2,130,097
Site 2 - CDOT Storage Facility near Empire, Co	110 m from target	June 7, 2010	ILRIS-3D	Before Movement 1	56,675
	286 m from target	June 7, 2010	ILRIS-3D	Before Movement 1	22,181
	110 m from target	June 7, 2010	ILRIS-3D	After Movement 1	33,005
	286 m from target	June 7, 2010	ILRIS-3D	After Movement 1	80,492
	110 m from target	June 7, 2010	ILRIS-3D	After Movement 2	121,475
	110 m from target	June 7, 2010	ISITE 8800	Before Movement 1	17,496
	110 m from target	June 7, 2010	ISITE 8800	After Movement 1	17,525

RESULTS OF POINT CLOUD PROCESSING OF THE COLORADO SCANS

Site 2: Near Empire, Colorado

Site 2 is discussed first since the results are a good reference for the analysis that was conducted at Site 1. Shown first are the results of Movement 1, analyzed from scans taken from a distance of 110 m (361 ft) from the artificial rock wall. The wall is broken up into 12 segments labeled A through L, as shown in Figure 28b, and the actual displacements in Movement 1 are given in Figure 28a. Figure 28c shows the difference point cloud from the Optech ILRIS-3D scans from a distance of 110 m (361 ft). Movement toward the scanner is shown in blue, movement away from the scanner is shown in red, and the threshold noise level for this difference cloud is about 1.1 cm (0.43 inch, shown in gray). Comparing Figure 28b and 28c, the blue patches agree with the actual displacements for all regions where a displacement greater than 0.4 inch was made (B2, C1, C2, D1, F2, H1, H2, I1, I2, K, L). Block J is red because it was removed between the scans.

Figure 28d shows cross sections through the difference point cloud through the top and middle plastic barriers, respectively. They provide additional details and show that the LIDAR scans taken from a distance of 110 m (361 ft)are capable of detecting change as small as 0.2 inch (see G1 and G2 locations in Figure 28d's bottom graph compared with actual movements given in

Figure 28a). Some of the waviness in these cross sections is due to the corrugations in the plastic barriers.

1st Move by hand - Upper Barriers
(measurement taken at base of barrier)

	Barrier	Movement (inches)	Notes
= Time - 12:00 to 12:10	A1	0.30	
	A2	0.20	
	B1	0.00	
	B2	1.70	
	C1	2.50	
	C2	2.50	
	D1	2.00	Barrier D was not intended to be moved. It moved with the barrier C movement
	D2	Not Recorded	No measurable movement from baseline
	E1	Not Recorded	No measurable movement from baseline
	E2	0.15	
	F1	Not Recorded	No measurable movement from baseline
	F2	3.30	Strain Guage #3 lost tension when moving this barrier. At approx 12:15 it was retensioned.

1st Move by hand - Concrete Board

	Board	Movement (inches)	Notes
= Start Time 12:30	G1	0.30	Movement of board measured from wall at approximate center. Boards moved with wooden wedges on each side except for board 'I', which we moved with one wedge only.
	G2	0.20	
	H1	0.40	
	H2	0.90	
	I1	0.60	
	I2	2.50	

1st Move by hand - Rocks in front of wall

	Board	Movement (inches)	Notes
Start time not recorded	J	NA	Rock movement is approximate. Rocks moved by pushing/rolling toward scanners. Rock J removed to simulate change detection.
	K	2.00	
	L	29.00	

Figure 28a. For Site 2, the actual displacements made to the artificial wall.

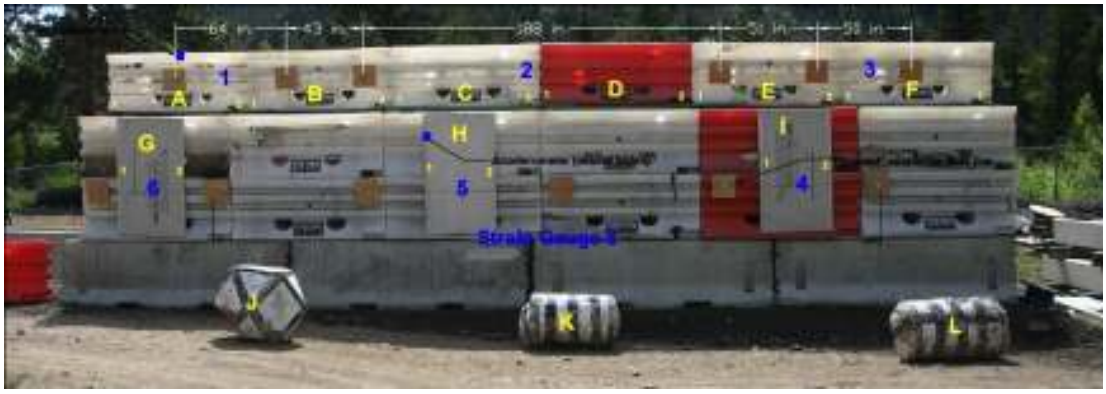

Figure 28b. For Site 2, the artificial wall with reference numbers.

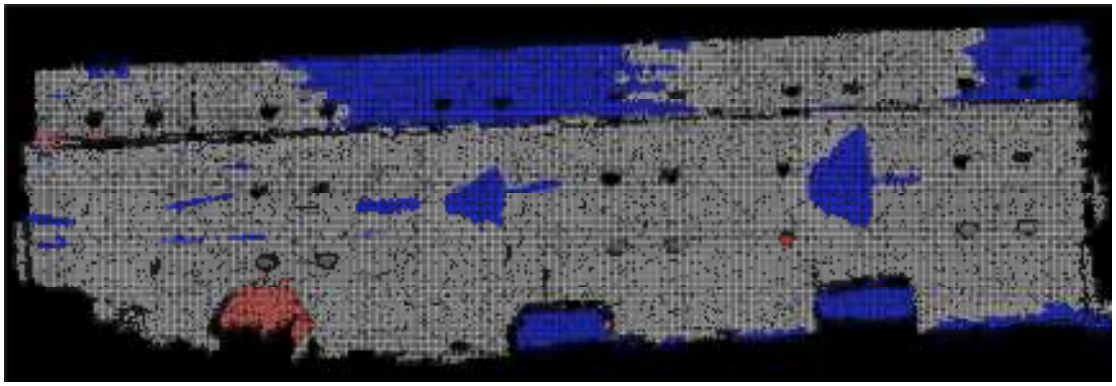

Figure 28c. For Site 2, the difference point cloud using Optech scanner at a distance of 110 m (361 ft).

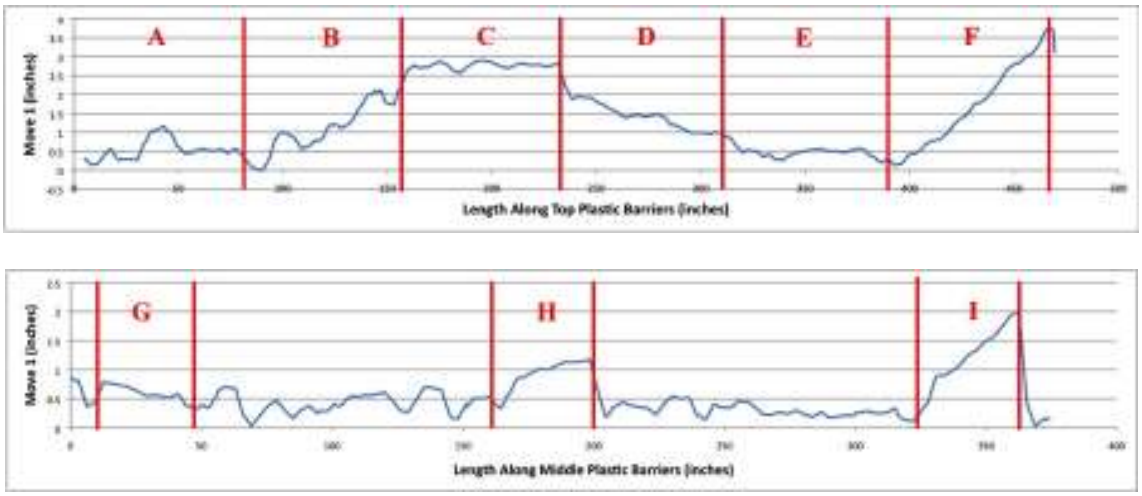

Figure 28d. For Site 2, the differences along upper barriers (top graph) and along middle barriers (bottom graph).

The results of Movement 1 taken from the 110-m distance with the ISITE 8800 scanner are shown in Figure 29a. It is not as accurate as Figure 28c, primarily because the point cloud point spacing is much larger. In the ISITE scan, the point spacing is 16 cm (6.3 inches) while in the Optech scan the point spacing is about 2.5 cm (1 inch). The resolutions of the two scanners are about the same. The results of Movement 1 taken from the 286-m (938 ft) distance with the Optech ILRIS-3D scanner are shown in Figure 29b. Figure 29b is not as accurate as Figure 28c because of the increased distance. The noise level for the difference point cloud shown in Figure 29b is 1.4 cm (.55 inch), compared to 1.1 cm (.43 inch) in Figure 28c. The results of Movement 2, taken from the 110 meter (361 ft) distance with the Optech ILRIS-3D scanner, are shown in Figure 29c. This can be compared with the actual movements shown in Figure 29d. Only movements were made to the upper barriers, as predicted by Figure 29c. There are some discrepancies between the difference cloud and the actual movements (e.g., red in the upper right of Figure 29c does not seem to match with actual movements, shown in plan view in Figure 29e).

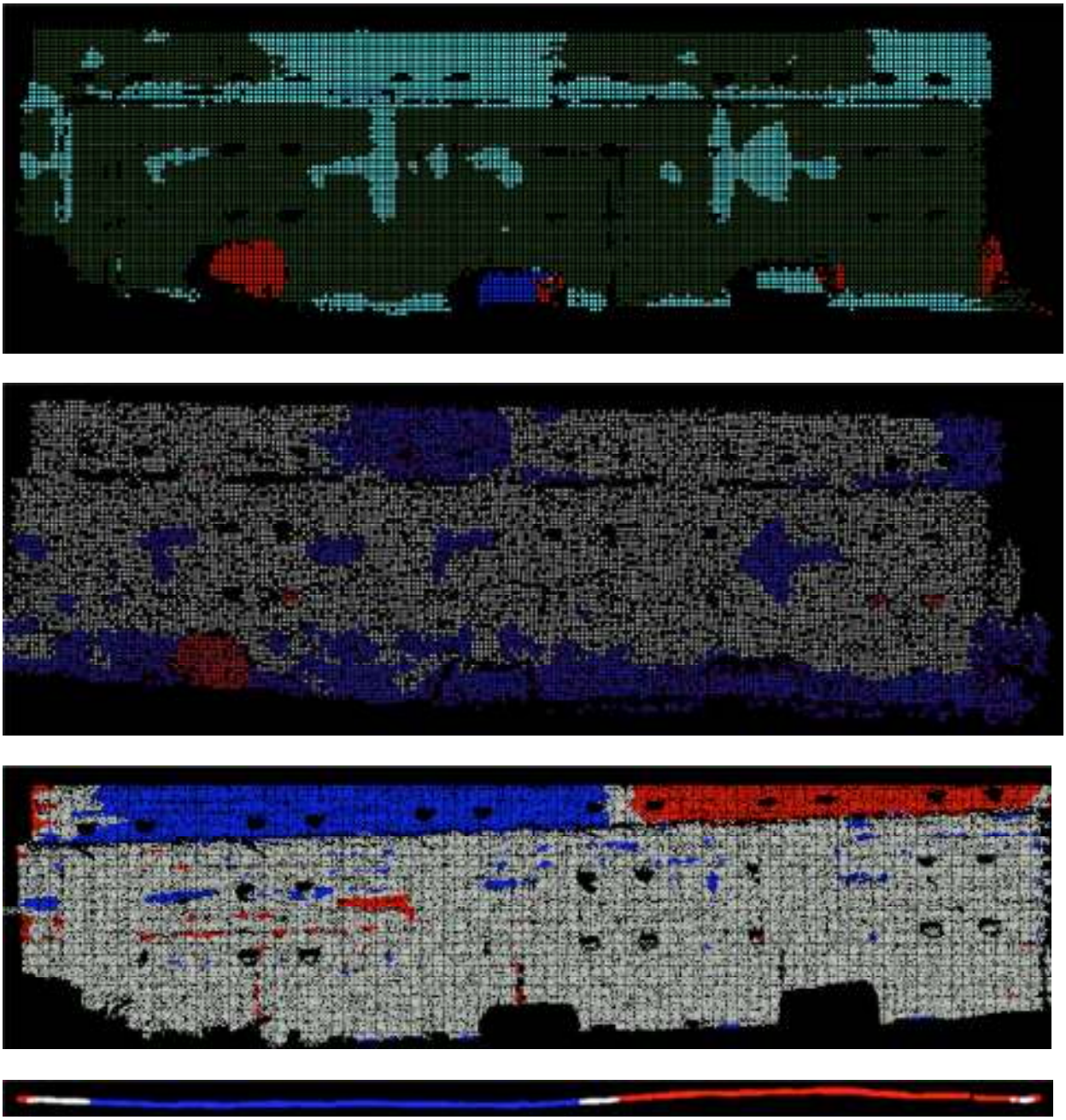

Figure 29a-d. Images are top to bottom (a) a difference point cloud from the ISITE scanner at a distance of 110 m (361 ft); (b) a difference point cloud from the Optech scanner at a distance of 286 m (938 ft); (c) a difference point cloud at a distance of 110 m for Movement 2 with the Optech scanner; and (d) a plan view of the difference cloud in shown in (c).

2nd Move by hand - Upper Barriers

(measurement taken at base of barrier - concrete board and rock not moved)

« Start Time - 12:55

Barrier	Movement (inches)	Notes
A1	0.00	An attempt made to "bow" barrier out from the center. The scan of the 1st move is the baseline for the second move. Some
A2	2.20	of the barriers moved back. Backward movement marked as negative.
B1	1.90	
B2	2.70	
C1	1.90	
C2	3.60	
D1	3.70	
D2	2.20	
E1	2.20	
E2	2.80	
F1	2.60	
F2	-0.40	

2nd Move by hand - Upper Barrier Aperture

(Aperture measued at top front of barrier)

Start Time not recorded

Barrier	Aperture (inches)	Notes
A - B	0.10	After 1st move it was noted (John Kemeny) that information regarding the movement of the "aperture" between barriers
B - C	0.50	should be recorded.
C - D	1.60	
D - E	0.40	
E - F	0.00	

Figure 29e. Charts of the actual movements made during movement 2.

Site 1: Along U.S. Route 285

The results from before scans (September 2009) and after scans (June 2010) taken at Site 1 are shown in Figure 30; Figure 30 also shows the difference point cloud of the left and middle parts of the slope; red indicates missing material and gray indicates movement less than the noise level. Because of the numerous small changes that occurred to the soil matrix in the nine months between the before and after scans, the background noise level is high – over 10 inches. Thus, only rockfall events with a size greater than 10 inches are shown in Figure 30's difference cloud. That image clearly shows several large rockfall events that have occurred, as well as a sign in the lower right that appears to have been bent at some point during the nine-month interval.

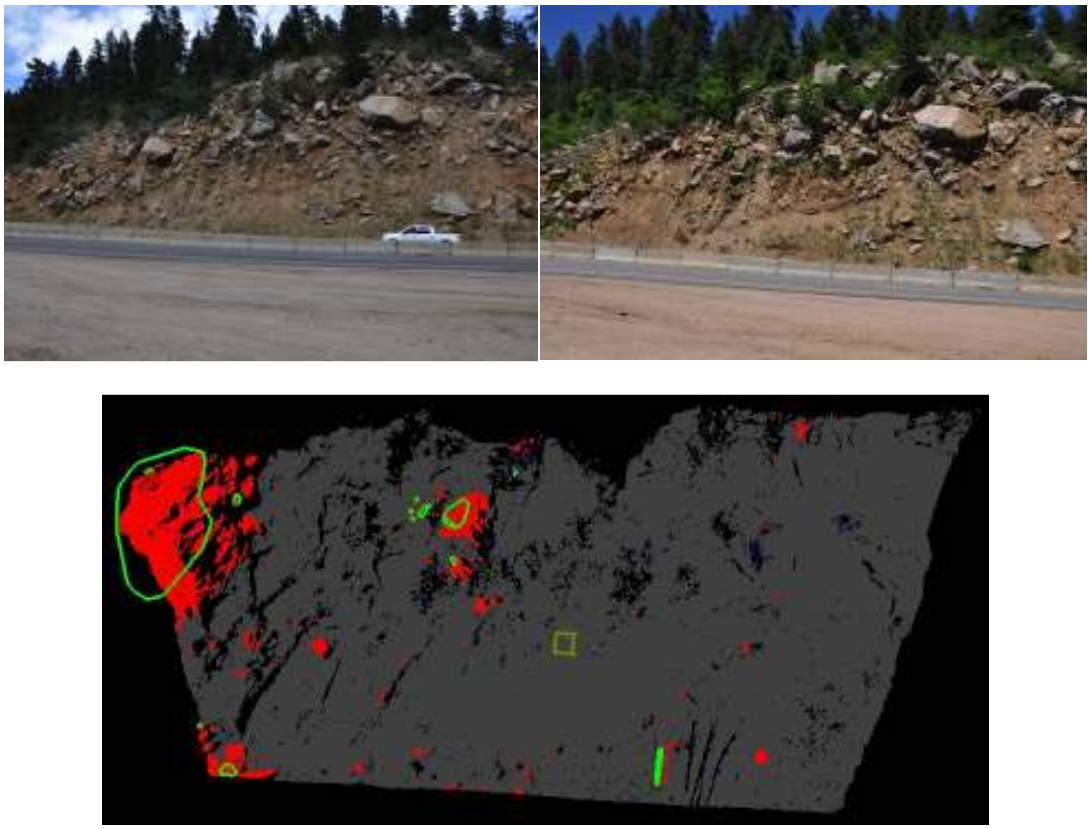

Figure 30. At Colorado Site 1 along U.S. Route 285, upper photos show, left to right, the conditions before (September 2009) and after (June 2010). The bottom image is a difference cloud for the site.

7. NEW HAMPSHIRE

This chapter discusses scanning that took place in New Hampshire as part of the LIDAR pooled fund project, as well as the results of analyzing the New Hampshire scans.

OVERVIEW OF THE NEW HAMPSHIRE SITE

The New Hampshire site for the pooled fund study is a rock slope on the east side of the northbound lanes of Highway 93, 1.5 mi north of Exit 30 near Woodstock, New Hampshire. The rock slope is approximately 260 m (853 ft) long and ranges in height from 17 (56 ft) to 40.5 m (132.8 ft). An andesite dike divides foliated and non-foliated regions of the rock mass. Rocks along the southern end of the cut are less foliated and are predominately gneiss, while the north end of the site is foliated schistose. The rock mass is intercepted by two major joint sets, which create a blocky rock mass structure. Mylonite seams dipping steeply toward the rock cut contribute to the instability of the rock mass. During the initial construction of the roadway, a rockslide occurred along a mylonite seam. The major causes of failures at this site are sliding and wedge failures mostly due to seasonal freeze-thaw and rain events. Figure 31 shows a picture of the southern part of the slope.

Figure 31. Southern section of the New Hampshire site.

As part of the pooled fund project, LIDAR scanning and point cloud processing of the New Hampshire site was conducted. New Hampshire State DOT (NHSDOT) hoped to learn several things from the scanning and analysis of results. First, the time required and cost of scanning and processing the point clouds would be compared with the time required and cost of employing conventional NHSDOT techniques. Second, NHSDOT was interested in quantifiable parameters that can be extracted from LIDAR scanning to evaluate geologic structure (i.e.,

stereonets) and the likelihood for slope failure and rockfall via their rock slope rating system. Additionally, LIDAR data may be useful in determining requirements for future rock bolting of the area.

LIDAR SCANNING AT THE NEW HAMPSHIRE SITE

A team from the Department of Mining and Geological Engineering at the University of Arizona performed LIDAR scanning of the New Hampshire site on May 13, 2010. Scanning used an Optech ILRIS3D time-of-flight scanner as shown in Figure 32. Seven scans were taken, referred to as Woodstock1 through Woodstock7; details of these scans are given in Table 15. An unregistered point cloud of the entire slope was produced from the seven scans that contained about 11 million points, but analysis was conducted on each scan individually. Scan times ranged from about 14 min (Woodstock7) to about 18 min, and in total about 3.5 hrs were spent at the site. The point spacing in the scans ranges from about 1.2 – 2.5 cm. In addition to the scans, a high-resolution digital image was taken at each of the seven locations using a Nikon D90 12 MP digital camera. These digital images were then draped over the point clouds to produce color point clouds. Figure 33 shows the color point cloud for Woodstock 6. At the time of the scanning, a number of locations were marked for surveying, and these points were surveyed by NHSDOT in the week following the scanning. The point clouds were registered using readings taken from a Brunton compass. The compass was used to measure the up-down and left-right tilts as well as the bearing of the scanner. Magnetic declination for the area was noted and adjustments were made in the Rocscience program Dips.

Table 15. Scan Information for the New Hampshire Site

Scan	Number of Points	Scan Time (approximate)	Average Slope Information			
			Length (m)	Height (m)	Dip	Dip Direction
Woodstock1	1,387,720	17 minutes	39.88	29.64	40.60	283.61
Woodstock2	1,894,251	18 minutes	44.86	31.47	33.06	281.09
Woodstock3	1,728,639	17 minutes	45.53	33.65	32.10	268.21
Woodstock4	1,632,855	18 minutes	40.56	24.27	33.06	279.86
Woodstock5	1,485,270	17 minutes	34.56	25.76	34.87	270.79
Woodstock6	1,760,900	16 minutes	33.57	40.57	48.65	258.10
Woodstock7	1,151,901	14 minutes	20.86	16.84	47.72	240.89
Total	11,041,527	2 hours				

Figure 32. Left to right, an example of scanning at the site using an Optech ILRIS 3D scanner, and the approximate locations of scans Woodstock1 to Woodstock7.

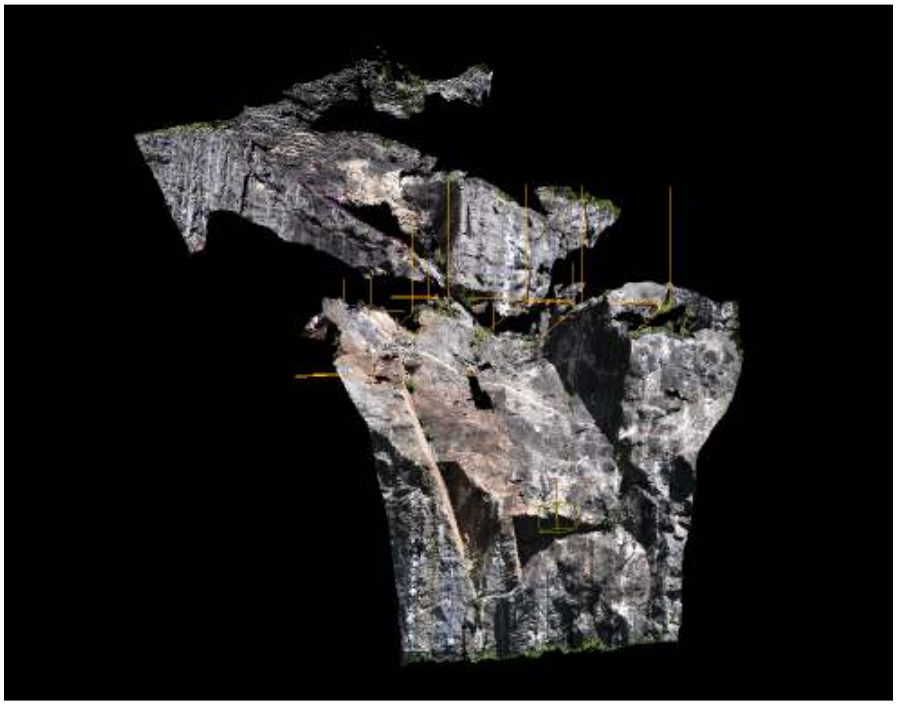

Figure 33. Color point cloud of the Woodstock6 LIDAR scan.

POINT CLOUD PROCESSING OF SCANS FROM THE NEW HAMPSHIRE SITE

For the New Hampshire site, point cloud processing was conducted for three main types of analysis, as described below.

Rock Mass Characterization

Important attributes of the geologic structure, including discontinuity orientation and spacing, were extracted from the point clouds. The orientation results were plotted on a stereonet and the primary joint sets were determined.

The geologic structure as determined from LIDAR scans Woodstock1-Woodstock7 is presented in Figure 34 and Table 16. Because the geologic structure was found to change from the north to south ends of the slope, the slope was broken up into three sections. The first section covers Woodstock1-Woodstock2, the second section covers Woodstock3-Woodstock5, and the third section covers Woodstock6-Woodstock7, as shown in the stereonets in Figures 34a to 34c, respectively. The primary discontinuity sets from each of the stereonets is given in Table 16. The stereonets in Figure 34 also show the orientation of the highway for each section, poles of blasting fractures that are parallel to the highway are shown in the stereonets and were not assigned to any set. Figure 34 shows that the geologic structure is similar between the different sections even though there are also some differences from section to section. The large medium-dipping mylonite planes, which pose a hazard for plane sliding, are a common structural feature seen in all the scans. The results in Figure 34 also reveal a number of joint sets that intersect to form possible wedge failures. An analysis of plane and wedge sliding is given below.

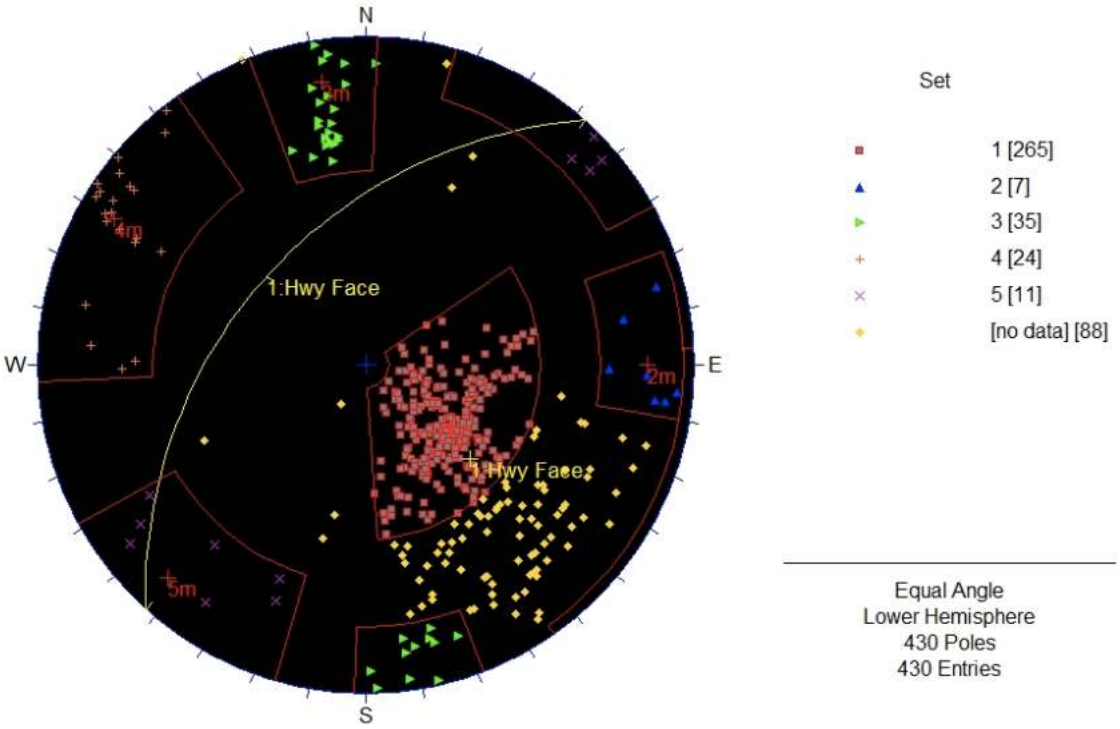

Figure 34a. Lower hemisphere stereonet plots for discontinuities at the New Hampshire site Woodstock1-Woodstock2 combined.

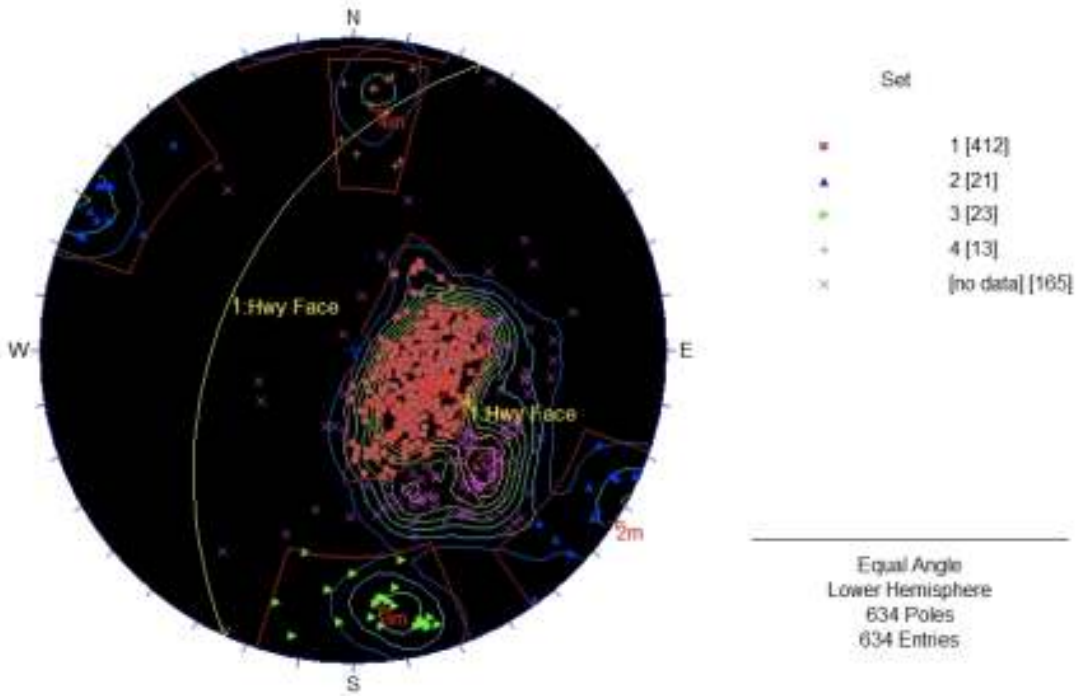

Figure 34b. Lower hemisphere stereonet plots for discontinuities at the New Hampshire site Woodstock3-Woodstock5 combined.

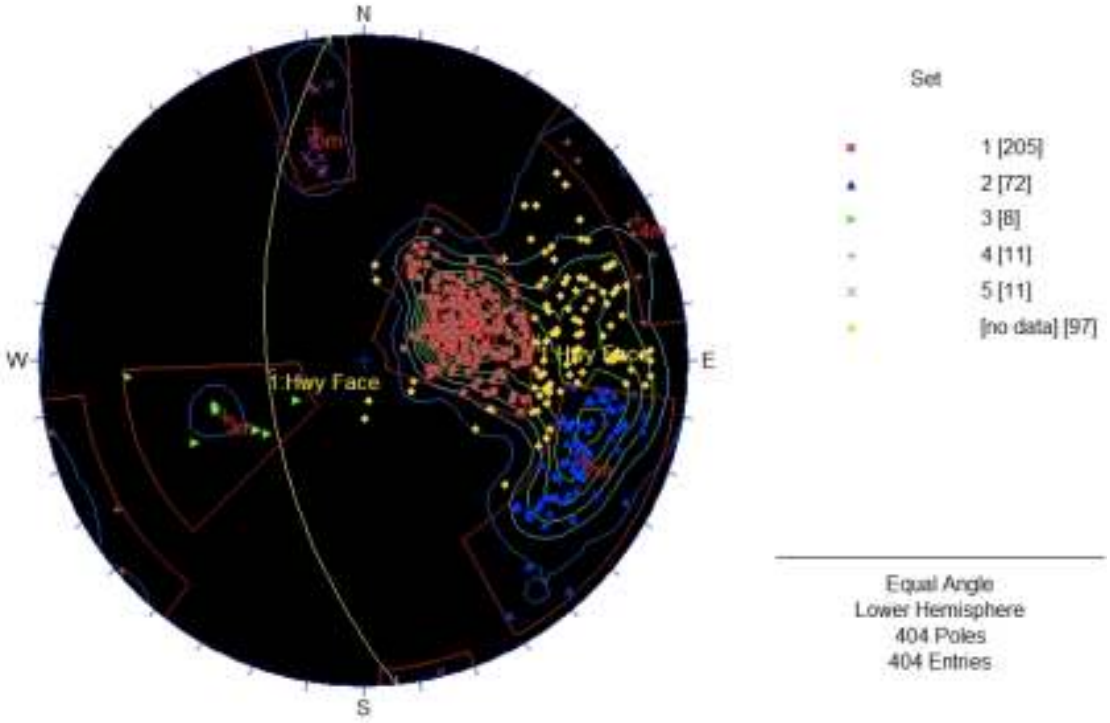

Figure 34c. Lower hemisphere stereonet plots for discontinuities at the New Hampshire site, Woodstock6-Woodstock7 combined.

Table 16. Mean Orientations for the Fracture Sets Shown in Figure 34

Set	Woodstock1-Woodstock2			Woodstock3-Woodstock5			Woodstock6-Woodstock7		
	Dip	Dip D.	Fisher	Dip	Dip D.	Fisher	Dip	Dip D.	Fisher
1	35	307	23	28	292	23	38	251	31
2	81	270	67	90	303	53	73	294	40
3	81	171	42	79	354	55	49	68	27
4	83	120	33	75	186	74	87	243	37
5	83	43	26				72	168	64

Analysis of Slope Stability

As described above, the slope was broken up into three structural sections, the section containing Woodstock1-Woodstock2, the section containing Woodstock3-Woodstock5, and the section containing Woodstock6-Woodstock7. For each section, a plane sliding analysis was conducted using the Rocscience Dips program, and a wedge sliding analysis was conducted using the Rocscience Swedge program. The results of the plane sliding analysis is shown in Figures 35a, 35b, and 35c, respectively, and the results of the wedge sliding analysis are shown in Tables 33a, 33b, and 33c, respectively.

Each of the stereonets in Figure 35 shows a friction circle (centered about the center of the stereonet) and a daylighting envelope. The friction circle was drawn assuming a friction angle of 32 degrees. Fracture poles that are outside the friction circle and inside the daylighting envelope are susceptible to plane sliding. For each of the three sections, Figure 5 shows that a subset of the mylonite seams are the primary discontinuities that fall within the plane sliding criterion. This agrees with the large plane failures that have occurred at the site, such as the one shown in Figure 31.

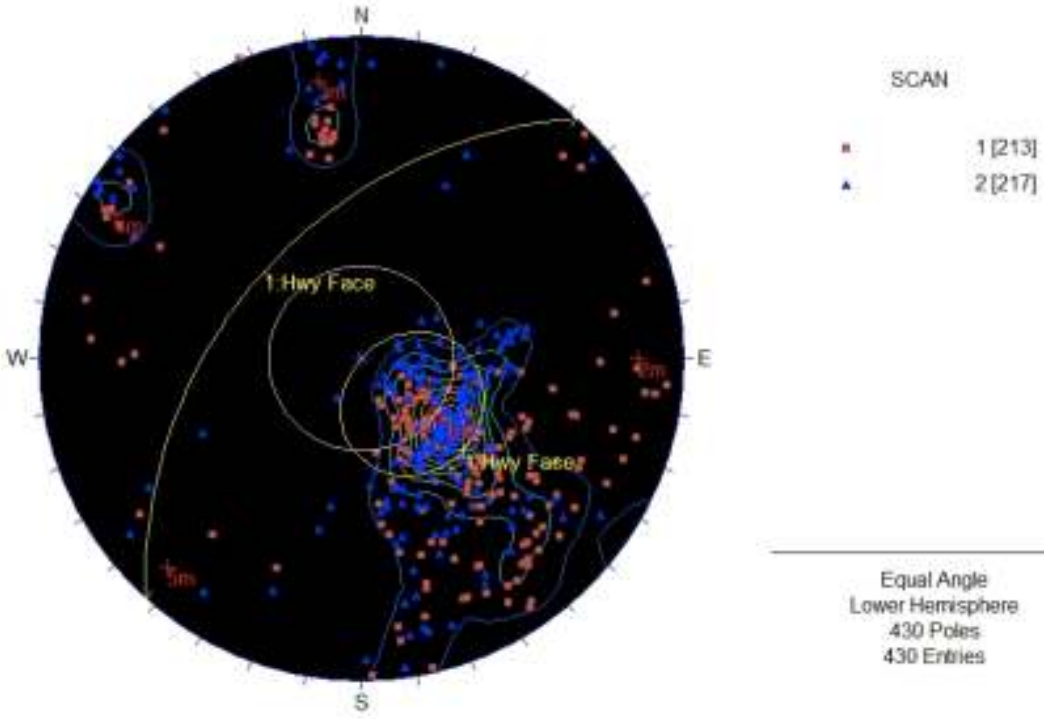

Figure 35a. Analysis of plane sliding at the New Hampshire site, Woodstock1-Woodstock2 combined.

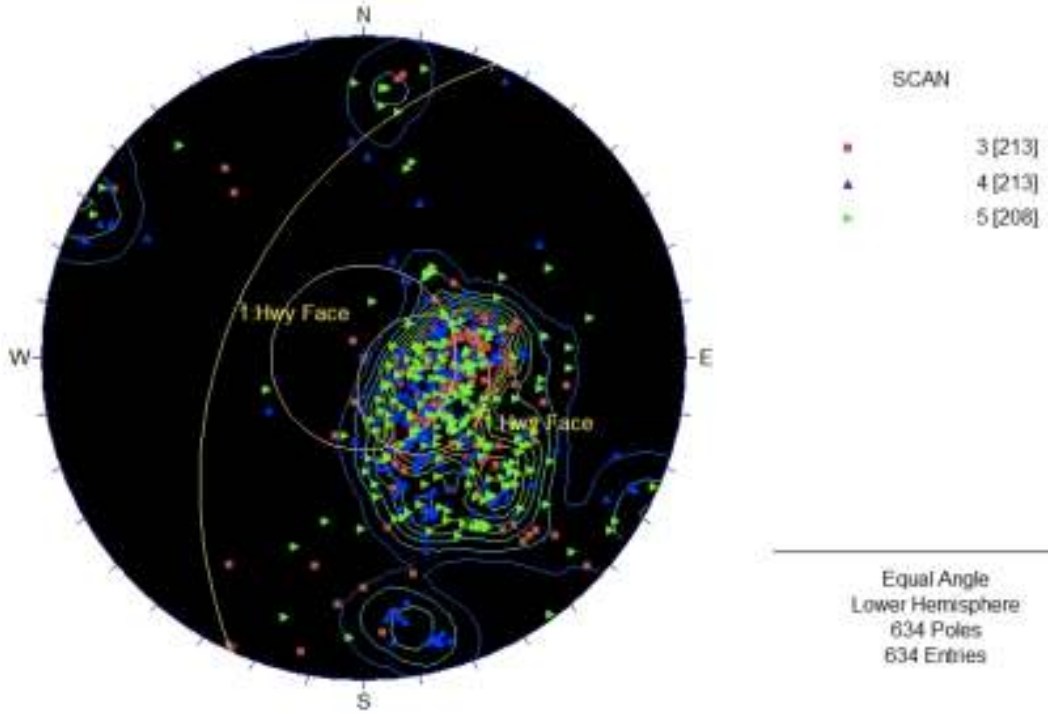

Figure 35b. Analysis of plane sliding at the New Hampshire site, Woodstock3-Woodstock5 combined.

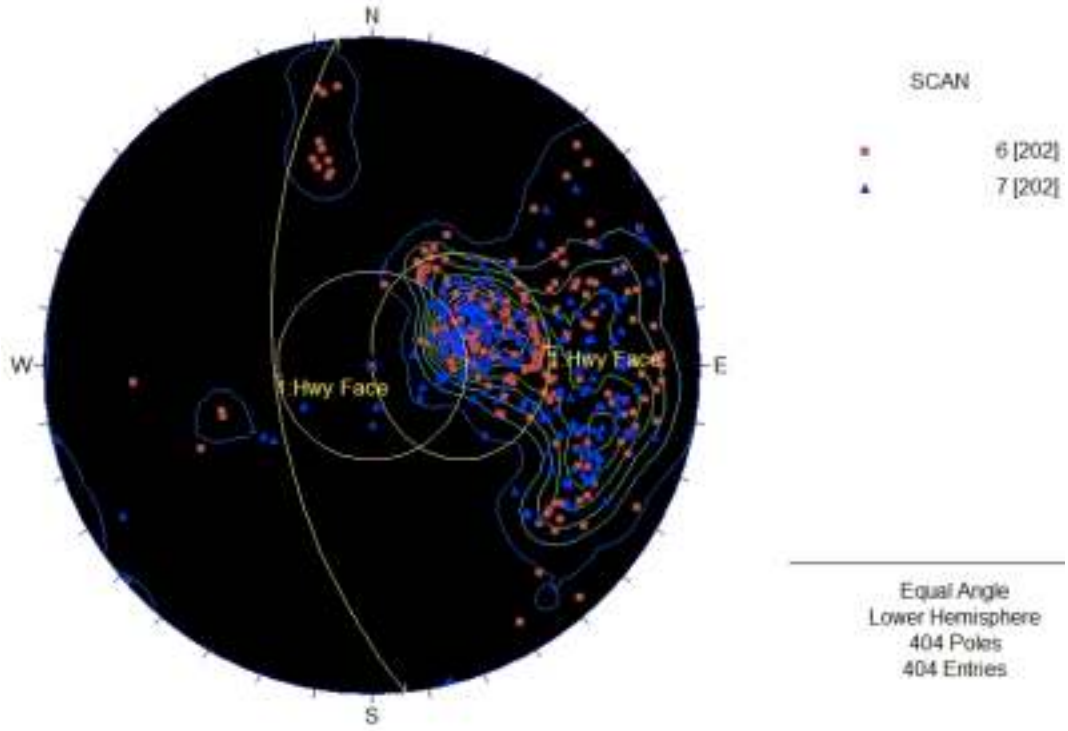

Figure 35c. Analysis of plane sliding at the New Hampshire site, Woodstock6-Woodstock7 combined.

The Rocscience Swedge modeling program was used to analyze wedge failure. For a given point cloud section, every possible combination of joint set pairs was analyzed for possible wedge failure. In the section containing Woodstock6-Woodstock7, for example, there are five joint sets resulting in 10 possible joint set pairs. For each joint set pair, the probability of wedge failure was calculated twice, once assuming dry (no water pressure) and once assuming wet (fractures filled with water) conditions. Dry conditions are shown in red and wet conditions are shown in blue. A friction angle of 32 degrees and zero joint cohesion were assumed. Additional parameters – the mean dip, mean dip direction, and Fisher constant – are given for each joint set in Table 16. The results are shown in terms of the probability of wedge failure for every possible joint set pair. Probabilities of failure can range from 0 to 100 percent, and a probability of failure greater than 20 or 30 percent indicates likelihood for wedge failure to occur. Table 17 shows that the section containing Woodstock6-Woodstock7 (the south end of the slope) has the highest probabilities of failure of the three sections. The high probabilities of failure in this section are coming from Joint Set 1 (mylonite seams) and Joint Sets 2 and 5 (joints). This agrees with the wedge failures shown in Figure 31, which are bounded by these three sets.

Table 17. Probabilities of Failure for Wedge Sliding

NH1&2 Swedge Slope Stability Analysis ϕ=32°					
Prob of Failure (Dry/Wet)					
Joint Set	1	2	3	4	5
1		33.42%	32.60%	9.80%	59.73%
2	12.50%		0.00%	0.06%	0.10%
3	11.20%	0.00%		0.04%	0.03%
4	3.03%	0.00%	0.00%		0.00%
5	2.37%	0.02%	0.00%	0.00%	

NH3-5 Swedge Slope Stability Analysis ϕ=32°				
Prob of Failure (Dry/Wet)				
Joint Set	1	2	3	4
1		10.91%	46.91%	48.28%
2	1.70%		0.00%	0.01%
3	14.40%	0.00%		17.83%
4	13.04%	0.00%	0.00%	

NH6&7 Swedge Slope Stability Analysis ϕ=32°					
Prob of Failure (Dry/Wet)					
Joint Set	1	2	3	4	5
1		66.09%	10.46%	17.55%	80.76%
2	49.11%		0.04%	0.24%	37.41%
3	5.85%	0.01%		3.69%	0.00%
4	11.32%	0.23%	0.00%		0.03%
5	52.82%	11.72%	0.00%	0.03%	

Analysis of Rockfall

Slope profiles can be generated from the point clouds to analyze the rockfall hazard associated with rock slopes. In this project, two types of analyses were conducted from the slope profiles. First, the OHF was calculated to indicate likely locations and sizes for rockfall events at a particular location. Second, the profiles were used to determine rockfall trajectories for those locations using programs such as the Colorado Rockfall Simulation Program (Jones et al. 2000). For this project the research team used the Rocscience program RocFall to determine rockfall trajectories (Rocscience 2010).

Details on the calculation of the OHF are given in the Analysis of Rockfall from Cross Sections section of the Arizona chapter of this report. OHFs greater than 4 or 5 percent indicated a possible rockfall hazard. As an example, Figure 36 shows a photo of part of the rock scanned in Woodstock6, plus the slope profile produced by making a cross section in the Woodstock6 point cloud. A small overhang is apparent in both the photo and the slope profile, but overall the OHF for this cross section is 1.8 percent, indicating low rockfall potential due to overhangs.

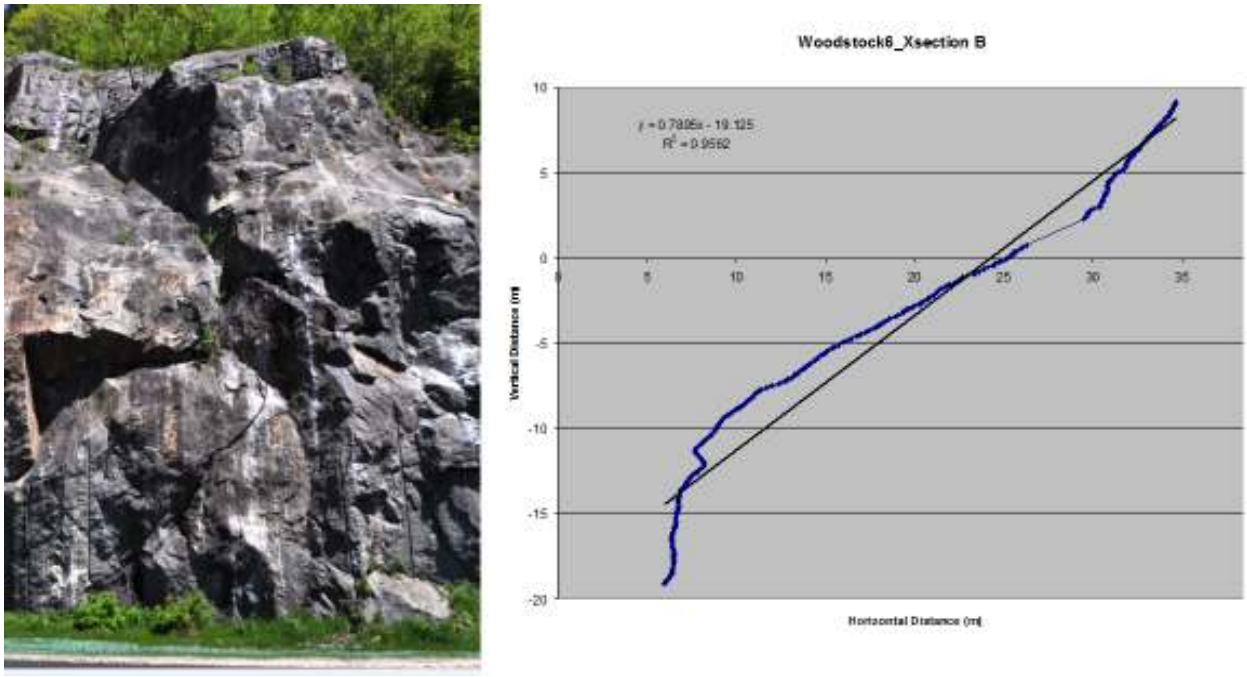

Figure 36. Left to right, a photograph of the Woodstock6 portion of the New Hampshire site, and a slope profile generated from the Woodstock6 scan.

Slope profiles from Woodstock1-Woodstock7 are given in Figure 37, and the OHFs from these profiles are given in Table 18. Overall, all OHFs are less than 4 percent except for one cross section in Woodstock7, indicating low potential for rockfall due to overhangs at the New Hampshire site.

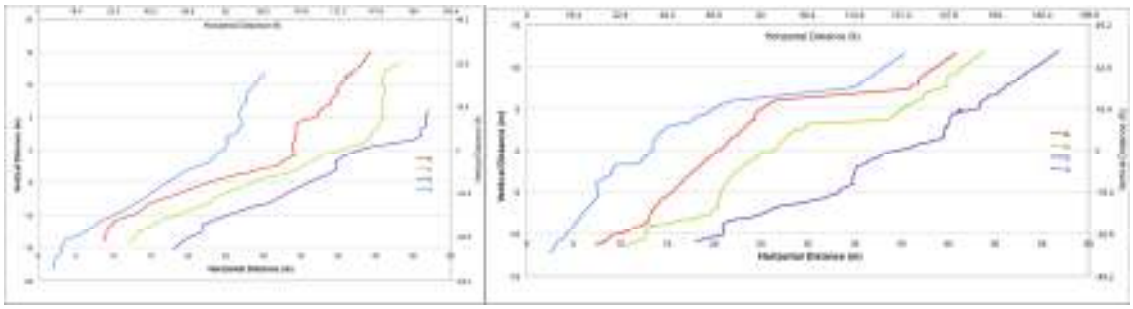

Figure 37a-b. Vertical cross sections for, left to right, a) Woodstock1 and b) Woodstock2.

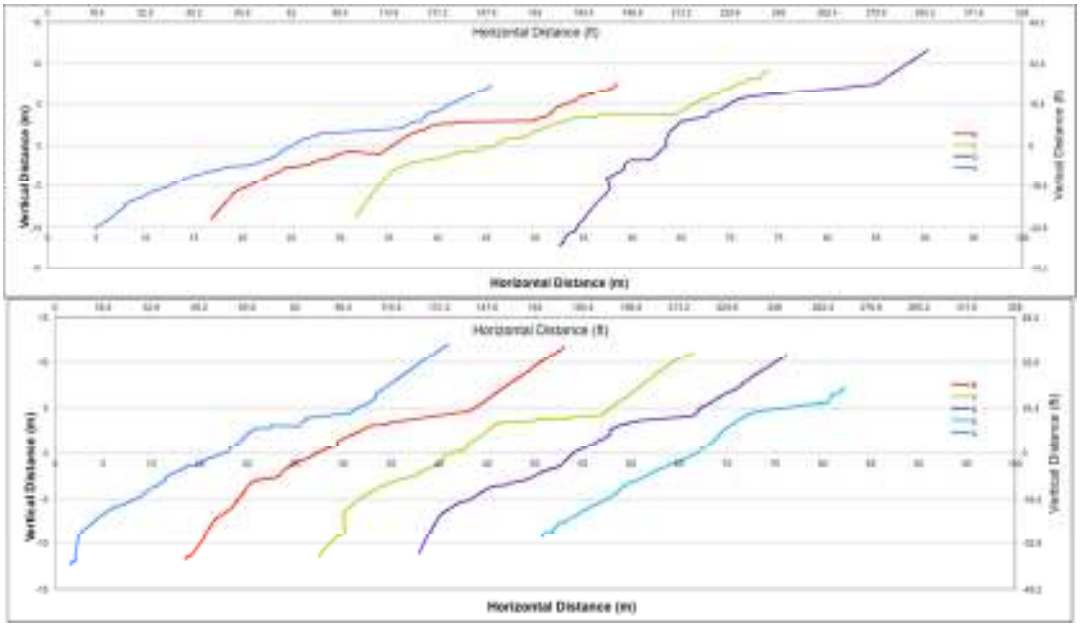

Figure 37c-d. Vertical cross sections for, top to bottom, c) Woodstock3 and d) Woodstock4.

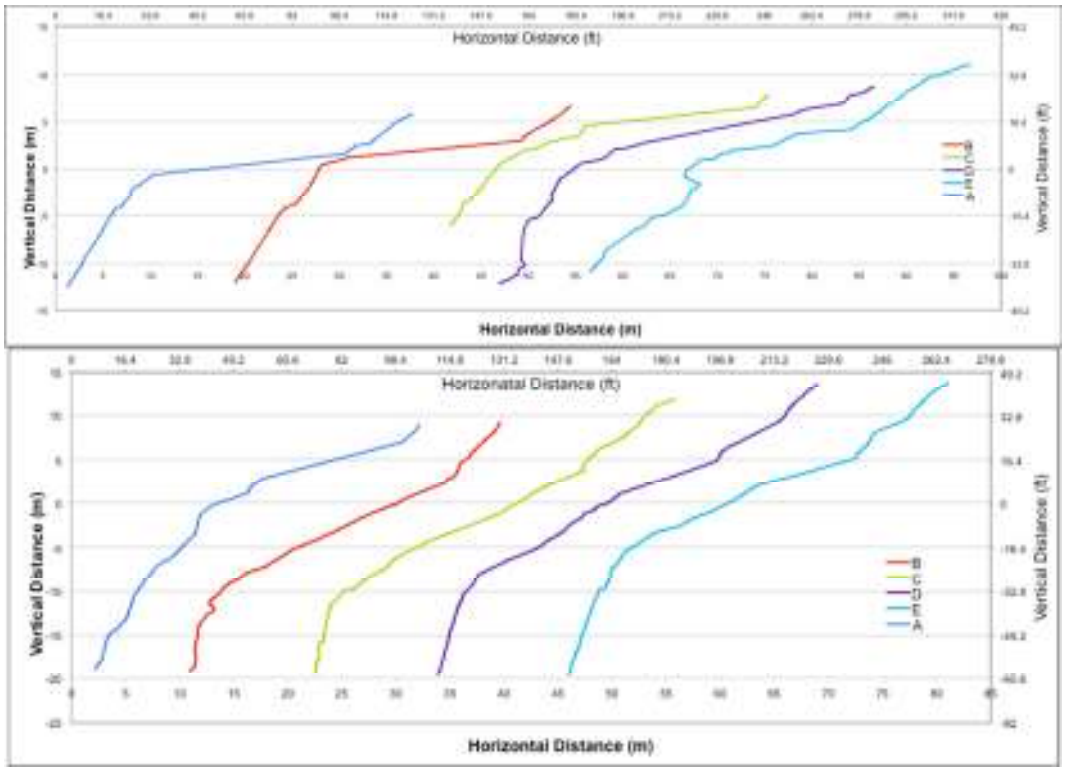

Figure 37e-f. Vertical cross sections for, top to bottom, e) Woodstock5 and f) Woodstock6.

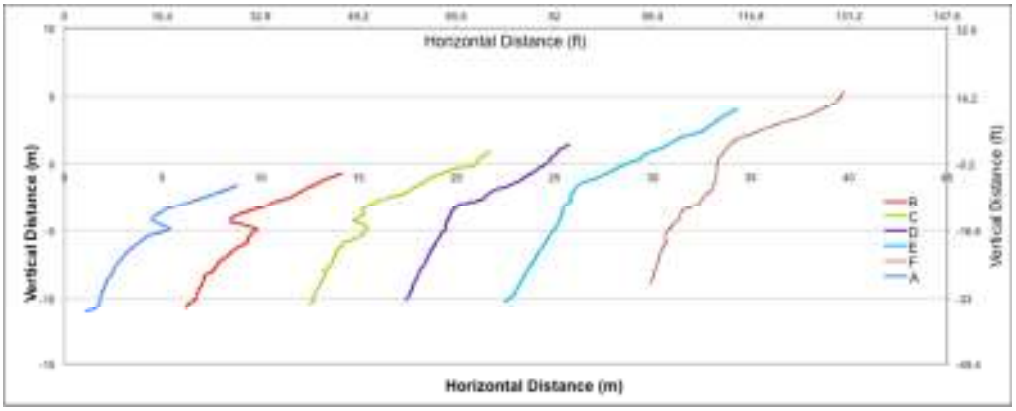

Figure 37g. Vertical cross sections for Woodstock7.

Table 18. OHFs for the Cross Sections Shown in Figure 37

Section	Woodstock 1	Woodstock 2	Woodstock 3	Woodstock 4	Woodstock 5	Woodstock 6	Woodstock 7
A	2.0	1.2	1.7	0.1	0	0.1	1.7
B	2.65	1.2	1.7	0	0	1.8	4.1
C	2.77	0.6	0.55	0.8	0	0.7	2.6
D	1.83	0.9	1.2	0.1	2.1	0	0.2
E				0.7	2.2	0.3	0.3
F							0.6

Figure 38 shows rockfall trajectories calculated using the Rocscience RocFall program, using cross section B from Woodstock6. A block size of 50 kg (110 lbs) was assumed. The impact and rebound properties for a hard unweathered rock were assumed. The properties of a soft soil were assumed for the ditch properties. Based on these input parameters, 100 trials were simulated with slight variations in the input parameters; the results are shown in Figure 38. The results indicate that there is a high probability that a falling rock could enter the roadway.

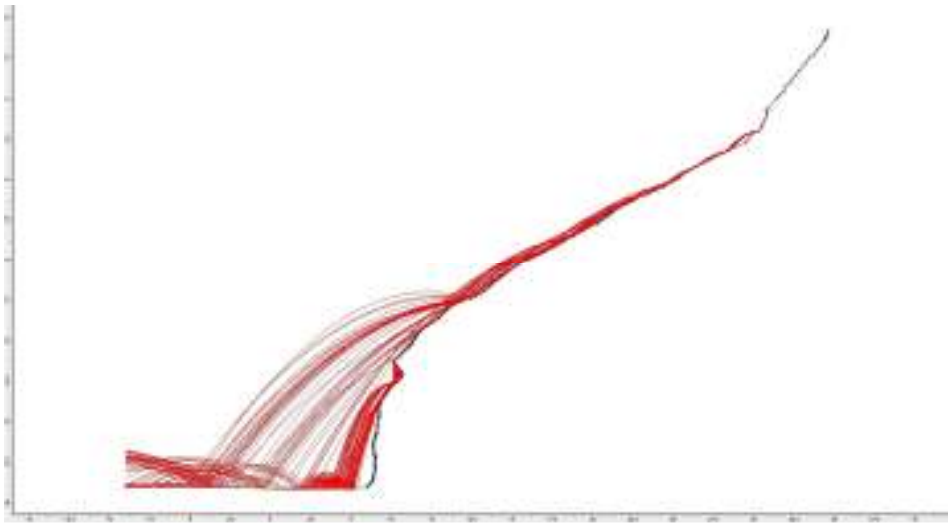

Figure 38. Trajectories for a 50-kg (110 lbs.) block in the Woodstock6 point cloud using the Rocscience RocFall program.

8. NEW YORK

This chapter discusses scanning that took place in New York as part of the LIDAR pooled fund project, as well as the results of analyzing the New York scans.

OVERVIEW OF THE NEW YORK SITE

The New York site for the pooled fund study is a rock slope on the north side of the westbound lanes of New York State Route 5 at the border of Schenectady and Montgomery counties. SR 5 follows the Mohawk River at this location and the site is about 15 mi from Schenectady. The rock slope is approximately 230 m (754 ft) long and ranges in height from 14 to 27 m (46 to 88.6 ft). The rock at the site is a horizontally bedded Ordovician limestone with near vertical jointing. The horizontal bedding varies from very thin to several feet in thickness. The site is near an old fault line; thus, large joints cut diagonally across the rock face. The major causes of failures at this site are sliding, toppling, and raveling failures mostly due to seasonal freeze-thaw events. A picture of the southern part of the slope is shown in Figure 39.

Figure 39. Southern section of rock slope at New York site showing the difference between pre-split (right) and conventional blasting (left).

The excavation of the rock slope used both conventional blasting and pre-split blasting. The rock in the westernmost part of the slope is in Schenectady County and was pre-split, while the rock in the remainder of the slope is in Montgomery County and was excavated using conventional blasting and benches. Today, a major difference can be seen between the integrity of the pre-split slope and that of the conventionally blasted slope, as shown in Figure 39. Pre-splitting the rock created a much smoother face that is holding up very well over time, while the conventionally blasted slope has become damaged and is subject to ongoing slope failure and

rockfall. A rockfall fence has been installed in front of the conventionally blasted slope, as shown in Figure 39.

LIDAR scanning and point cloud processing of the New York site were conducted as part of the pooled fund project. New York State DOT (NYSDOT) hoped to learn several things from the scanning and analysis of results. First, the time required and cost of scanning and processing the point clouds would be compared with the time required and cost of conventional NYSDOT techniques. Second, NYSDOT was interested in quantifiable parameters that can be extracted from LIDAR scanning to evaluate geologic structure (i.e., stereonets) and the likelihood for slope failure and rockfall. Third, the LIDAR scanning would be used by NYSDOT to evaluate recut or scaling of the slope.

LIDAR SCANNING AT THE NEW YORK SITE

A team from the Department of Mining and Geological Engineering at the University of Arizona performed LIDAR scanning of the New York site on May 11, 2010. Scanning was conducted using an Optech ILRIS3D time-of-flight scanner as shown in one image in Figure 40. Seven scans were taken, referred to as Mohawk 1 through Mohawk7, and details of these scans are given in Table 19. Scans were taken about every 33 m (108 ft) down the slope with about 20 percent overlap on each side, as shown in the second image of Figure 40. An unregistered point cloud of the entire slope was produced from the seven scans that contained about 8.6 million points, but analysis was conducted on each scan individually. Scan times ranged from about 12 min (Mohawk2) to about 20 min (Mohawk5), and in total about 3.5 hrs were spent at the site. The point spacing in the scans ranges from about 1.2 cm (.47 inch) at the bottom of the slopes to 2.5 cm (1 inch) at the top of the slopes. It should be noted that the viewing window was unable to capture the entire slope for the scans at the site due to limited room to place the instrument. The bottom 5-10 m (16.4 to 32.8 ft) of the scan was not captured, so the listed slope heights are smaller than the actual heights.

In addition to the scans, a high-resolution digital image was taken at each of the seven locations using a Nikon D90 12 MP digital camera. These digital images were then draped over the point clouds to produce color point clouds. Figure 41 shows the color point cloud from Mohawk1. At the time of the scanning, a number of locations were marked for surveying, and these points were surveyed by NYSDOT during the week following the scanning. The point clouds were registered using readings taken from a Brunton compass. The compass was used to measure the up-down and left-right tilts as well as the bearing of the scanner. Magnetic declination for the area was noted and adjustments were made in the Rocscience program Dips. The Split-FX stereonets represent the raw data and were not adjusted for the magnetic declination, but the data in the tables show the corrected results.

Table 19. Scan Information for the New York Site

Scan	Number of Points	Scan Time (approximate)	Average Slope Information*			
			Length (m)	Height (m)	Dip	Dip Direction
Mohawk1	854,704	13 minutes	23	14	57.8	222.8
Mohawk2	765,350	12 minutes	21.1	15.4	58.7	247.2
Mohawk3	1,468,579	19 minutes	30.7	24	47.8	235.5
Mohawk4	1,526,312	20 minutes	38.8	22.4	49.95	239.2
Mohawk5	1,561,891	20 minutes	38.8	25.8	58.5	236.8
Mohawk6	1,319,869	18 minutes	39	27.1	58.8	238
Mohawk7	1,165,306	17 minutes	38.7	24.9	54.6	244.7
Total	8,662,011	2 hours	Ave 32.9	Ave 21.9	Ave 55.2	Ave 237.7

*Slope height is measured from top of slope to bottom of scanning window and cuts off the bottom 5-10 m (16.4 to 32.8 ft) of the slope

Figure 40. Left to right, an example of scanning at the site using an Optech ILRIS 3D scanner, and the approximate locations of scans Mohawk1 to Mohawk7.

Figure 41. Color point cloud of the Mohawk1 LIDAR scan.

POINT CLOUD PROCESSING OF SCANS FROM THE NEW YORK SITE

For the New York site, point cloud processing was conducted for three main types of analysis, as described below.

Rock Mass Characterization

Important attributes of the geologic structure are extracted from the point clouds, including discontinuity orientation and spacing. The orientation results are plotted on a stereonet and the primary joint sets are determined.

Figures 42a to 42g are lower hemisphere stereonet plots of delineated fractures from Mohawk1 through Mohawk7, respectively. Also, joint sets in each of the stereonets are shown. As an example, statistical joint set information for Mohawk7 (average dip, average dip direction, Fisher constant, average spacing) is given in Table 20.

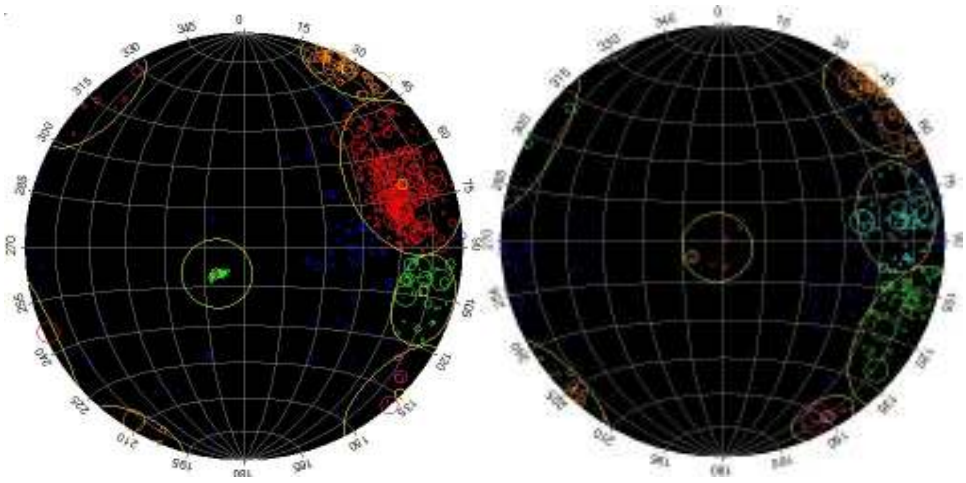

Figure 42a-b. Lower hemisphere stereonet plots for the discontinuity orientations extracted from LIDAR scans of, left to right, a) Mohawk1 and b) Mohawk2.

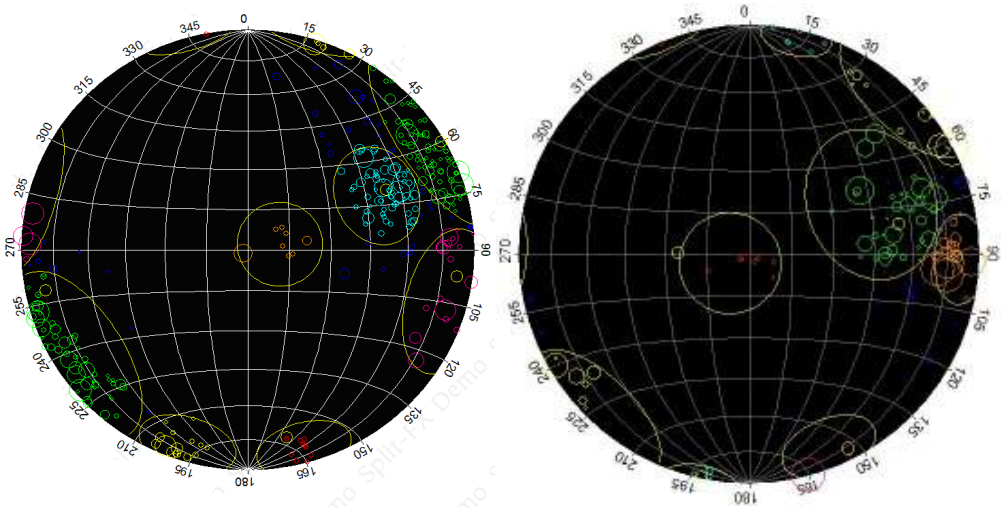

Figure 42c-d. Lower hemisphere stereonet plots for the discontinuity orientations extracted from LIDAR scans of, left to right, c) Mohawk3 and d) Mohawk4.

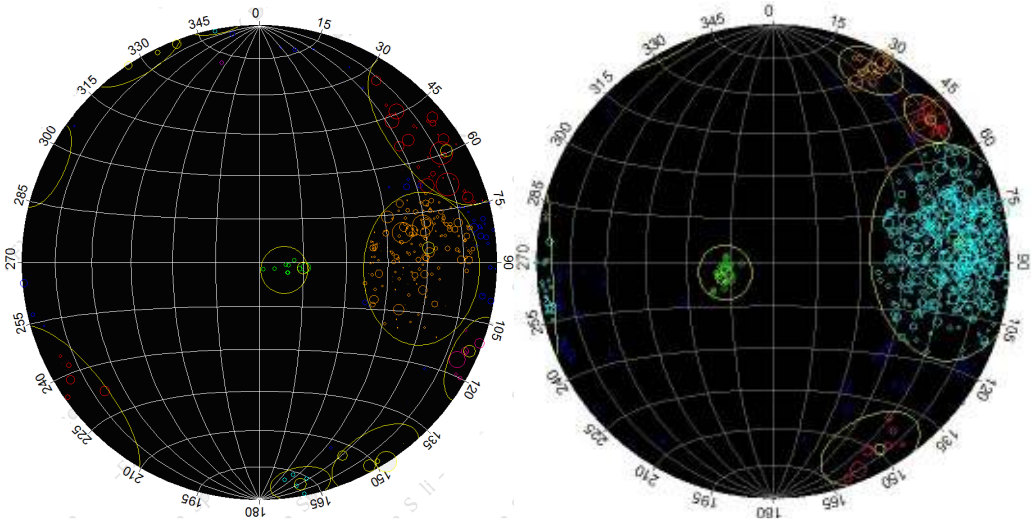

Figure 42e-f. Lower hemisphere stereonet plots for the discontinuity orientations extracted from LIDAR scans of, left to right, e) Mohawk5 and f) Mohawk6.

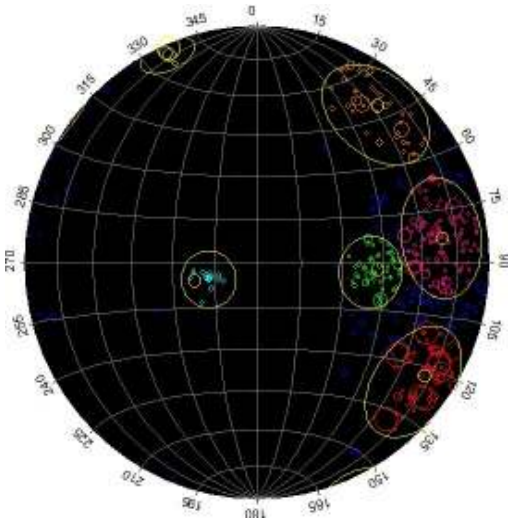

Figure 42g. Lower hemisphere stereonet plot for the discontinuity orientation extracted from LIDAR scan of Mohawk7.

Table 20. Average Results for the Joint Sets in Mohawk7

Set	Average Dip	Ave. Dip Dir.	Fisher Constant	Ave. Joint Spacing
1 (red)	78.40	279	67.1	1.11
2 (pink)	74.94	190.74	63.39	0.59
3 (green)	45.44	245.99	75.87	0.49
4 (blue)	16.94	47.16	721.29	0.27
5 (orange)	70.44	239.17	43.71	0.54
6 (yellow)	84.67	131.67	371.85	0.92

Figure 42 shows that the geologic structure is similar between the different scans, even though there are also some differences from scan to scan. A common structural feature seen in all the scans are the sub-horizontal bedding planes, with average orientations differing slightly from scan to scan. The other primary geologic structures are the sub-vertical joints. The combination of the sub-vertical joints and the sub-horizontal bedding results in blocks that can be as large as 1 m^3 but more often results in small blocks that pose a rockfall hazard. Figure 42 shows that the orientation of the sub-vertical joints differs from scan to scan. Discontinuities subparallel to the slope face are also seen in the stereonets. The slope has an average dip direction of about 240 degrees, as shown in Table 19. Many of these discontinuities may be blasting fractures, as they are parallel to the strike and the dip of the overall slope.

Blocks are formed by the combination of bedding planes and two vertical joint sets, and because the bedding plane spacing is often 0.4 m (1.32 ft) or less (see Table 40), many small blocks are formed that create a rockfall hazard. The analysis of rockfall is discussed in the next section.

Analysis of Rockfall from Cross Sections

To analyze the rockfall hazard associated with rock slopes, slope profiles can be generated from the point clouds. This report describes two types of analyses that were conducted from the slope profiles. First, the OHF was calculated to indicate likely locations and sizes for rockfall events at a particular site. Details on the calculation of the OHF are given in the Point Cloud Processing of the Scans from the Arizona Site section of the Arizona chapter. Second, the profiles were used to determine rockfall trajectories for those locations using the Rocscience program, RocFall (Rocscience 2010). Other programs, such as the Colorado Rockfall Simulation Program (Jones et al. 2000), can also be used for rockfall analysis. Rocscience Rocfall was chosen for its availability at the University of Arizona.

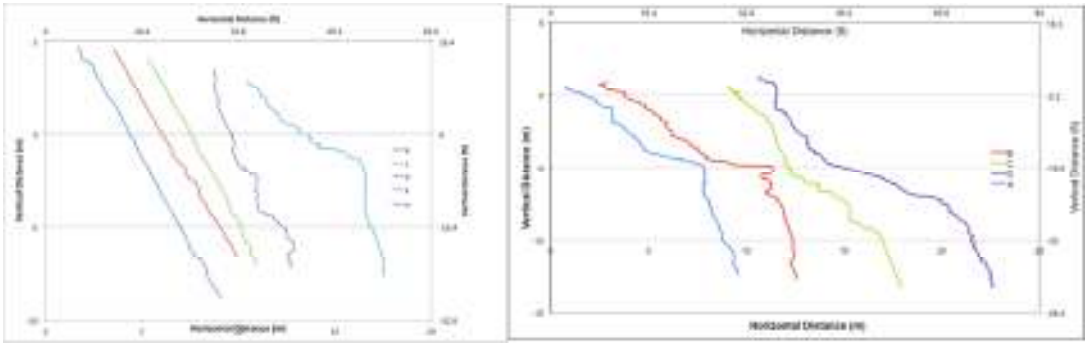

Figure 43a-b. The slope cross sections from Mohawk1 (left) and Mohawk2 (right).

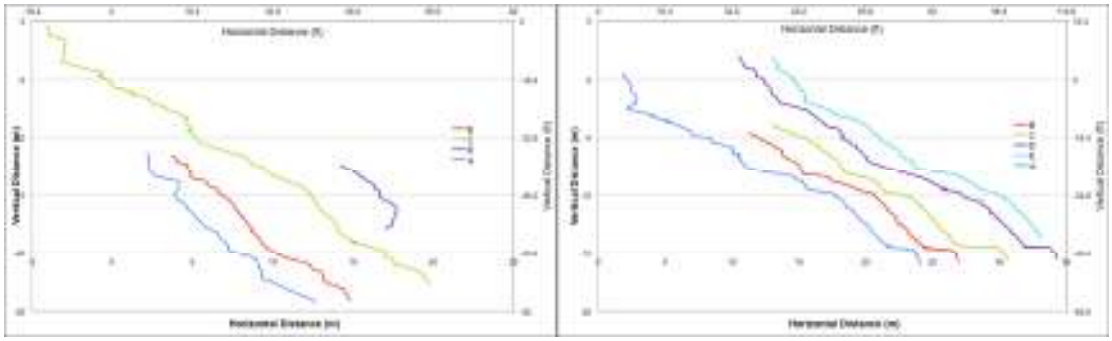

Figure 43c-d. The slope cross sections from Mohawk3 (left) and Mohawk4 (right).

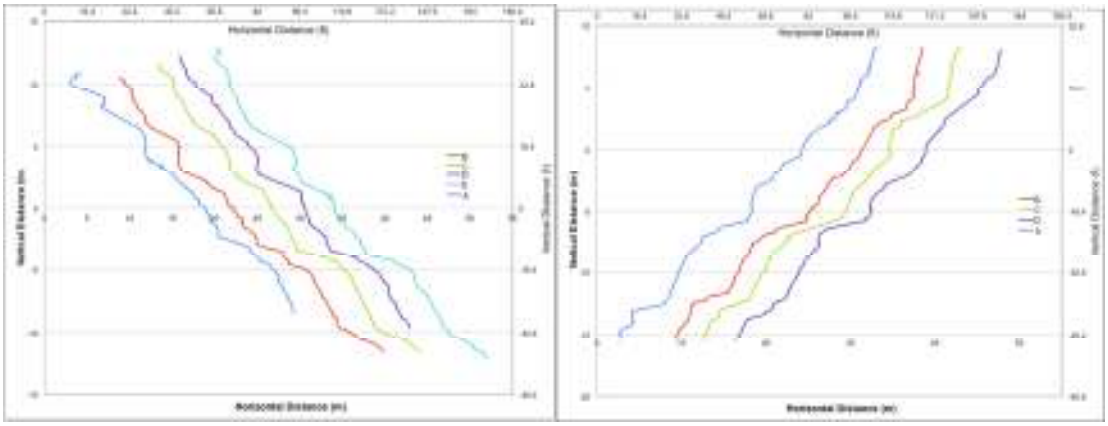

Figure 43e-f. The slope cross sections from Mohawk5 (left) and Mohawk6 (right).

Figure 43g. The slope cross sections from Mohawk7.

Figures 43a to 43g present vertical cross sections from Mohawk1-Mohawk7, respectively. Figure 43a shows very clearly the difference between pre-split slopes (Sections A to C) compared with non-pre-split slopes (Sections D and E). Cross sections with prominent overhangs are seen in Figure 43b and 43g. Figure 44 shows details associated with Cross Section B in Mohawk2 (Figure 43b).

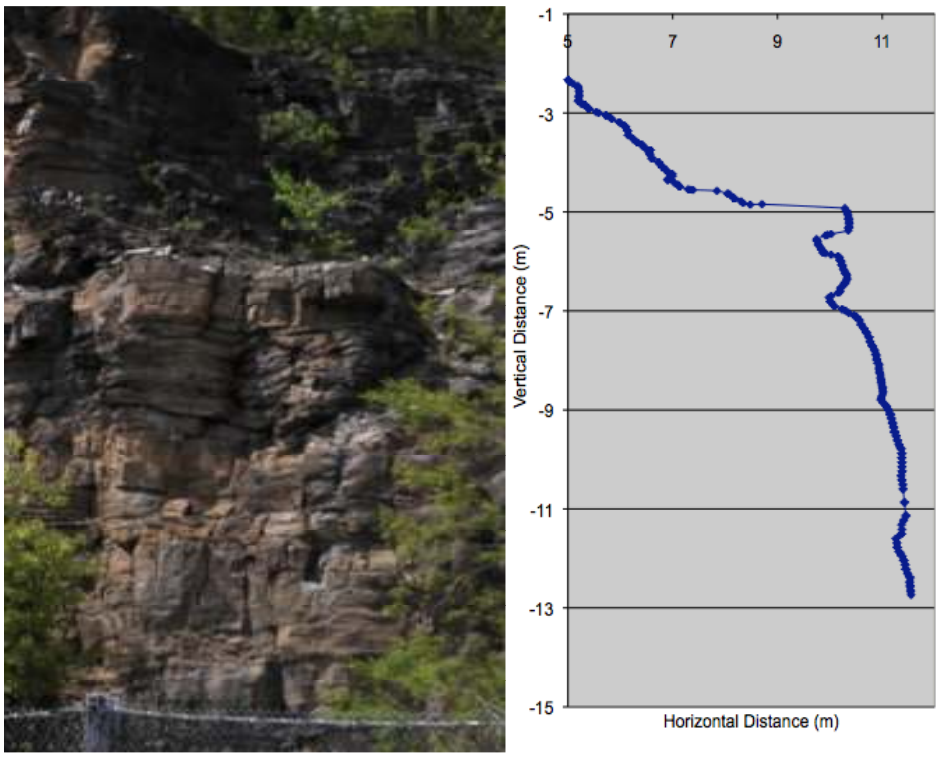

Figure 44. Left to right, a photo of a portion of the New York site, and a slope profile generated from the Mohawk2 scan.

The OHF is a measure of the amount of overhangs that occur along a given cross section (details of the calculations are explained in the Analysis of Rockfall from Cross Sections section of the Arizona chapter of this report). Table 21 gives the OHFs for the cross sections shown in Figure 43. From experience, OHFs greater than 4 percent indicate a hazard from rockfall. Most of the scans have cross sections with OHFs over 4 percent, indicating that rockfall is a potential hazard, which is consistent with site observations.

Table 21. OHFs for the Cross Sections Shown in Figure 43

Section	Mohawk1	Mohawk2	Mohawk3	Mohawk4	Mohawk5	Mohawk6	Mohawk7
A	0	1.89	2.1	2.99	6.5	2.2	0.8
B	.15	4.72	0.28	0.30	1.4	1.2	4.5
C	.44	1.97	3.2	0.09	0.26	1.9	0.36
D	3.88	1.98	10.0	0.34	2.4	0.76	0.42
E	2.23			0.40	4.3		

A special rockfall issue at the New York site was an overhanging block that was captured in Cross Section A in Mohawk4. In this cross section a large block is overhanging near the top of the slope. Figure 45a shows a photo of the slope with an arrow pointing to the large overhanging block. Figure 45b shows a close-up of the point cloud of the overhanging block. From the point

cloud, it was determined that the large block has dimensions of about 4 m x 3 m (13 ft x 10 ft) with a 1.2 m (4 ft) overhang. Also, a small block that has moved can be seen in the lower left with dimensions of about 0.7 m x 0.4 m x 0.4 m (2.3 ft x 1.3 ft x 1.3 ft), and several small blocks are being held up by rock bolts. The block is about 30 m (98 ft) above the highway. The scans taken have cut off approximately the bottom 5-10 m (16.4 to 32.8 ft) of the rock slope due to limitations of scanner placement on the side of the road. Figure 45c shows the slope profile, which shows the overhanging block with an OHF of about 3 percent.

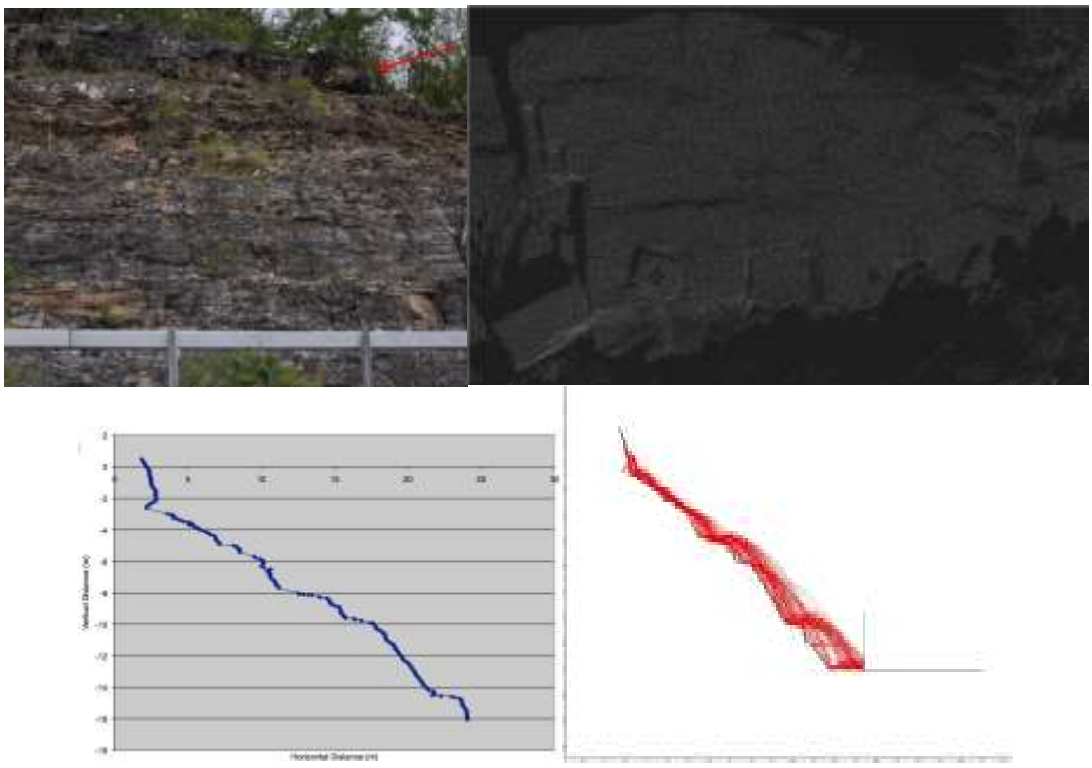

Figure 45. Upper left, a) an overhanging block in a scan of Mohawk4; upper right, b) a point cloud of the block; lower left, c) a slope profile of the block; and lower right, d) the trajectories of the block using the Rocscience RocFall program.

Figure 45d shows rockfall trajectories for this block calculated using the Rocscience RocFall program. A block size similar to the small block in the lower left of Figure 45b was assumed. The impact and rebound properties for a hard unweathered rock were assumed. Also, a ditch and fence were placed at the bottom of the slope and the properties of a soft soil were assumed for the ditch properties. Based on these input parameters, 100 trials were simulated with slight variations in the input parameters; the results are shown in Figure 45d. The results indicate that there is a high probability that the block will hit the fence but a 0 percent probability that a rock will land on the highway.

The trajectory model for the New York site can be calibrated using a past rockfall event. Previous to the scanning visit in May 2010, a rock block had fallen in the area of the Mohawk7 scan and hit the rockfall fence. Figure 46a shows the rock block behind the fence and also

indicates where the rock block hit the fence. Using the same material parameters as in Figure 45d and using the slope profile from Mohawk 7 (and assuming the boulder initiated near the top of the slope), Figure 46b shows the results of 100 trials. It shows a high probability of the boulder hitting the lower part of the fence, which is consistent with the photo.

Figure 46. Comparison of an actual rockfall event (left) with the RocFall trajectory modeling results (right).

Analysis of Slope Stability

A slope stability analysis for the New York site was conducted using the discontinuity orientation information obtained from the point clouds and discussed previously (see Figure 42 and Table 20). There are many slope stability programs available for the analysis of plane and wedge failure. Here are used the Rocscience Swedge program (Rocscience 2010).

Wedge failure was not expected to be a major issue at this site, since the structure is mostly horizontal bedding planes and near-vertical joints. As an example, the report considers the results from Mohawk7 shown in Figure 42g and Table 20. Table 20 shows that there are six joint sets, one of which (Set 3) is parallel to the rock face. For each joint set, the mean dip, mean dip direction, and the Fisher constant have been calculated, as shown in Table 20. The Fisher constant is a measure of the amount of scatter in the poles; the lower the Fisher constant the more scatter in the poles. The Rocscience Swedge program considers two joint sets at a time and searches for unstable wedges formed from the combination of these sets and the orientation of the free face. To produce a wedge, it randomly picks an orientation from each set and calculates the factor of safety. It does this 10,000 times for each pair of discontinuity sets. The probability of failure is the percentage of trials that results in a failed wedge. There are six discontinuity sets in Mohawk7, but since one set is parallel to the face (Set 3), slope stability calculations were conducted on the other five sets and the average rock face orientation (with a dip of 54.6 and a dip direction of 244.7). A friction angle of 35 degrees was used.

The wedge sliding results are presented in Table 22. Probabilities of failure can range from 0 to 100 percent, and a probability of failure greater than 20 or 30 percent indicates likelihood for wedge failure to occur. Table 22 shows that all probabilities of failure (wet and dry) are less than

6 percent, indicating that wedge failure is not a primary mechanism for slope failure at the New York site. This is also supported by field observations at the site.

Table 22. Probabilities of Failure for Wedge Sliding

New York Swedge slope stability analysis Φ=35 degrees					
Dry (red) / Wet (blue)					
Joint Set	**1**	**2**	**4**	**5**	**6**
1		.55	0	1.37	5.82
2	0.54		0	3.06	0.34
4	0	0		0.8	0
5	1.01	1.79	0.04		2.9
6	0	0.09	0	2.17	

9. PENNSYLVANIA

This chapter discusses scanning that took place in Pennsylvania as part of the LIDAR pooled fund project, as well as the results of analyzing the Pennsylvania scans.

OVERVIEW OF THE PENNSYLVANIA SITE

The Pennsylvania site for the pooled fund study is a rock slope along State Road 11/15-351, 2 miles north of New Buffalo, Pennsylvania. The rock slope is approximately 560 ft long and ranges up to 130 ft in height. It is located along a slight curve or the road and the highway slope has been excavated within the last 15 years. It is a steep slope with overhang in some areas. Geotechnical surveying using traditional methods is very difficult due to the risk of physical injury to field personnel, particularly for the higher portions of the outcrop.

The geology of the site includes highly strained clastic sedimentary rocks of the Irish Valley Member of the Catskill Formation (Dciv) that are folded into anticlines and synclines that were subsequently displaced along sub-horizontal thrust faults. Dciv is composed of interbedded arkosic sand and shale beds. Well-developed cleavage is common in the shaley horizons and mesoscopic brittle faults are common in the sandy layers. The material variability has resulted in permeability contrasts that are manifested by seeps that undermine portions of the exposure. The competency contrast between the shaley and sandy beds resulted in different dominant mechanisms of strain accomplishment in the exposure. Competent sandy beds accommodate shortening by the development of wedge faults, while the plastic shaley horizons accommodate shortening via cleavage development. The wedge faults and cleavage are not oriented parallel to one another and in places are folded, thus creating a wide range in orientations of planes of weakness. A picture of a portion of the Pennsylvania site is shown in Figure 47.

Figure 47. A portion of the Pennsylvania site.

LIDAR SCANNING OF THE PENNSYLVANIA SITE

Pennsylvania DOT (PennDOT) personnel conducted scanning in January 2009 using a Cyrax time-of-flight scanner. Two registered color point clouds of the entire slope, the North Area scan and the South Area scan, were produced by PennDOT personnel. Each of these scans was broken up into five sections. The sections of the North Area scan are referred to as NA1 through NA5. The sections of the South Area scan are referred to as SAtc (top center), SAtr (top right), SAbl (bottom left) SAbc (bottom center) and SAbr (bottom right). There are several reasons for breaking the slope into sections. First, since the point cloud of the entire slope contains over 3 million points, this allows for manageable subsets of point cloud data. Second, the geologic structure varies along the length of the slope, and this allows geotechnical analysis of subsections of the slope. Details on the point clouds from the five SA sections are given in Table 23.

Table 23. Summary of the South Area Point Clouds

Scan	Number of Points	Average Slope Information			
		Length (ft)	Height (ft)	Dip	Dip Direction
SAtc	267,601	121.9	72.98	72.5	105.3
SAtr	431,797	147.48	65.8	67.9	98.9
SAbr	1,426,353	155.6	44.5	66.7	104.1
SAbc	583,168	113.01	47.5	62.3	104.2
SAbr	614,752	151.4	38.7	57.6	100.5
Overall Slope	3,323,671	560.8	128.5	56	102.8

Figure 48. Left, a portion of the South Area scan, and at right, a portion of the North Area scan.

Portions of the South Area and North Area scans are shown in Figure 48. The point cloud from SAtr is shown in Figure 49 and contains about 430,000 points. The length of this point cloud is about 148 ft and the height ranges up to 65 ft. The average dip of the rock slope in scan SAtr is 67.9 degrees and the average dip direction is 98.9 degrees.

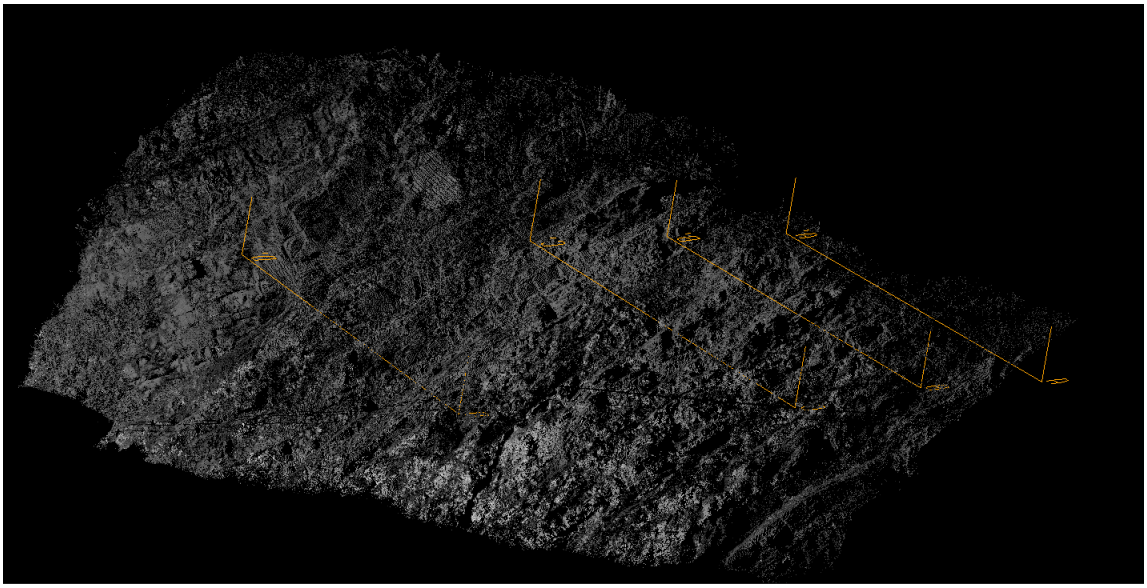

Figure 49. Point cloud of SAtr.

POINT CLOUD PROCESSING OF SCANS FROM THE PENNSYLVANIA SITE

For Pennsylvania, point cloud processing was conducted for three main types of analysis, as described below.

Rock Mass Characterization

Important attributes of the geologic structure, including discontinuity orientation and spacing, are extracted from the point clouds. The orientation results are plotted on a stereonet and the primary joint sets are determined.

The geologic structure at the Pennsylvania site is complex, and it was not possible to combine the geologic structure into a single stereonet. Similarly, it was not possible to make one stereonet of the geologic structure in the South Area and one for the North Area. However, it was possible to combine the data into two groups to represent the geologic structure at the Pennsylvania site. Group 1 combines the fracture data from scans NA1, NA2, SAbl, Satc, and SAtr, and Group 2 combines the fracture data from scans NA3, NA4, NA5, SAbc, and SAbr. Figure 50a shows the combined data representing Group 1, and Figure 50b shows the combined data representing Group 2. For each group, the major discontinuity sets were determined, resulting in four discontinuity sets for Group 1 and six discontinuity sets for Group 2. Figures 50c and 50d are stereonet plots showing the discontinuity sets for Groups 1 and 2, respectively. The joint set information (mean dip, mean dip direction, and Fisher constant) for each of the sets in Group 1

and Group 2 is shown in Table 24. Some fracture poles in Groups 1 and 2 have not been assigned to any of the sets. These are either random orientations not associated with a group of fractures, or fractures parallel to the rock face that appear to be blasting fractures.

Table 24. Discontinuity Set Information for the Pennsylvania Site

Set	Group 1			Group 2		
	Dip	Dip D.	Fisher	Dip	Dip D.	Fisher
1	84	241	33	90	238	48
2	82	329	17	87	90	42
3	65	75	31	29	340	22
4	42	134	24	87	149	72
5				42	106	37
6				57	150	34

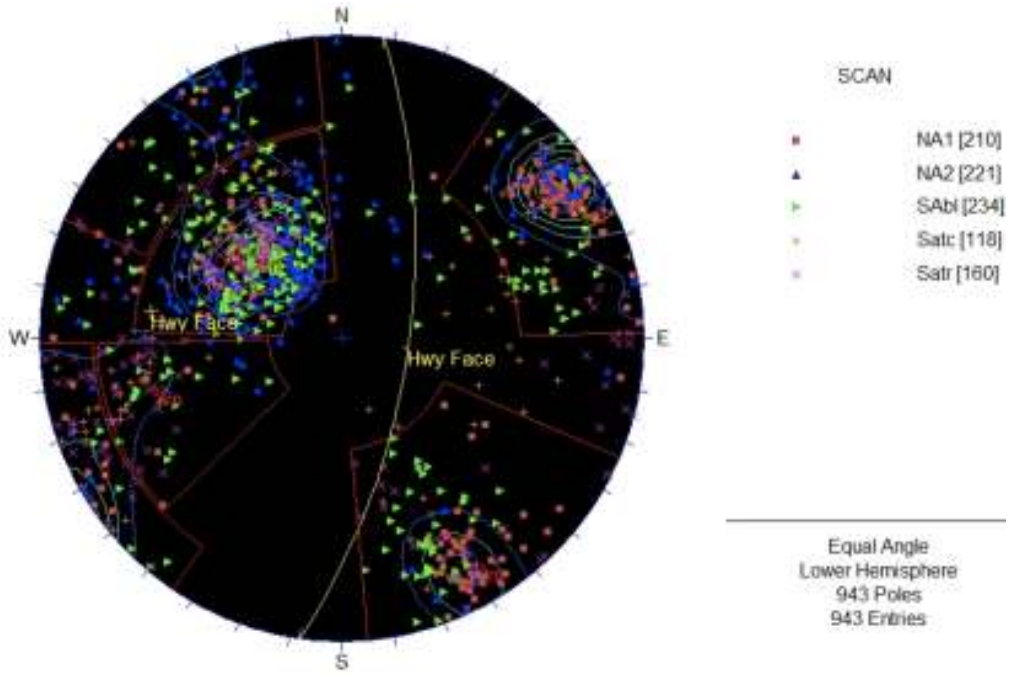

Figure 50a. Lower hemisphere plot of fracture poles from the Pennsylvania site, Group 1 separated by scan.

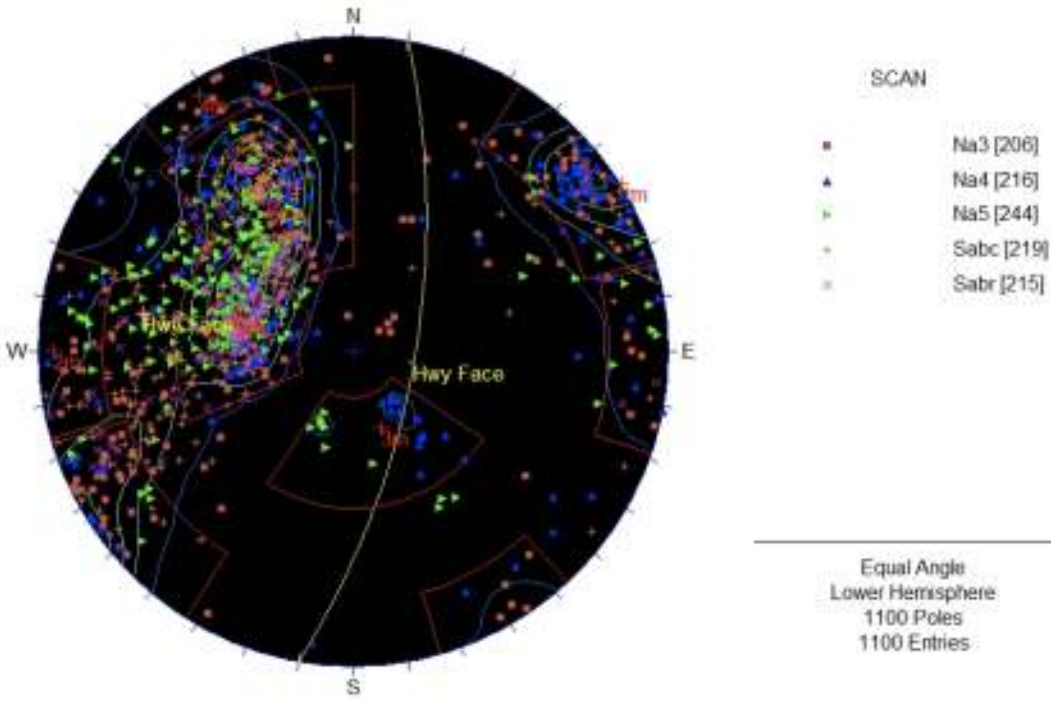

Figure 50b. Lower hemisphere plot of fracture poles from the Pennsylvania site, Group 2 separated by scan.

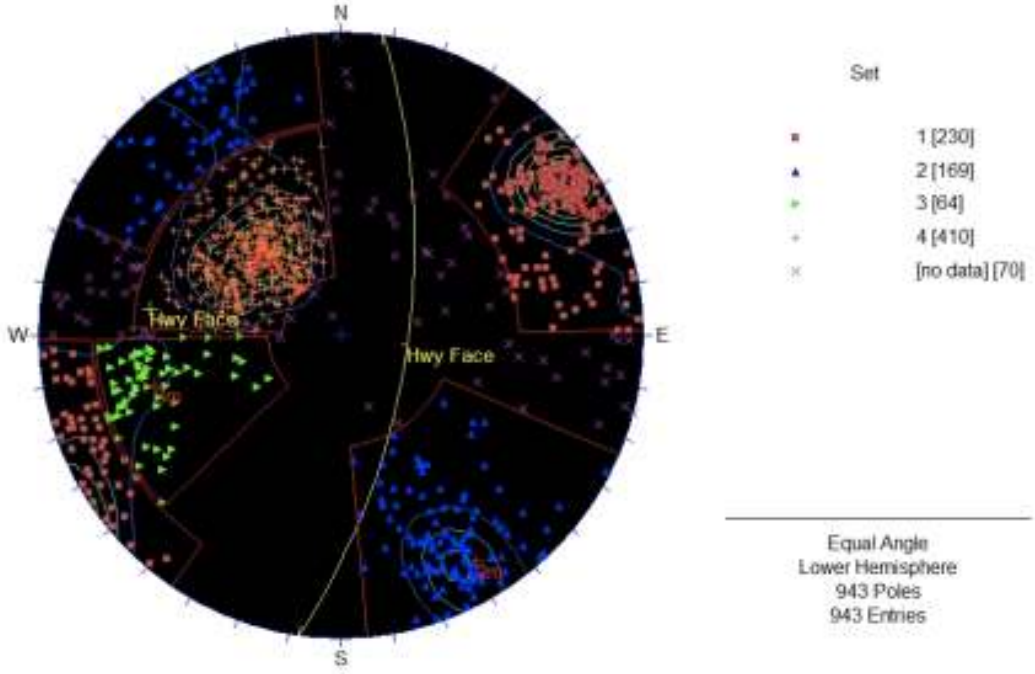

Figure 50c. Lower hemisphere plot of fracture poles from the Pennsylvania site, Group 1 separated by set.

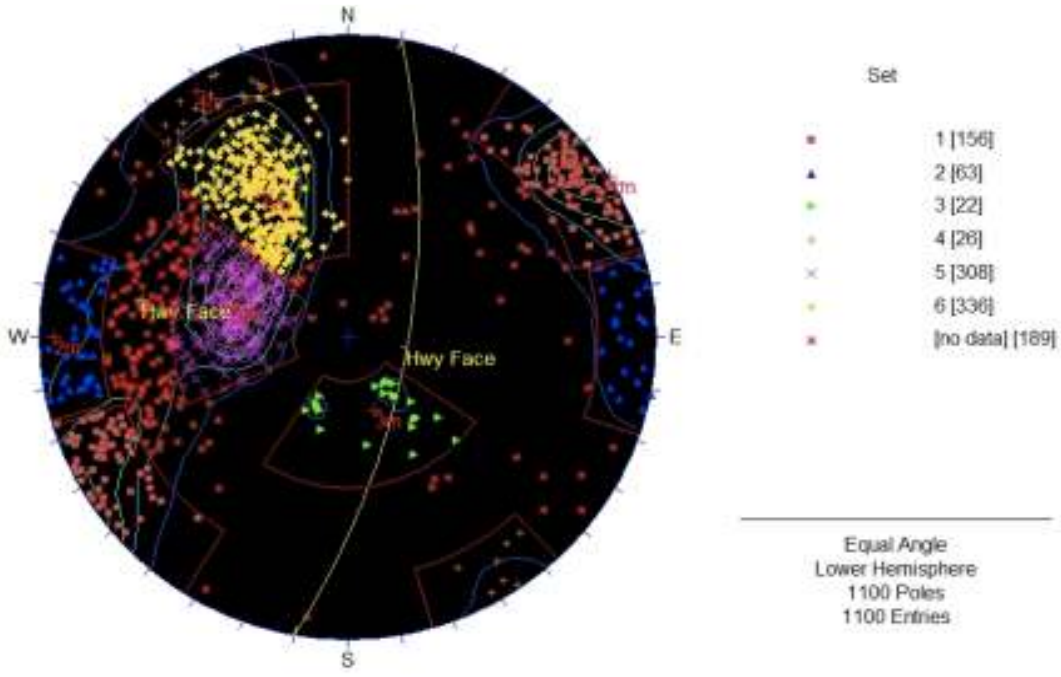

Figure 50d. Lower hemisphere plot of fracture poles from the Pennsylvania site, Group 2 separated by set.

Analysis of Slope Stability

For the Pennsylvania site, a kinematic analysis of plane failure and a probabilistic analysis of wedge failure have been conducted. The plane sliding analysis was conducted using the Rocscience Dips program, and the wedge sliding analysis was conducted using the Rocscience Swedge program (Rocscience 2010).

The kinematic analyses for plane failure for Groups 1 and 2 are shown in Figures 51a and 51b, respectively. The analysis follows the procedure described in Rocscience (2010). All fracture poles from Groups 1 and 2 have been included. The stereonets in Figure 51 show a friction circle (centered about the center of the stereonet) and a daylighting envelope. The friction circles were drawn assuming a friction angle of 35 degrees. Fracture poles that are outside the friction circle and inside the daylighting envelope are susceptible to plane sliding. The plane sliding analysis in Figure 51 identifies Set 4 in Group 1 and Set 5 in Group 2 as those susceptible to plane sliding.

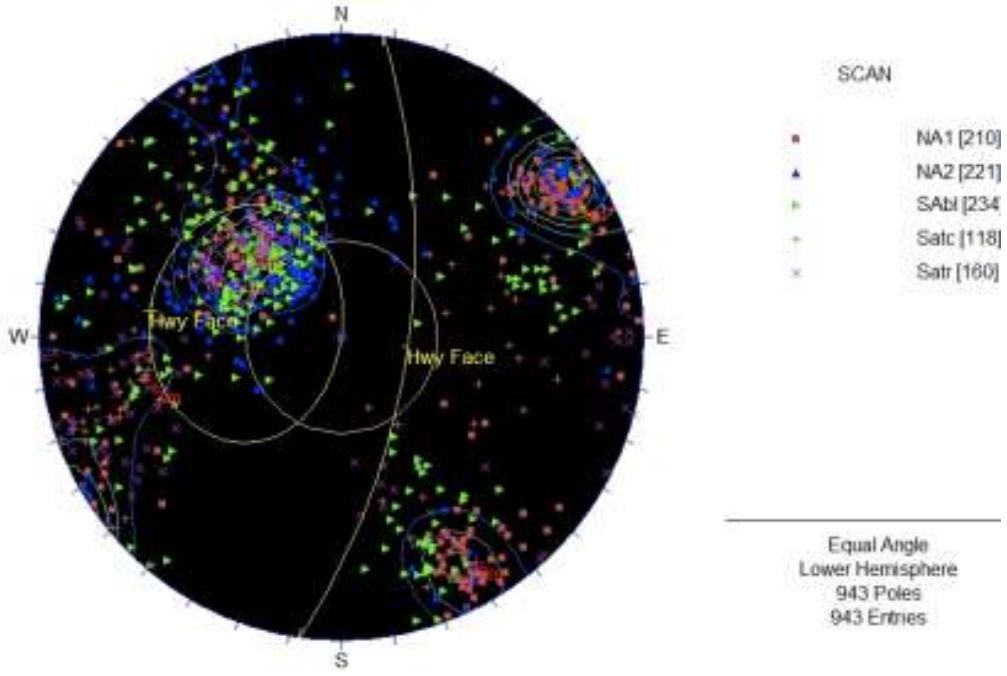

Figure 51a. Plane sliding analysis, Group 1 poles.

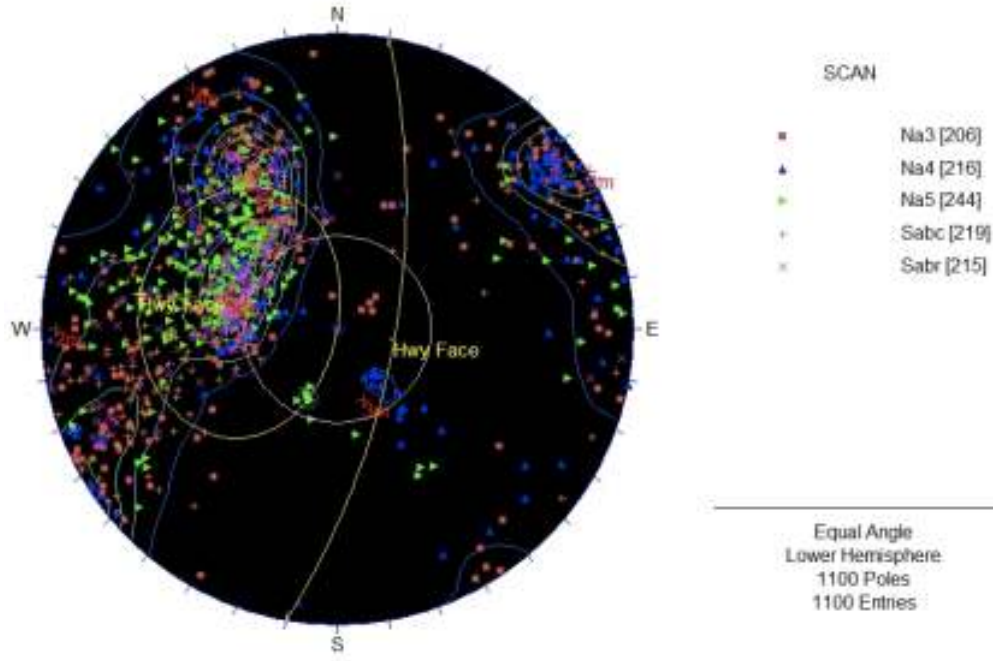

Figure 51b. Plane sliding analysis, Group 2 poles.

The probabilistic analysis for wedge failure in Groups 1 and 2 is shown in Table 25. The wedge failure analysis utilizes the information on the rock face and discontinuity sets listed in Tables 23 and 24 (average dip, average dip direction, Fisher constant, and average highway cut orientation). Every possible combination of joint set pairs was analyzed for possible wedge failure. Therefore, for the four discontinuity sets in Group 1, there were six possible joint set pairs, and for the six discontinuity sets in Group 2, there were 15 possible joint set pairs. The probability of failure for each joint set pair was calculated by making 10,000 picks from a Fisher distribution for orientation of each fracture making up the joint set pair. The percent of the picks that results in wedge failure is the probability of failure. For each joint set pair, the probability of wedge failure was calculated assuming dry (no water pressure) and wet (fractures filled with water) conditions. Dry conditions are shown in red and wet conditions are shown in blue in Table 25. A friction angle of 35 degrees and zero joint cohesion were assumed.

Probabilities of failure can range from 0 to 100 percent, and a probability of failure greater than 20 to 30 percent indicates likelihood for wedge failure to occur. Table 25 shows that the highest probabilities of failure for Group 1 are associated with Joint Set 4 (4/1 and 4/3), which is also associated with possible plane failure. Similarly, the highest probabilities of failure for Group 2 are associated with Joint Set 5 (5/1, 5/2, 5/3, 5/4, 5/6), which is also associated with plane failure.

Table 25. Probabilities of Failure for Wedge Sliding

Pennsylvania 1 Swedge Slope Stability Analysis ϕ=35°				
Prob of Failure (Dry/Wet)				
Joint Set	1	2	3	4
1		0.48%	15.21%	71.90%
2	0.44%		32.14%	10.07%
3	1.63%	31.32%		88.98%
4	53.82%	3.04%	68.38%	

Pennsylvania 2 Swedge Slope Stability Analysis ϕ=35°						
Prob of Failure (Dry/Wet)						
Joint Set	1	2	3	4	5	6
1		4.89%	0.00%	0.53%	67.80%	55.02%
2	0.53%		2.46%	1.25%	42.11%	11.23%
3	0.00%	0.15%		4.04%	31.56%	1.19%
4	0.53%	1.07%	0.28%		45.57%	2.27%
5	52.54%	32.53%	19.01%	27.51%		67.77%
6	51.05%	10.78%	0.04%	0.09%	47.98%	

Analysis of Rockfall

Slope profiles generated from the point clouds can be used to analyze the rockfall hazard associated with rock slopes. This report describes two types of analyses that were conducted from the slope profiles. First, the OHF was calculated to indicate likely locations and sizes for rockfall events at a particular site. Second, the profiles were used to determine rockfall trajectories for those locations using the Rocscience program, RocFall (Rocscience 2010). Other

programs, such as the Colorado Rockfall Simulation Program (Jones et al. 2000), could have been used.

Slope profiles from the five scans in the South Area are shown in Figure 52, and the OHFs from these profiles are given in Table 26. Details on the calculation of the OHF are given in the Arizona chapter of this report. The use of the OHF is new, but based on the results in this pooled fund study, OHFs greater than 4 or 5 percent indicate a possible rockfall hazard. Overall, Table 26 shows that OHFs greater than 4 percent are found in four of the five scans in the South Area, indicating a potential for rockfall due to overhangs in the areas around those four scans. This is consistent with rockfall events that have occurred at the Pennsylvania site.

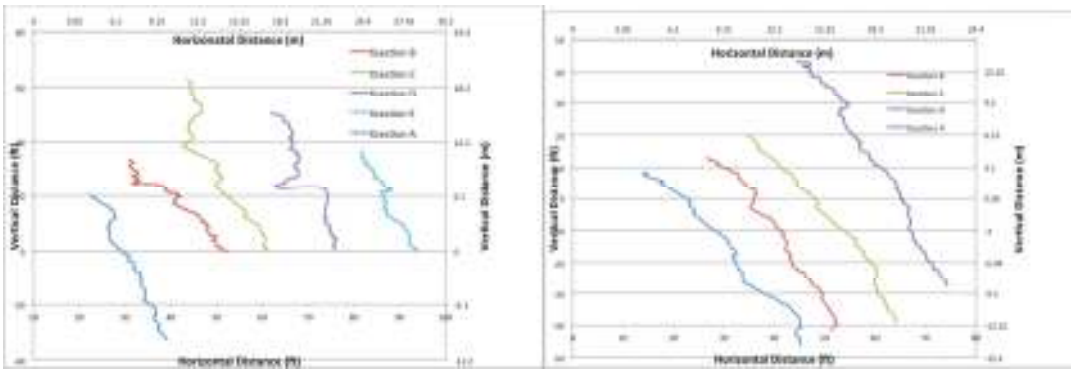

Figure 52a-b. Vertical cross sections for scans, from left, a) SAtc and b) SAtr.

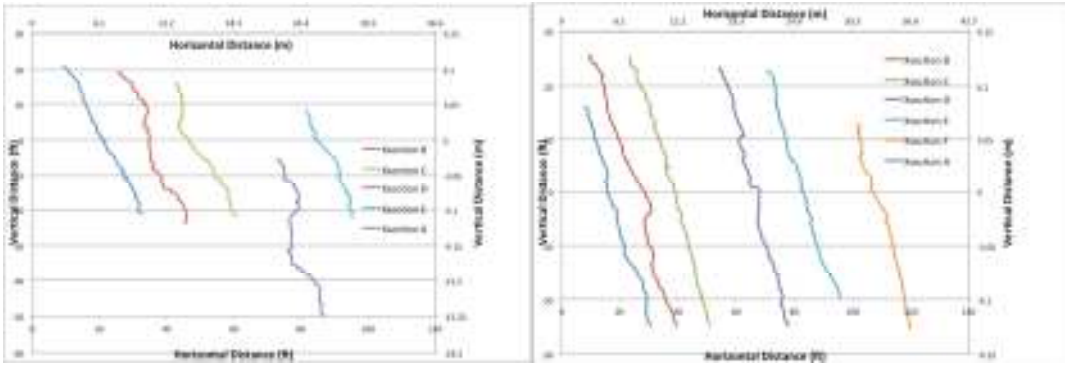

Figure 52c-d. Vertical cross sections for scans, from left, c) SAbl and d) SAbc.

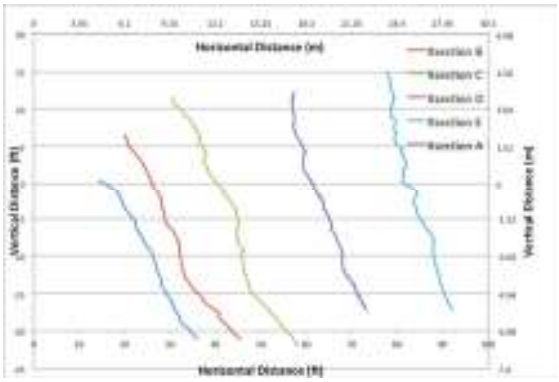

Figure 52e. Vertical cross sections for scans SAbr.

Table 26. OHFs for the Cross Sections Shown in Figure 52

Section	Scan SAtc	Scan SAtr	Scan SAbl	Scan SAbc	Scan SAbr
A	5.24	2.11	2.86	3.41	0
B	6.67	3.94	4.32	5.68	0
C	12.07	1.28	5.02	2.71	4.02
D	14.92	3.57	10.07	6.30	2.06
E	4.88		5.38	1.07	7.06
F				3.20	

Cross sections have also been used to simulate the trajectories of rock blocks that become dislodged from the slope. Figure 53 shows an example of rockfall trajectories calculated from one of the Pennsylvania cross sections using the Rocscience RocFall program. This cross section is on the right section of the slope and includes the top portion, bottom portion, and bench. A small block was used to simulate loose rock dislodging from both the upper and lower portions of the slope. Impact and rebound properties of a weathered rock and talus cover were used, with vegetation and soil cover at the bottom of the slope. A small ditch was also added between the slope and the highway. Based on these input parameters, 100 trials were simulated. The results indicate that there is a moderate probability that falling rock could enter the roadway if a failure occurs, with most of the rock that enters the roadway originating from dislodging at the top of the slope.

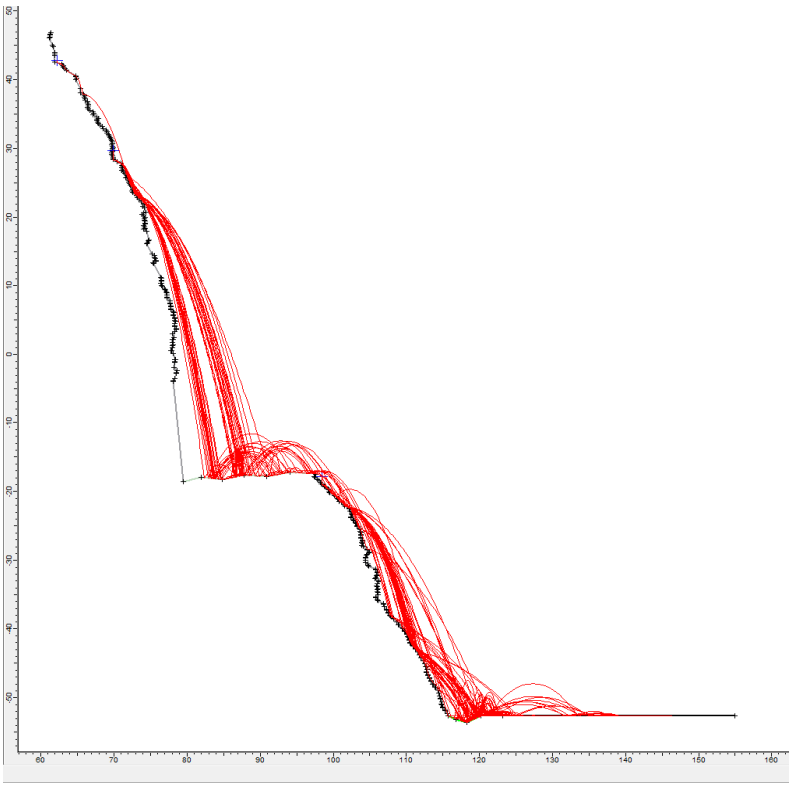

Figure 53. Rockfall trajectories from a cross section on the right side of the slope.

10. TENNESSEE

This chapter discusses scanning that took place in Tennessee as part of the LIDAR pooled fund project, as well as the results of analyzing the Tennessee scans.

OVERVIEW OF THE TENNESSEE SITE

The Tennessee site for the pooled fund study is a rock slope along Interstate Highway 24 westbound (I-24W) near milepost 137.1. Since it is heavily traveled, a lane closure would entail considerable expense to the state and severely inconvenience the motoring public. The Tennessee Department of Transportation (TDOT) assigned the site their Rockfall Hazard Rating System (RHRS) rating of 578 (McCarter 2004) out of a maximum of 850 (Mauldon et al. 2007). The rock slope is on a curve in the highway where it shifts from heading west to northwest, with limited decision site distance. The slope is approximately 750 ft in length along the highway with an approximate maximum height of 190 ft. It strikes 292 degrees with an average dip of approximately 51 degrees to the northeast. The three rock units at the site are horizontally bedded Paleozoic sandstones, limestones, and shales (TDG 2011). The rock mass is most notably affected by the differential weathering of the shale beds between more competent layers of limestone and sandstone, creating overhangs of sandstone and limestone bedding with smooth shale talus slopes underneath. Toppling due to a sub-horizontal overhanging joint set and raveling of small blocks also contributes to the instability of the slope. Raveling of smaller loose blocks is present, but small block size limits the hazard. A picture of the highway showing the slope is shown in Figure 54.

Figure 54. View of the highway cut on Interstate 24 westbound (Photo courtesy of TDOT).

The climate at the I-24 site in Tennessee is classified as Humid Subtropical, a zone of subtropical climate characterized by hot, humid summers and generally mild winters (Peel et al. 2007). Monthly average rainfall ranges from a high of 6.94 inches in March to a low of 4.04 inches in August. Monthly average temperatures vary from July's high/low range of 83.4/65.8 degrees Fahrenheit to January's high/low range of 43.2/26.2 degrees (SRCC 2011). The climate conditions at the site present a high probability for maximum water pressure and seepage conditions due to the plentiful rainfall. Also, the winter temperature range presents the potential for freeze-thaw cycles and rapid deep snowpack melting combined with heavy rain events.

LIDAR scanning and point cloud processing of the Tennessee site was conducted as part of the pooled fund project. TDOT hopes to learn several things from the scanning and analysis of results. The primary goal was to use the LIDAR rock mass analysis results to conduct a Rockfall Hazard Rating of the scanned slope. TDOT plans to determine the effectiveness and efficiency of LIDAR for use in their Tennessee Rockfall Hazard Rating system. TDOT is interested in quantifiable parameters that can be extracted from LIDAR scanning to evaluate geologic structure (i.e., stereonets), geotechnical engineering properties, and the likelihood for slope failure and rockfall.

LIDAR SCANNING OF THE TENNESSEE SITE

The scan for the I-24 project was conducted in February 2011 to reduce the limitations imposed by heavy foliage that is present at the site during other times of the year. The scan was completed by two TDOT crews (Region 1 and Region 2). Although the project fell within Region 2 (Chattanooga), Region 1 (Knoxville) performed the scan, because Region 2 did not have a scanner. The Leica C10 scanner was used and captured a complete 360-degree point cloud at each location. The section of I-24 analyzed took five setups to capture, with each scan taking approximately 12 min to complete. The five scans were registered together with Leica's Cyclone software and all scan data on the opposite side of I-24 were removed. The scans were also cleaned up using Cyclone to minimize the effects of traffic noise, vegetation, temporary barriers, and large pieces of ice. Traditional survey data were added to show the base of the rock slope, as well as the edges of pavement due to the barrier blocking the scanner's line of sight (Shane Snoderly, Civil Engineer, TDOT, personal communication, November 2011).

The registered point cloud of the entire slope was sent by TDOT personnel and analyzed using the Split-FX point cloud processing software, referred to as the I-24 scan. For Tennessee, the entire scan was analyzed in one section. There are several reasons for keeping the slope in one piece. First, since the point cloud of the entire slope contains just under 3 million points, this allows for manageable manipulation of point cloud data. Second, the geologic structure is consistent along the length of the slope; this allows for a single geotechnical analysis of the entire slope, as was done by TDOT in categorizing this site with the RHRS. In addition, an overhang analysis for Tennessee was conducted using this point cloud. A second scan of the entire slope, including the highway and some of the ditch, was provided, referred to as the I-24 With Lanes scan (Figure 55). This was useful for ditch and highway measurements and rockfall trajectory analysis. The general scan and slope information are given in Table 27.

Table 27. Summary of Slope Information

Scan	Number of Points	Average Slope Information			
		Length (ft)	Max Height (ft)	Dip	Dip Direction
I-24	2,953,411	750	118 – 190	51.5	22.1
I-24 With Lanes	15,586,542	1654	118 – 190	20.5	22.2

Figure 55. Location of I-24 scans showing ditch and highway (upper slopes not visible) (Photo courtesy of TDOT).

The point cloud from the I-24 With Lanes scan is shown in Figure 56 and contains about 15.5 million points. The length of this point cloud is about 1650 ft and the height of the rock outcrops ranges from 115 to over 190 ft. The average dip of the rock slope in the scan is 20.5 degrees and the average dip direction is 22.2 degrees. The steeper and more hazardous section of the I-24 scan is visible in the middle of the bend.

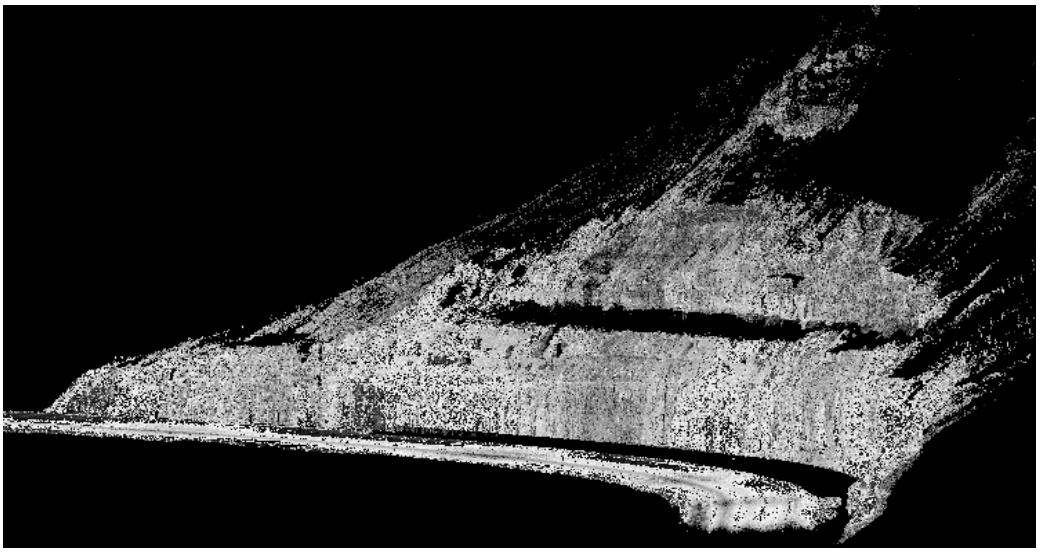

Figure 56. Point cloud of the I-24 with lanes scan.

POINT CLOUD PROCESSING OF SCANS FROM THE TENNESSEE SITE

For Tennessee, point cloud processing was conducted for three main types of analysis, as described below.

Rock Mass Characterization

Important attributes of the geologic structure are extracted from the point clouds, including discontinuity orientation and spacing. The orientation results are plotted on a stereonet and the primary joint sets are determined.

The results of the rock mass characterization of the I-24 point cloud are shown in Figure 57 and Table 28. Figure 57a shows the point cloud and Figure 57b shows the triangulated surface mesh. The delineated fracture surfaces are shown in Figure 57c, the lower hemisphere stereonet plot of the fracture poles is shown in Figure 57d, and the measurement of fracture spacing of the horizontal fractures is demonstrated in Figure 57e. Figure 57d shows the occurrence of four primary joint sets; statistical information about these joint sets is given in Table 28. The two most prominent joint sets are the vertical (teal) and the horizontal (red) road-facing fractures. But the most problematic structural features are the horizontal (red) and the 55-degree overhanging (orange) joint sets that sit above the loose talus layers of shale that are sitting at the angle of repose (seen clearly in Figure 54). Combined with the large average joint spacing of the joints at the site, the potential for large block rockfall is definitely present. Based on the joint sets present and their orientations, it was determined kinematically that there is no hazard from wedge or planar failures.

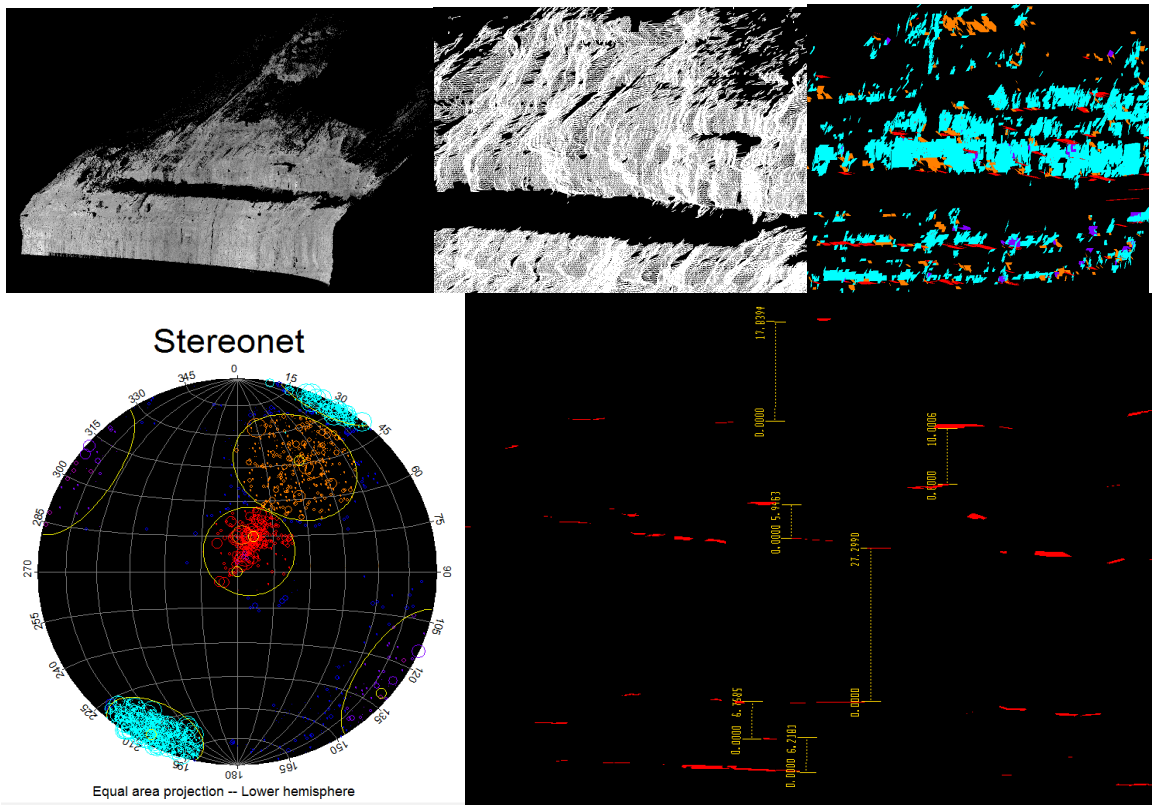

Figure 57. Basic steps using Split-FX for rock mass characterization using the Interstate 24 scan, at upper left, a) point cloud; at center, b) triangulated mesh (zoomed in), and, upper right, c) automatic fracture delineation (zoomed in); at bottom left, d) lower hemisphere stereonet of plot fracture poles, and, bottom right, e) measurement of average joint spacing for Joint Set 1 (red).

Table 28. Average Results for the I-24 Scan Joint Sets in Figure 57d

Set	Average Dip	Ave. Dip Direction	Fisher Constant	Ave. Joint Spacing (ft)
1 (red)	14.50	207.87	66.13	5.18
2 (orange)	55.62	208.04	26.95	10.58
3 (purple)	87.03	308.54	34.01	11.14
4 (teal)	84.1	26.54	66.0	3.9

Analysis of Rockfall

This section describes two types of rockfall analyses that were conducted from the Tennessee point cloud. First, an OHF was calculated to determine an approximate percentage of the slope that contains moderately to severely overhanging rock. A 3D extension of the OHF approach was developed here that used the entire triangulated mesh rather than 2D cross sections, as has been used for the other states. Second, selected cross sections were used to determine rockfall

trajectories for the most potentially hazardous locations using the Rocscience program, RocFall (Rocscience 2010).

3D Overhang Factor

The OHF indicates the approximate areal percentage of the slope that is moderately to severely overhanging. It is a simple calculation that can be made in a spreadsheet program. Details on how the OHF is calculated using 2D slope profiles are given in the Analysis of Rockfall from Cross Sections section of the Arizona chapter of this report. To calculate the 3D OHF, a triangulated mesh was created in Split-FX for the entire point cloud of the Tennessee slope, using an average triangle density of 3.5 triangles per square foot. Figure 58 shows overhanging sections in the triangular mesh created from the I-24 scan, and Figure 59 is a photo of the slope showing overhanging sections.

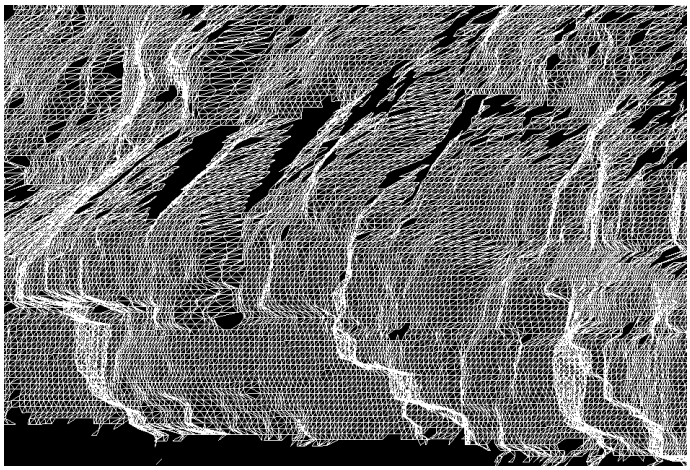

Figure 58. Triangular mesh created in Split-FX for use in the OHF calculation.

Figure 59. Photo of overhangs present on I-24 slope.

In order to determine the degree of overhang present in the slope using a spreadsheet, angles and orientations of all the small triangular elements must be acquired. The point cloud processing software generates dip and dip direction data for each mesh triangle. The dips and dip directions were exported from Split-FX and imported into an Excel spreadsheet. Each triangle's dip and dip direction were then evaluated for their overhang ratings. A non-overhanging slope was given a 0 rating, a slightly overhanging slope (dip of 70-90 degrees) was given a rating of 1, a moderately overhanging slope (dip of 50-70 degrees) was given a rating of 4, and a severely overhanging slope (dip of 0-50 degrees) was given a rating of 10. Of course, in order for a triangle to even get a rating other than 0, it also has to have a dip direction outside of +/- 90° of the slope dip direction of 22°. The OHF was then calculated in the spreadsheet using the following equation:

$$= \frac{\sum Ratings}{(\#Triangles * 10)} * 100\%$$

Table 29 shows a small portion of the spreadsheet using the equation above to determine the OHF.

Table 29. Example of OHF Spreadsheet Analysis from a Small Section of the Slope

Dip	Dip Dir.	Rating	Σ Ratings	# of Triangles*10	Overhang Factor (OHF)
77.5	242.4	1	17	170	10%
71.5	3.7	0			
65.2	220.8	4			
80.5	69.2	0			
84.7	61.3	0			
44	261.7	10			
67.6	58	0			
75.2	282.2	1			
58.1	31.6	0			
51.4	58	0			
76.9	44.6	0			
35.2	31.5	0			
86.9	229.8	1			
68.2	37.2	0			
68.7	39	0			
53.6	26.1	0			
73.7	49.5	0			

The result of the full analysis for 342,020 triangles was an OHF of 7.16 percent for the I-24 scan. Table 30 shows the results from the spreadsheet. An analysis of OHFs on other slopes (Kemeny

et al. 2011) indicates that factors over 4 percent pose a rockfall hazard. Thus, the OHF of 7.16 percent, along with the very visible overhangs in the photos, indicates a rockfall hazard from overhanging rock slabs. In the future, the OHF will be enhanced to include other important slope and overhang information such as the size of overhanging sections and the height above the roadway.

Table 30. Results of OHF Analysis for the Tennessee I-24 LIDAR Scan

# Triangles	Σ Ratings	# Triangles*10	Overhang Factor (OHF) (%)
342020	244736	3420190	7.155626

Rockfall Trajectories

Rockfall trajectory analysis was conducted using cross sections created from the I-24 point cloud and the Rocscience RocFall program, as presented in Figures 60 through 62 below. First, a number of vertical cross sections were created in Split-FX, as shown in Figure 60. In general, the cross sections were chosen to be in locations with the highest potential for rockfall. Cross Section A is shown in Figure 61a, and at this point there are still gaps in the profile due to missing LIDAR data in those areas. The x,y data from this cross section were then imported into AutoCAD, converted to dxf, and imported into the Rocscience RocFall program. This process fills in the gaps as shown in Figure 61b.

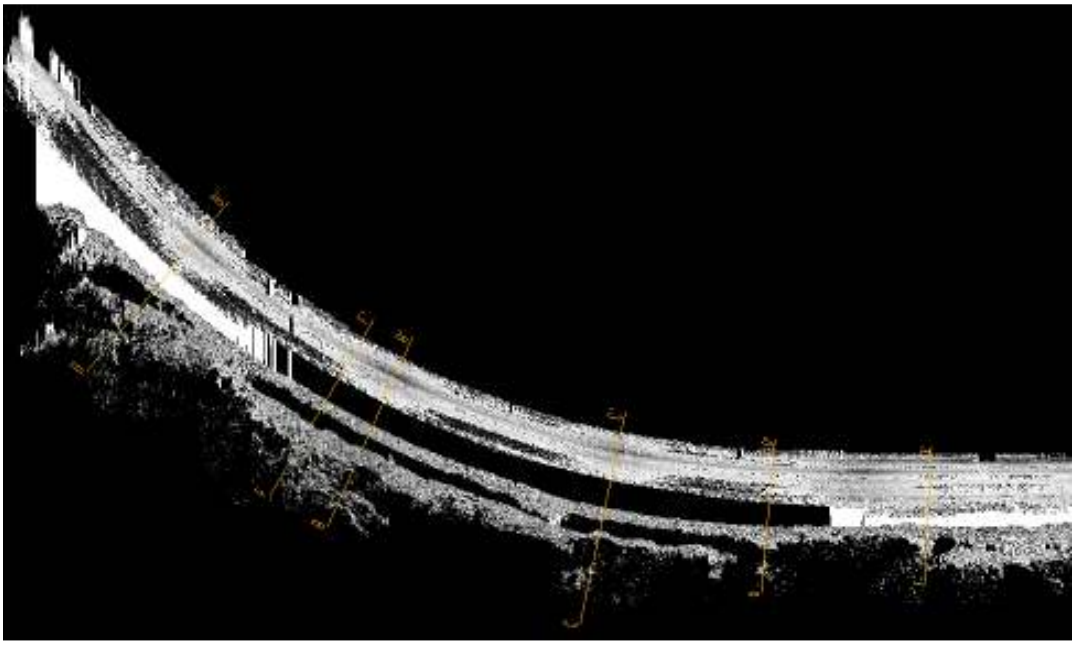

Figure 60. Aerial view (z direction) of I-24 with lanes scan, showing Sections A–F.

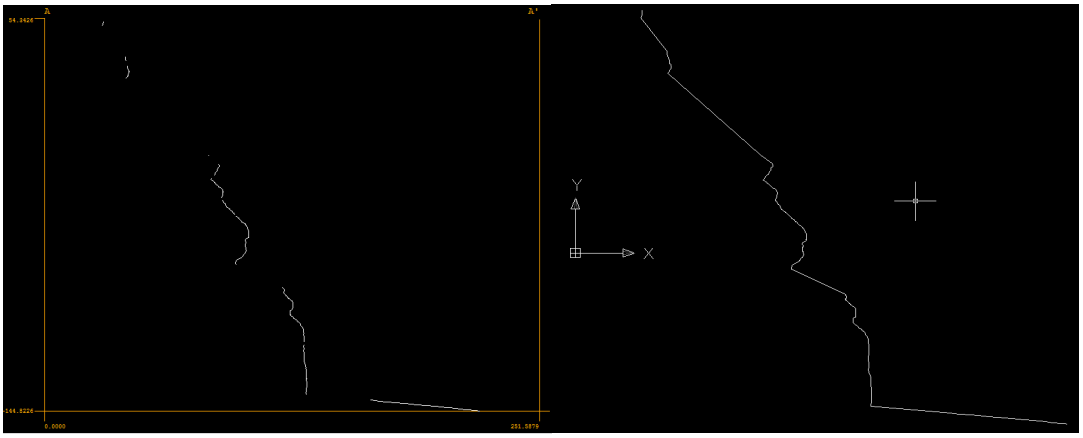

Figure 61. Left to right, a) Cross Section A profile generated by Split-FX, b) Cross Section A slope profile exported from Split-FX and imported into AutoCAD.

Figure 62 shows the rockfall trajectories calculated by the Rocfall program for Cross Section A. A block size of 50 kg (110 lbs) was assumed. The impact and rebound properties for a "soil with vegetation" were assumed for all talus slopes and the ditches, due to prolific vegetation growth at the site. Based on these input parameters, 100 trials were simulated for each of five variations in rockfall initiation heights. The results indicate that there is a high probability that a falling rock could enter the roadway from a height of approximately 115 ft or greater.

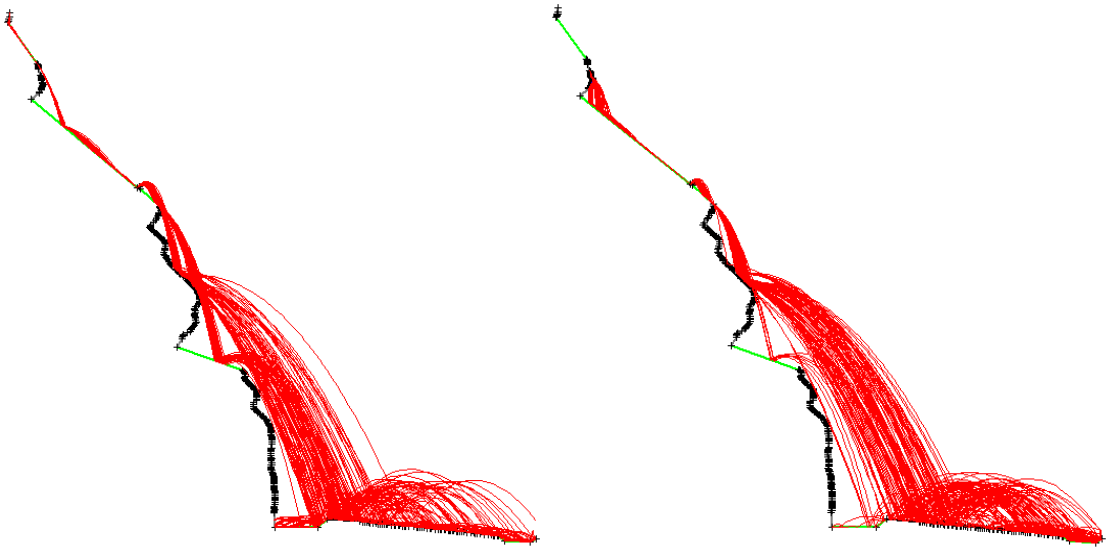

Figure 62a-b. Rockfall trajectories for Cross Section A shown in descending initiation heights, left to right, a) 190 ft, and b) 155 ft.

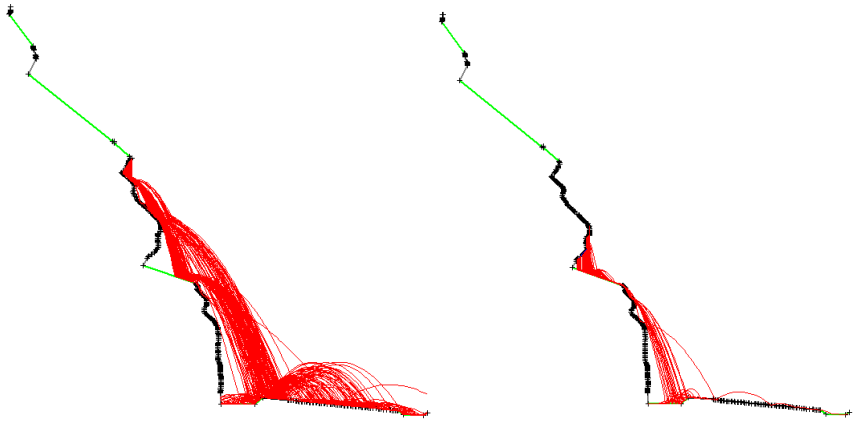

Figure 62c-d. Rockfall trajectories for Cross Section A shown in descending initiation heights, left to right, c) 115 ft. and d) 80 ft.

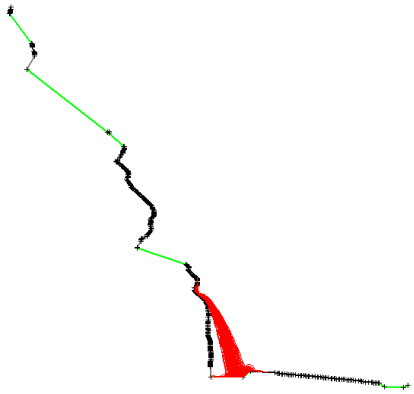

Figure 62e. Rockfall trajectories for Cross Section A shown at final initiation height of 45 ft.

Tennessee Rockfall Hazard Rating System (RHRS)

Since TDOT already has a rockfall hazard rating system in place, it was important to know how LIDAR data could be used in this system and how its results would compare to the existing rating. Tennessee's RHRS is based on the National Highway Institute's (NHI) RHRS, which instituted systematic identification and prioritization of highway slopes for remediation and/or monitoring. The geologic details of potential failure modes were made more explicit in the Tennessee system to improve characterization of ditch width and to allow reproducible field evaluation of rockfall hazards. Geologic characterization was improved by explicitly rating potential rockfall modes, measuring the abundance of the failure modes, and summing the scores for all potential rockfall modes at a rockcut (Mauldon et al. 2007).

The official Tennessee RHRS rating assessment results for the I-24 site are shown in Table 31. Using the same rating system, the site was evaluated using LIDAR scans and the point cloud processing software Split-FX. The results of the LIDAR-based rating are shown in Table 32. The

results of the LIDAR analysis gave a noticeably higher rating of 675 out of 850 compared to the TDOT rating of 578. It appears that the total height of the slope was the main difference that caused the hazard rating from the LIDAR analysis to be higher; The TDOT analysis used a slope height of 100 ft, while the LIDAR clearly shows significant rock outcrops up to 190 ft. The significance of this height difference is not just due to the slope height score increasing from 81 to 100, but is also based on other rating criteria that are influenced by height. One main score change due to the height difference was in the ditch effectiveness score, which is based on ditch width as related to the height and verticality of the slope. Using the LIDAR analysis height of 190 ft, the actual ditch width to design width ratio was 1/3. This 33 percent "of Design Catchment Width" rating put this slope into the <50 percent category with a maximum score of 81. The score of 81 for ditch effectiveness is much higher than the score of 9 from TDOT, accounting for 74 percent of the total hazard rating difference. The other six points of difference are due to a block size designation difference for raveling (Mauldon et al. 2007).

Completing the RHRS form using the LIDAR was straightforward, but some data had to be taken from the existing form. Certain information could not be obtained purely from the scans. Items that were just copied over from the existing form are: water conditions, average daily traffic (ADT), and rockfall history. Another issue with using the LIDAR scans without a site visit was the discrepancy in the slope height, as discussed in the previous paragraph. Vegetation was removed from the point cloud by Tennessee personnel, and without knowing the vegetation conditions, there is some uncertainty about the rockfall potential from the highest rockfall points. Photos of the site used for the study show that the upper slope was forested. The highest rock outcrop was not visible in the photos due to the trees, but it clearly showed in the LIDAR scans. This outcrop was responsible for the major score differences in the RHRS scores. During Rocscience RocFall analysis, all talus slopes had their material properties set as "soil with vegetation" to be conservative about the possible effects of dense vegetation.

Table 31. TDOT Rockfall Hazard Rating Table for I-24 Site with Total RHRS Score

TDOT Go.

Rockfall Managment System

Geotechnical Engineering Section

Rockfall Hazard Rating

File No.:	58I0024001137.10LRF				Preliminary Rating	A	
RN:	I0024	BLM:	137.1	Length	920	RCL:	L
County	58	County:	Marion	CS:	1	SC:	0
Date:	7/27/2004	Geologist:	McCarter			Region:	2

Site Geometry

Criteria		Score	Criteria		Score
ADT:	32000		Slope Height:	100	81
Slope Length	920		Ditch Width:	20	
Speed Limit	55		Other Ditch Features		
AVR:	422	100	Catchment 6:1 or steeper?	☐	
Road Width:	60	0	Launching Features Present?	☐	
%DSD:	Limited	27	Ditch Effect:	Moderate	9

Site Geology

Max Geo Score? ☑

Plane Shear Failure		Score	Wedge Failure		Score
Abundance:			Abundance:		
Block Size:			Block Size:		
Friction:			Friction:		
Steepness:			Steepness:		

Differential Weathering Failure		Score	Ravelling Failure		Score
Abundance:	<10%	3	Abundance:	<10%	3
Block Size:	>6	81	Block Size:	<1	3
Relief:	3-6	27	Shape:	blocky	9

Toppling/Bedding Release Failure		Score	Other Considerations		Score
Abundance:	<10%	5	Water:	Flowing	27
Block Size:	>6	122	Rockfall History	Constant	81

Total RHR Score 578

Table 32. LIDAR-Generated Rockfall Hazard Rating Table with Total RHRS Score

Rockfall Management System						
Geotechnical Engineering Section						
Rockfall Hazard Rating						
Preliminary Rating:		**A**				
RN:	I0024	BLM:	137.1	Length	750	
County	58	County:	Marion			
Date:	9/1/2011	Geologist:	Lyons, J.			
Site Geometry						
Criteria		Score	***Criteria***			Score
ADT:	32000		Slope Height:	190		100
Slope Length:	750		Ditch Width:	20		
Speed Limit:	55		Other Ditch Features:			
AVR:	344	100	Catchment 6:01 or Steeper?:			
Road Width:	60	0	Launching Features Present?:			
%DSD:	Limited	27	Ditch Effect:			81
Site Geology						
Plane		Score		***Wedge***		Score
Block Size:		0		Block Size:		0
Friction:		0		Friction:		0
Steepness:		0		Steepness:		0
Diff. Weathering		Score		***Raveling***		Score
Abundance:	<10%	3		Abundance:	<10%	3
Block Size:	>6	81		Block Size:	1-2	9
Relief:	3-6	27		Shape:	blocky	9
Toppling/Bedding		Score		***Other Considerations***		Score
Abundance:	<10%	5		Water:	Flowing	27
Block Size:	>6	122		Rockfall History:	Constant	81
		365				310
Total RHR Score						
675						

11. TEXAS

This chapter discusses scanning that took place in Texas as part of the LIDAR pooled fund project, as well as the results of analyzing the Texas scans.

OVERVIEW OF THE TEXAS SITE

The Texas site consists of a series of rock slopes located along a 15-mile section of State Loop 375, located just west of El Paso, Texas. Loop 375 has two 12-ft lanes in each direction with a 6-ft inside shoulder and a 10-ft outside shoulder. There are approximately 16 ft between the edge of pavement and the right-of-way line. The roadway was constructed in 1966. The benched cuts cut at a maximum slope of 0.25:1; the lower bench has a 40-ft height while the upper cut varies in height. Pictures from the Texas site are shown in Figure 63.

Figure 63. Pictures of Texas site, along with the Leica Scanstation 2 scanner.

Along the slopes in the test site, major rockfall events have occurred after heavy rains, periods of freeze and thaw, or high winds. The normal mode of failure appears to be minor block fall; however, large mass movements due to wedge, key block, and toppling failures have occurred. Raveling and minor block fall has reduced the effectiveness of the benched section as a fallout catchment. District personnel have used a T501 concrete barrier along the edge of pavement to contain rockfall. The barriers are positioned approximately 20 ft from the rock face. More recently, less competent sections of rock have failed, resulting in lane closures.

Site characterization along this extensive section of roadway is very difficult, time-consuming, and expensive. Collection of data using conventional methods may result in missed or erroneous data. LIDAR is an attractive alternative due to the efficient and repeatable method of data collection. Currently, the response to rockfall in this section of roadway is reactive. Texas DOT wishes to minimize the risk to motorists by eliminating the sections of cut that pose the greatest risk. This can only be done once a detailed survey has been conducted and evaluated.

The road cuts of interest along Loop 375 are through the Franklin Mountains , a block-faulted mountain range that contains a thick section of Paleozoic rocks on the west side overlying a

section of Precambrian rocks exposed on the steep east flank. For details on the geology of the Franklin Mountains, see Cornet (2008). Failure modes vary from basic block fall to potential wedge, toppling, and raveling. Most rockfall is minor and is contained in ditch catchments; however, several failures have resulted in lane closures.

LIDAR SCANNING AT THE TEXAS SITE

The Texas site for the pooled fund study is a rock slope along Loop 375 (Transmountain Road) in the Franklin Mountains near El Paso, Texas. The rock slope is approximately 870 ft long and ranges in height from 40 to over 125 ft. A team from the Department of Mining and Geological Engineering at the University of Arizona conducted scanning in August 2009 using a Leica Scanstation time-of-flight scanner. Three scans were taken at the site and registered color point clouds of the entire slope were produced by personnel from Darling Surveying. Scan 4 is the western part of the slope, Scan 2 is the middle section of the slope, and Scan 3 is the eastern part of the slope. Details of the scans are given in Table 33. As an example, the approximate boundaries for Scan 2 are shown in Figure 64.

Table 33. Summary of Slope Information

Scans (listed from west to east)	Number of Points	Average Slope Information			
		Length (ft)	Height (ft)	Dip	Dip Direction
Scan 4	1,329,278	252.8	119.5	55.6	193.1
Scan 2	1,522,296	279.8	125	57.6	192.7
Scan 3	1,416,701	338	123.7	60.3	187
Total	4,268,275	870		57.83 (Avg)	190.93 (Avg)

Figure 64. Approximate location of the Scan 2 point cloud.

The point cloud from Scan 2 is shown in Figure 65 and contains about 1.5 million points. The length of this point cloud is about 280 ft and the maximum height is about 125 ft. The average dip of the rock slope in Scan 2 is 57.6 degrees and the average dip direction is 192.7 degrees.

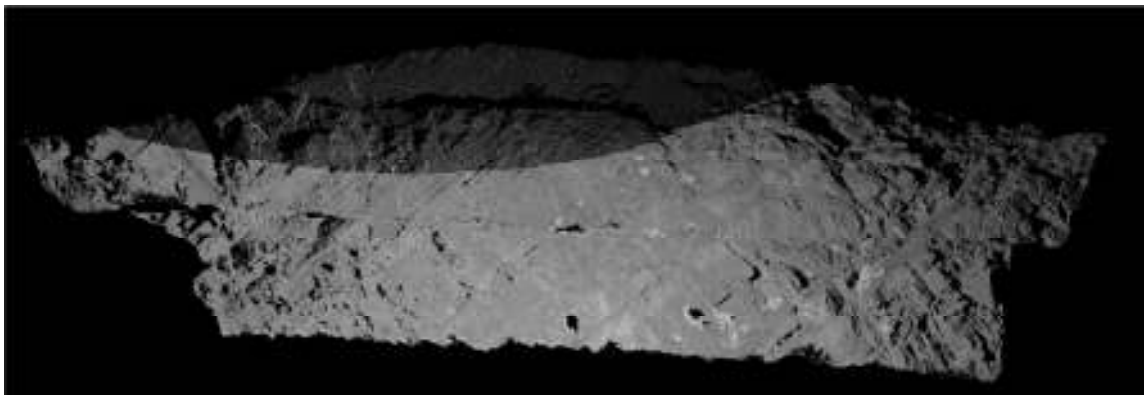

Figure 65. Point cloud of Scan 2.

POINT CLOUD PROCESSING OF SCANS FROM THE TEXAS SITE

For Texas, point cloud processing was conducted for three main types of analysis, as described below.

Rock Mass Characterization

Important attributes of the geologic structure, including discontinuity orientation and spacing, are extracted from the point clouds. The orientation results are plotted on a stereonet and the primary joint sets are determined.

The stereonet results for LIDAR Scans 2, 3, and 4 are shown in Figure 66 and Table 34. In Figure 66a, the fracture poles are separated by scan, and this shows the geologic structure is very similar between the three scans. This justifies a structural analysis of the site from the combined data. Figure 66b shows the four primary joint sets that were extracted from the fracture poles. There are a number of poles not assigned to any of the sets, and these are primarily blasting fractures parallel to the highway cut. The average fracture information from the four sets is given in Table 34.

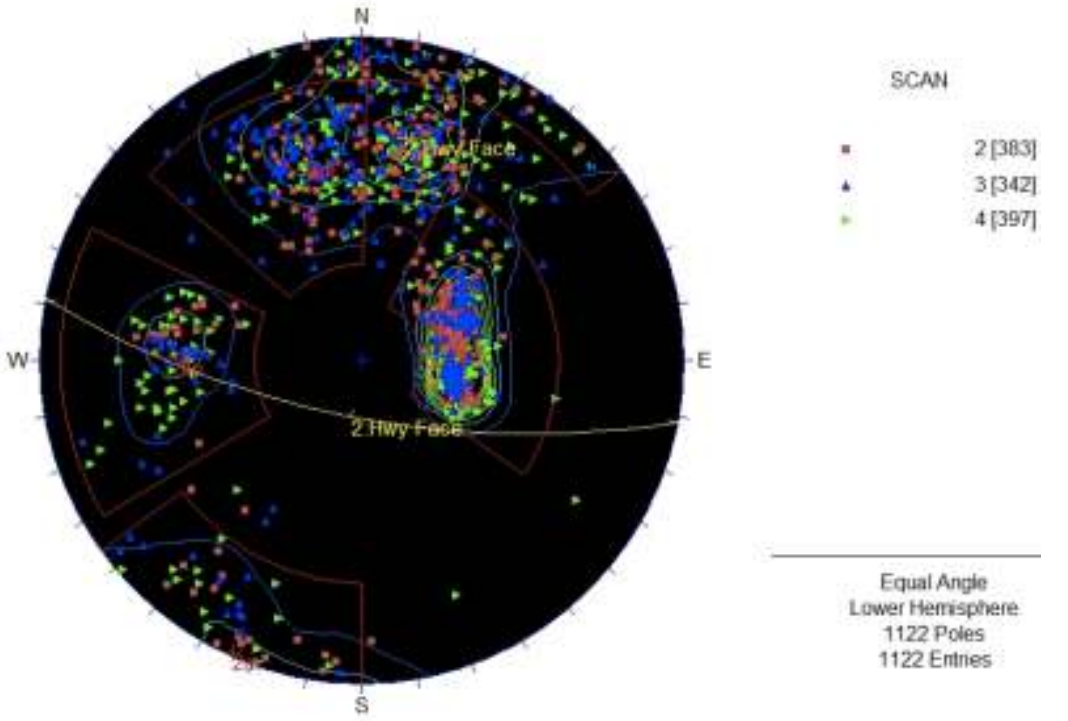

Figure 66a. Geologic structure from combined data from Scans 2, 3, and 4, separated by scan.

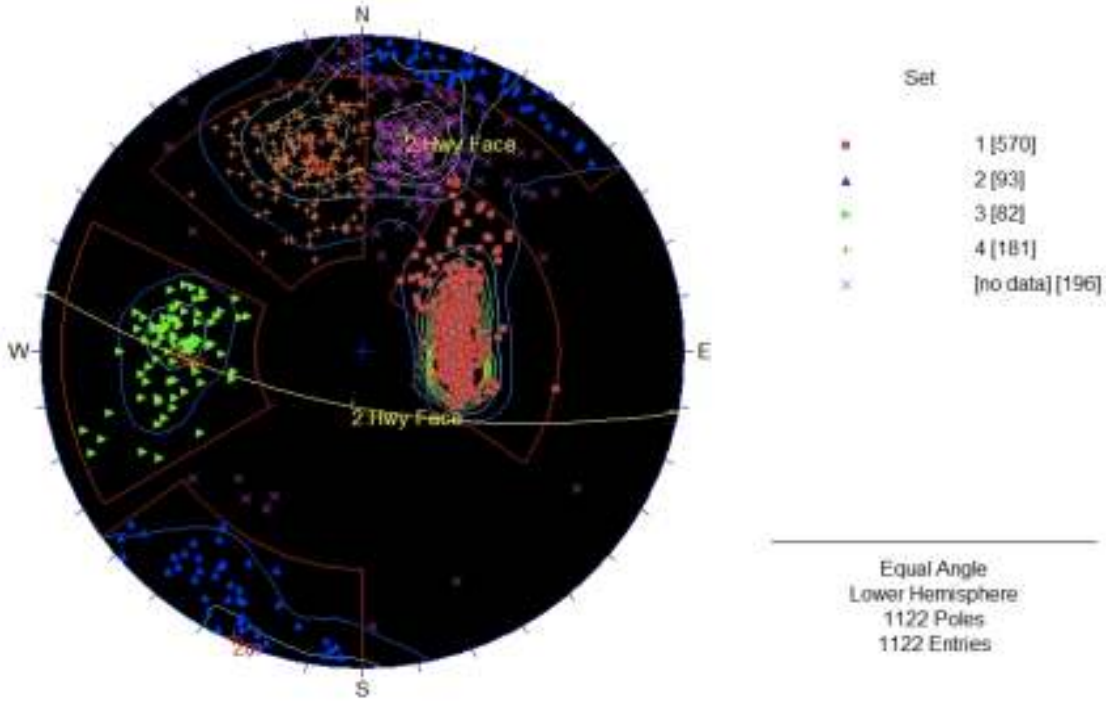

Figure 66b. Geologic structure from combined data from Scans 2, 3, and 4, separated by joint set.

Table 34. Average Results for the Joint Sets in Figure 65

Set	Average Dip	Ave. Dip Direction	Fisher Constant
1	34	262	35
2	89	24	28
3	60	91	36
4	65	165	37

Slope Stability

A kinematic analysis for plane failure is shown in Figure 67. The analysis follows the procedure described in Rocscience (2010). All fracture poles from Scans 2-4 have been included. The stereonet in Figure 67 shows a friction circle (centered about the center of the stereonet) and a daylighting envelope. The friction circle was drawn assuming a friction angle of 35 degrees. Fracture poles that are outside the friction circle and inside the daylighting envelope are susceptible to plane sliding. The plane sliding analysis in Figure 67 clearly identifies portions of Sets 1 and 4 as those susceptible to plane sliding. This is consistent with plane sliding apparent in Figure 63b.

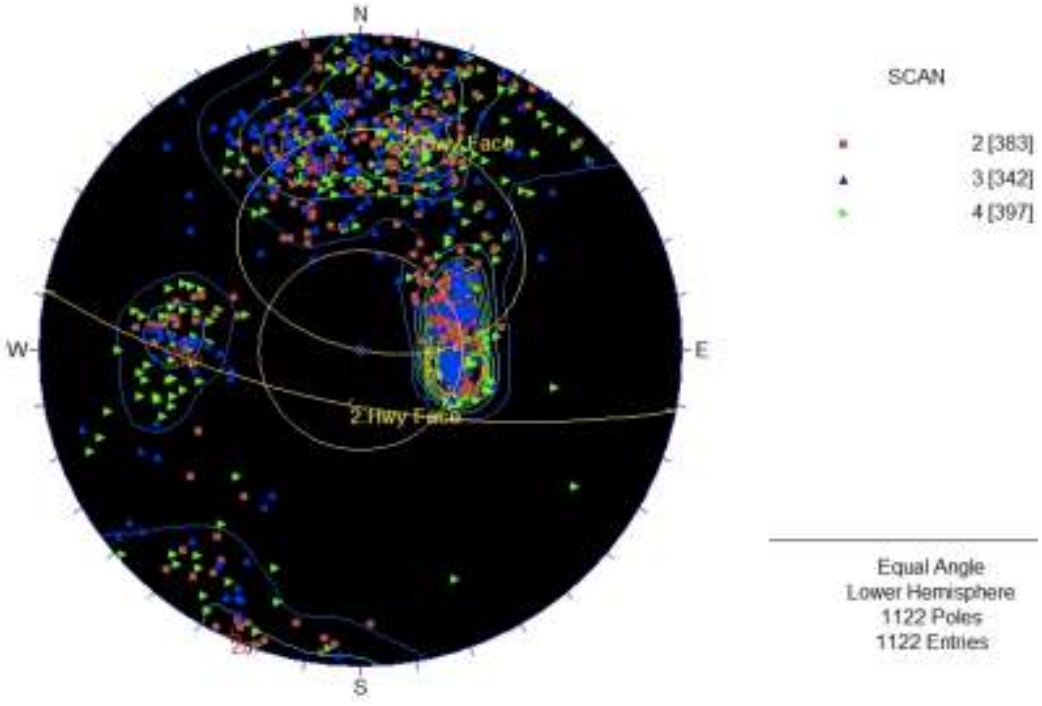

Figure 67. Plane sliding analysis from the combined data from Scans 2, 3, and 4.

Using the structural data presented in Table 34, a wedge sliding analysis was conducted using the Rocscience Swedge program. The Swedge program takes the mean dip, mean dip direction, and Fisher constant for each set and does a probabilistic slope stability analysis. In particular, to

determine the probability of failure for potential wedges between any two discontinuity sets and the rock face, it randomly picks a fracture from each set and determines the factor of safety. It does this 10,000 times for each pair of discontinuity sets. The probability of failure is the percentage of trials that results in a failed wedge. Slope stability calculations were conducted between the sets and the average rock face orientation. Friction angles of 35 degrees and zero cohesion were assumed for each joint set. The results are shown in Table 35. Results are presented for both dry and fully saturated (such as after a heavy rainfall) conditions. The results are presented in terms of the probability of failure for wedges formed from any two sets and the slope surface. Probability-of-failure percentages greater than about 20 percent indicate a potential slope hazard. The results indicate that slope instability at the Texas site is associated with wedges formed from Sets 1 and 4, indicating a 14.5 percent probability of failure under dry conditions and a 71.5 percent probability of failure under wet conditions. This is very consistent with the wedge failures observed at the site, as shown in Figure 68.

Table 35. Probabilities of Failure for Wedge Sliding at the Texas Site

Texas Swedge Slope Stability Analysis ϕ=35°				
Prob of Failure (Dry/Wet)				
Joint Set	1	2	3	4
1		0.57%	0.49%	71.50%
2	0.08%		4.62%	0.99%
3	0.00%	0.35%		6.97%
4	14.45%	0.94%	6.31%	

Figure 68. Wedge failures at the Texas site formed by discontinuity Sets 1 and 4 (see Figure 66b and Table 34).

Rockfall Analysis Using Vertical Cross Sections

Vertical cross sections from Scans 2, 3, and 4 are shown in Figures 69a, 69b, and 69c, respectively. In the pooled fund project, two types of analysis were conducted using the vertical cross sections. First, the OHF was calculated for each cross section, as described in the Analysis of Rockfall from Cross Sections section of the Arizona chapter of this report. The OHFs for the

cross sections shown in Figure 69 are given in Table 36. From experience, the research team has found that OHFs greater than 4 percent represent potential hazards for rockfall. Table 36 indicates that five of the 12 cross sections have OHFs greater than 4 percent. This indicates likelihood for rockfall at the Texas site and is consistent with field experience.

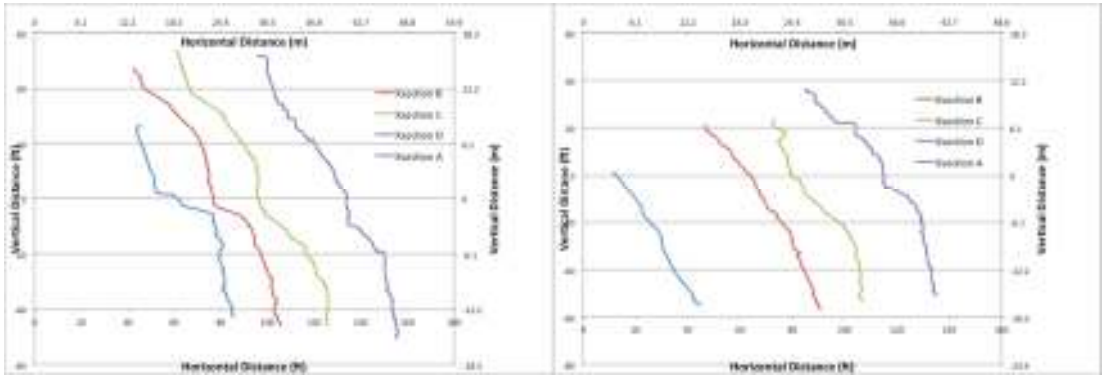

Figure 69a-b. Cross sections from, left to right, a) Scan 2, and b) Scan 3.

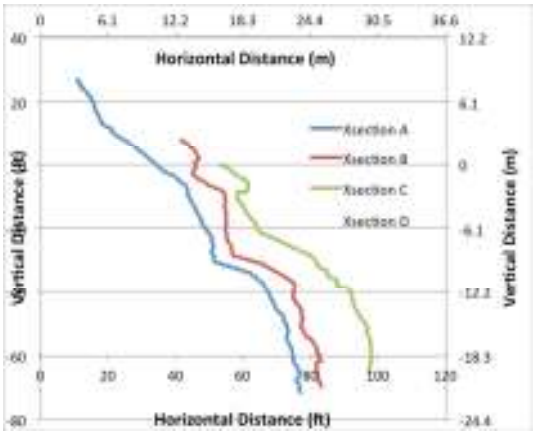

Figure 69c. Cross sections from Scan 4.

Table 36. OHFs for the Cross Sections in Figure 69

Section	Scan 2	Scan 3	Scan 4
A	5.55	0.06	1.81
B	2.18	0.76	4.71
C	2.23	4.11	5.12
D	2.35	2.00	13.46

The second type of analysis that was conducted on the vertical cross sections from the Texas site was an analysis of rockfall trajectories. Figure 70 shows the rockfall trajectories calculated using the Rocscience RocFall program. A small block size was used to simulate loose rock being

dislodged from the top and the middle of Cross Section C in Scan 2. Impact and rebound properties of clean bedrock were used, with a vegetation cover at the bottom of the slope. A small ditch was also added between the slope and the highway. Based on these input parameters, 100 trials were simulated. The results indicate that there is a high probability that falling rock could enter the roadway if a failure occurs higher up on the slope, while rock falling from the middle of the slope would likely land in the ditch.

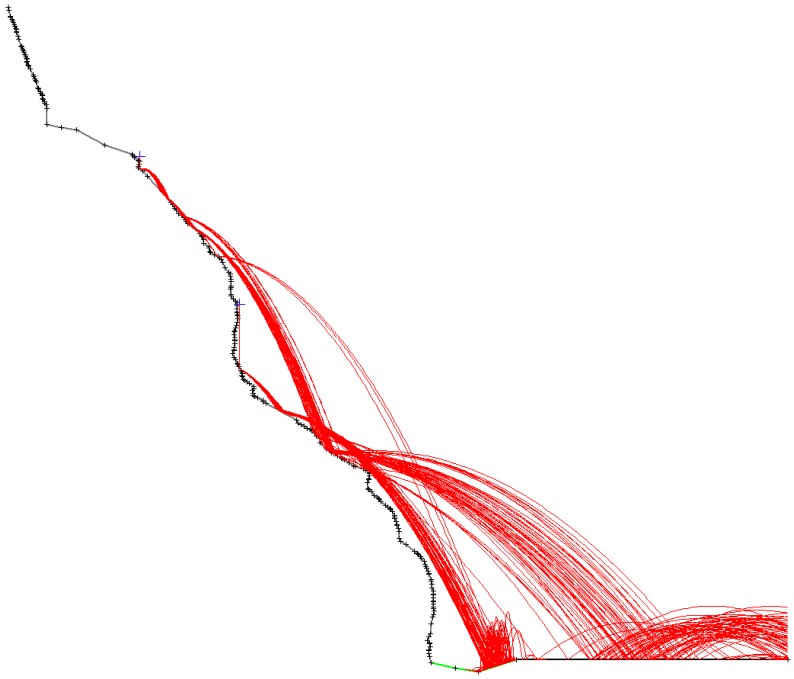

Figure 70. Trajectories from Cross Section C from Scan 2, analyzed with the RocFall program.

12. DISCUSSIONS AND CONCLUSIONS

SUMMARY AND OUTCOMES

This final report has presented results from Transportation Pooled Fund Project TPF-5(166), titled "Application of Three-Dimensional Laser Scanning for the Identification, Evaluation, and Management of Unstable Highway Slopes." Participants in the pooled fund study include Arizona, California, Colorado, New Hampshire, New York, Pennsylvania, Tennessee, and Texas. As part of the pooled fund project, LIDAR scanning was conducted in each state, and the resulting point clouds were analyzed to look at rock mass characterization, rockfall, slope stability, and change detection. The purpose of the pooled fund project was to demonstrate geotechnical applications of ground-based LIDAR for highway slopes, and to train state DOTs on the use of point cloud processing software.

The LIDAR pooled fund project:

- Conducted ground-based LIDAR scanning, and analyzed the resulting point clouds, in each of the eight states
- Developed best practices for field LIDAR scanning (see the Best Practices for LIDAR Field Scanning section, below)
- Developed efficient and repeatable ways to process LIDAR data for highway geotechnical applications (see the Best Practices for Point Cloud Processing section, below)
- Developed some new analysis techniques to analyze overhangs, joint persistence, and joint friction angle
- Had continued discussions over the three-year project period with highway geotechnical personnel from each of the eight state DOTs
- Trained DOT geotechnical personnel on LIDAR scanning and point cloud processing
- Distributed a copy of the Split-FX point cloud processing software to each of the eight states
- Published several papers and gave several invited talks on the LIDAR pooled fund project

Based on the results of the three-year LIDAR pooled fund project, it is recommended that ground-based LIDAR be used for highway geotechnical applications. Some specific recommendations on how to utilize ground-based LIDAR in highway geotechnical applications are given in the next few sections. The Best Practices for LIDAR Field Scanning section of this chapter describes best practices for field scanning that were developed from the many case studies in the project. This includes estimating the time required for scanning as well as details on how the scanning should be conducted. The Best Practices for Point Cloud Processing section of this chapter describes best practices for the point cloud processing of LIDAR data, and includes estimating the time required for processing as well as details on how the data should be processed for geotechnical analysis. Some remaining issues with ground-based LIDAR for geotechnical applications are described in the Issues with the Use of Ground-Based LIDAR section of this chapter, and recommended future studies are described in the Recommended Future Studies section that follows.

BEST PRACTICES FOR FIELD LIDAR SCANNING

Based on the LIDAR scanning that was conducted as part of the pooled fund project, some efficient methods for LIDAR scanning, registration, and data formats have been developed, as discussed below.

Planning for Scanning

The approximate times spent in the field for the LIDAR scanning that was conducted in the eight states is shown in Table 37. Variations are expected due to variations in the site conditions and the particular scanner used, but overall the average amount of rock surface scanned per eight-hour day is about 85,000 ft^2 (assuming six hours at the field site and two hours commuting). That is the equivalent to about 1000 feet of scanning a day for a slope 85 feet high. These times do not include surveying.

Table 37. Time Spent in the Field at Scan Sites for the Pooled Fund Project

State	Approx. Time Spent in the Field	Approximate Area Scanned (ft^2)	Scanner
AZ	unknown	240,000	Leica Scanstation
CA	5 hours	60,000	Optech ILRIS-3D
CO	3 hours (before and after scans)	50,000	Optech ILRIS-3D
CO	5 hours	600	Optech ILRIS-3D ISITE 8800
NH	4 hours	85,000	Optech ILRIS-3D
NY	4 hours	53,000	Optech ILRIS-3D
PA	unknown	72,000	Cyrax 2500
TN	unknown	92,000	Leica C10
TX	1.5 days	150,000 (includes some areas not in report)	Leica Scanstation

Scanning Locations

In four of the eight states, scanning was conducted from the highway median, as shown in Figures 71a and 71b for New York and New Hampshire, respectively. At these sites, a number of scanning positions were used, and scanning progressed from one side of the slope to the other. In this technique, the scans are as perpendicular to the highway cut as possible, and there is a small overlap between the scans. Scanning using this technique is preferred if it is possible at a site. Figure 71c shows scanning at the California site , where scanning was conducted from the opposite side of the highway. Because of the narrow highway, scanning was not perpendicular to the highway cut, resulting in point clouds that have numerous occluded areas.

Figure 71. Top left, a) Scanning from the highway median at the New York site; top right, b) Scanning from the highway median at the New Hampshire site; and bottom, c) Difficult scanning from across a narrow highway at the California site.

Scan Point Spacing

The point spacing in the point cloud is one of the most important variables in field scanning. Scan distances in the scanning conducted for the pooled fund project varied from less than 30 m (98 ft) to over 250 m (820 ft). For time-of-flight scanners such as the Leica C10 and the Optech ILRIS-3D, and when scanning distances between 50 and 250 m, a point spacing of 2-3 cm (.8 to 1.2 inches) is ideal. This allows significant detail in the point cloud and triangulated mesh for delineating medium to large fractures [greater than 0.3 m (1 ft)]. For scan distances greater than 250 m, a point spacing greater than 5 cm (2 inches) may be necessary, due to accuracy and scan time considerations. This will still allow large fractures [greater than 1 m (3.3 ft)] to be delineated. For scans at distances less than 50 m (164 ft) and when using either time-of-flight or phase shift scanners that have a higher range accuracy, a point cloud spacing of 1.5 cm (.6 inch) or less is ideal. This allows even small fractures (10 cm or .4 inch) to be delineated.

Universal Data Formats

For the pooled fund project, scanning was conducted with a number of different scanners, including the Optech ILRIS-3D, Leica Scanstation, Leica C10, Cyrax 2500, and ISITE 8800. Each of these scanners has its own format for the point cloud. These formats are not very useful for point cloud processing unless the scanner manufacturer's own software is being used for the processing. The research team recommends that, in addition to storing scan files in the manufacturer's own format, the scans are also stored in the universal xyz format, which is normally an ascii file containing columns with x, y, z, intensity, red, green, and blue. The output to xyz format should be completed after the point cloud has been registered, which normally would be done using the manufacturer's software.

Supplementary Data

A registered point cloud is a stand-alone file that allows a geotechnical engineer to extract rock mass characterization, slope stability, and rockfall information from a site, even if the engineer has never physically been to the site. This is very useful as it allows a geotechnical project to be efficiently divided into two tasks: field scanning by a surveying crew and data analysis and interpretation by trained geotechnical engineers. However, in order to aid the analysis of the point clouds, some supplementary data can be very useful. Most important are high-resolution digital images of the site that can aid in differentiating structural features such as joints, bedding planes, and faults, from other features such as talus slopes and blasting fractures. Also, the point cloud does not capture certain features of the rock mass such as fracture fill, fracture weathering, and intact rock strength. These data could be collected in the field at the same time that the scanning is conducted.

BEST PRACTICES FOR POINT CLOUD PROCESSING

Based on the point cloud processing that was conducted as part of the pooled fund project, some efficient point cloud processing methods for highway geotechnical analyses have been developed, as described below.

Planning for Processing

The time spent on point cloud processing for each of the eight states was not accurately recorded. Some very approximate times are given here. In general, point cloud processing consisted of the tasks listed in Table 38 (times are based on processing and reporting on all the scans from a given state.

For the pooled fund project, most of these tasks were conducted by the two graduate students with the exception of change detection, finalizing the reports, and overseeing all the point cloud processing, which were conducted by the principal investigator (PI). These times assume one graduate student working half-time (20 hours per week), along with frequent interactions with the PI.

Table 38. Time Spent on Point Cloud Processing

Task	Approx. Time
Getting registered point clouds into the Split-FX software and ready for processing	1 week
Fracture delineation, stereonet plotting, and geologic structure interpretation	2 weeks
Other rock mass characterization properties (spacing, slope dimensions, and orientations)	0.5 weeks
Slope stability analyses (Dips and Swedge)	1.5 weeks
Making cross sections and calculating the OHFs	1 week
Trajectory analysis on one or two cross sections	1 week
Joint persistence, roughness, and friction angle (CA only)	1.5 weeks
Rockfall hazard ratings (TN only)	2 weeks
Change detection (CO only)	2 weeks
Writing the state report	3 weeks
Total average time per state	10 weeks

Point Cloud Clean-Up and Optimizing the Triangulated Mesh

Point cloud cleanup and optimizing the mesh are the first two point cloud processing tasks but both of these steps are very important, since the accuracy of everything that follows depends on these steps. It is now common to start with a single large point cloud from a site. This is the typical output from a Leica or Trimble scan project, for example. It is not usually efficient, however, to process the single point cloud. It is usually better to break up the point cloud into sections for the following reasons:

- Point cloud viewing and processing will be much faster
- Meshing is more efficient for sections of a highway cut with a uniform slope angle and direction (i.e., break up a highway cut that goes around a corner)
- Each section can represent a geologic structural domain
- Non-geologic features between sections of rock can be eliminated
- Each bench level can be analyzed separately for clouds that have multiple benches

After breaking up the point cloud into sections, the next steps are to clean up each section and then create a triangulated mesh for each section. Clean-up can include removing vegetation, the roadway, unnecessary detail behind a slope face, and other non-geologic features. The triangulated mesh should capture the same amount of detail that can be seen in the point cloud. This step is very important, and close inspection should be made to make sure the mesh is not blurring detail that is in the point cloud. Figure 72 shows some examples of properly triangulated meshes.

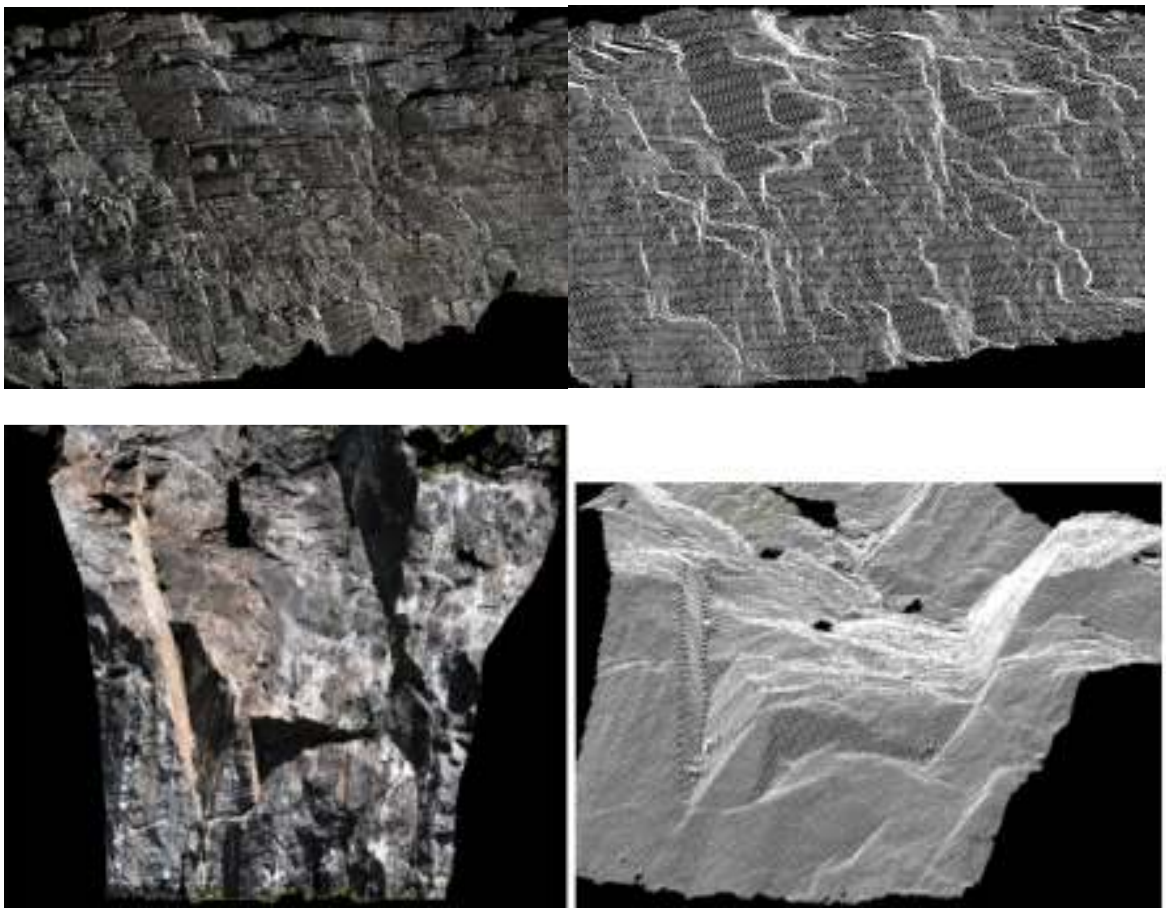

Figure 72. Properly triangulated meshes capture the same amount of detail as the point cloud.

Fracture Delineation and Stereonet Plotting

This is a fairly straightforward step, but some common mistakes are to 1) not plot fracture poles as a function of fracture area and 2) miss one or more discontinuity sets. Figure 73 illustrates these two problems. Figure 73a shows a proper plotting of the fracture surface (circles) and fracture traces (triangles). In this case, circle sizes are plotted from zero to 0.3 m^3, (10.6 ft^3) the maximum size for fracture areas, and fracture areas above 0.3 m^3 are given the maximum circle size. Figure 73b shows the stereonet plot if the circle size is not a function of area. In this case, the important structural features are masked by the large number of more randomly oriented smaller fractures. Stereonet contour plotting can also be used to highlight geologic structure, particularly if the stereonet contouring program takes into account the individual fracture areas (as it does in the Split-FX program). Generally, rock masses have at least three structure sets and often four or five sets. If the stereonet shows only one or two primary sets, then it usually means that automated fracture surface delineation is missing these sets. Usually, this occurs when a structure set dips away from the scanner or if the fracture surfaces cannot be seen because of smoothly blasted rock faces. In these cases, additional inspection of the point cloud by manual surface or trace delineation is required. It is important to carefully examine the point cloud and make sure that all discontinuity sets are represented in the stereonet. For example, in

Figure 73a, the large triangles represent a fracture set that was delineated from traces and was not apparent from analyzing fracture surfaces alone.

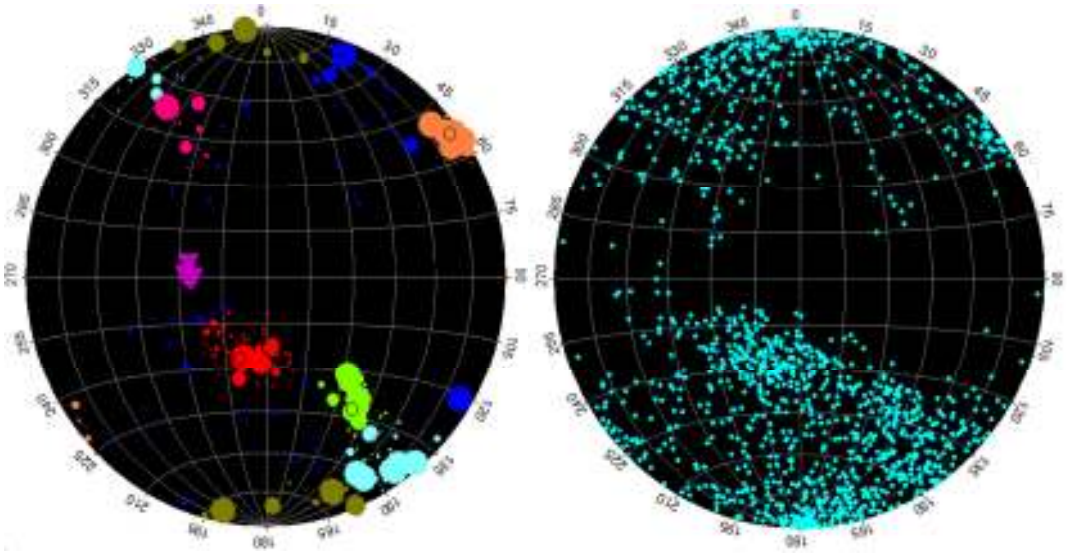

Figure 73. Stereonet plotting of the poles from the fractures shown in Figure 2b, at left, a) icon for delineated fracture surfaces (circles) plotted as a function of fracture area and some delineated fracture traces shown (triangles) and, at right, b) poles not plotted as a function of area for fracture surfaces and no fracture traces shown.

Interpreting the Geologic Structure

Interpreting the geologic structure and determining discontinuity sets from the stereonet plot is a difficult but very important step in point cloud processing for geotechnical analysis. Slope stability analysis generally involves routine slope stability calculations once the geologic structure has been defined. Looking through the many stereonets shown in this final report, the research team sees that sometimes the geologic structure is fairly distinct, such as in the example in Figure 73a, while in other cases a group of fractures must be divided into two or more structural sets, such as with the example from the California site shown in Figure 74. It is important to communicate with geological and geotechnical staff familiar with the site to check the geologic interpretation before further analysis of the data.

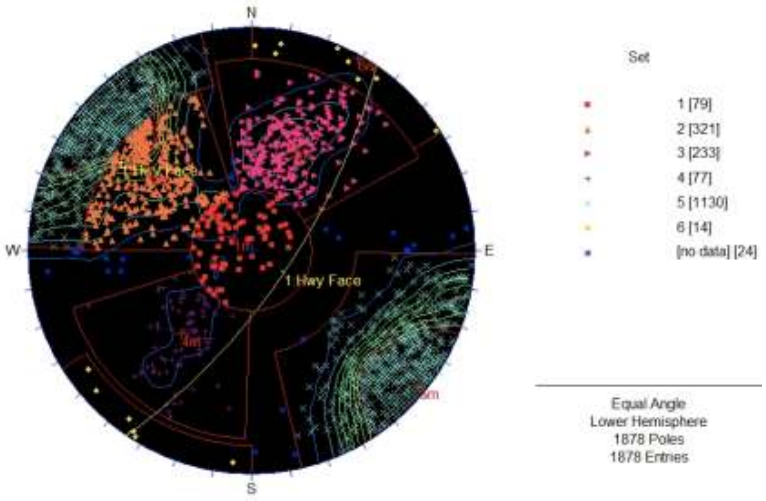

Figure 74. Structural interpretation of the California site into six discontinuity sets.

Slope Stability

This report contains a number of examples showing how the fracture orientation data from point cloud processing can be used in slope stability calculations. The individual fracture data can be exported from point cloud processing software into slope stability programs, or statistical information can be calculated from the orientation data (mean orientation and Fisher constant for each set, for example) and exported to slope stability programs. Slope stability programs that can directly use fracture information from point cloud processing software include Swedge (Rocscience 2012), RockPack (RockWare 2012), 3DEC (Itasca 2012), and many others. In addition to the fracture orientation data, other point cloud information that can be used in slope stability calculations includes the slope geometry (slope height, slope angle, and orientation), fracture spacing and persistence, and joint roughness. As shown with the California site, the delineated fractures in a point cloud can be used to estimate the persistence for each joint set. This information can then be used to determine the largest expected plane failure or wedge failure at a site. Also shown with the California site, the large-scale joint roughness can be calculated and used to provide an estimate for the additional joint friction angle due to roughness. The techniques for estimating joint persistence and the roughness component to the joint friction angle have not been validated using traditional techniques, and future work in this area is recommended.

Rockfall

This report provides many examples that show how point cloud data can be used to evaluate the potential for rockfall, and the effects of rockfall at a site. Overhanging rock slabs are an important source of rockfall. Ground-based LIDAR scanning is very good at providing information on overhanging rock slabs because of the high density of points and the high resolution, and also because ground-based LIDAR is often pointed up at a slope, thus providing detail on the underside of overhanging slabs. This report describes (for most sites) how to use vertical cross sections from the point cloud to calculate the severity of overhangs at a site, referred to as the OHF. At one site (Tennessee), it was demonstrated how to use the 3D

triangulated mesh to calculate the OHF. In the future, the OHF will be enhanced to include other important slope and overhang information, such as the size of overhanging sections and their height above the roadway. Point clouds and vertical cross sections can also be exported to rockfall trajectory programs to simulate the trajectory of rock blocks that become dislodged from the slope. A trajectory analysis based on vertical cross sections was conducted for most of the states in the pooled fund project, using the Rocscience RocFall program. More advanced trajectory simulations can be made using recently developed 3D trajectory programs (CFLH, 2012), and it is expected that point clouds or triangulated meshes could be directly imported into these programs in the near future.

Processing Photogrammetry Point Clouds

All the point cloud processing techniques and software described in this report can be directly applied to point clouds derived from ground-based photogrammetry in addition to ground-based LIDAR. In some applications, it may be desirable to use digital cameras and photogrammetry to generate point clouds rather than ground-based LIDAR. A comparison of advantages and disadvantage of these two technologies for geotechnical applications is given in Kemeny and Turner (2008). If photogrammetry is used to generate point clouds, the same resolution and point cloud spacing requirements need to be met, as discussed in Chapter 2 of this report.

ISSUES WITH THE USE OF GROUND-BASED LIDAR FOR HIGHWAY GEOTECHNICAL APPLICATIONS

Nine case studies were conducted as part of the LIDAR pooled fund study. This included LIDAR scanning that was conducted in eight states, as well as the processing of the point clouds. Overall, the results indicate that ground-based LIDAR scanning is very useful to assist with highway geotechnical applications. The pooled fund project did reveal some issues and limitations of the use of ground-based LIDAR, as discussed below.

Learning Curve in Using Point Cloud Processing Software

Point clouds are three-dimensional, and like CAD software, a learning curve is involved in becoming proficient with point cloud processing software for geotechnical applications. As point clouds become more readily available for field sites of interest, it will make more sense for companies and government agencies to have personnel trained in the use of point cloud processing software. Also, in the future, it is expected that training materials and the ability to get training online will improve, allowing users of point cloud processing software to come up to speed more quickly.

Interoperability with Other 3D Software

Moving the results from point cloud processing software to other 3D and slope stability programs is not seamless. The data files can be very large, and software manufacturers often have their own proprietary data formats. When exporting information such as meshes and delineated fracture data, there are often conflicts between point cloud software and other programs with the file formats used. In the future, the situation is expected to improve as the

use of point cloud processing software becomes more commonplace, and as point cloud software manufacturers provide more options for data output and input.

Change Detection Difficulties

The two field sites in Colorado were used to investigate the use of ground-based LIDAR for monitoring ground movement and rockfall. The case studies were very successful and indicated that movements as small as 0.2 inch from a distance of 110 m (361 ft) and 1.5 cm (0.6 inch) from a distance of 286 m (938 ft) can be detected. A second scan at the Arizona site was also conducted to investigate the use of ground-based LIDAR for change detection. This test was unsuccessful, due to difficulties in properly matching the "before" and "after" scans. Because change detection using LIDAR scans is relatively new, the sophistication and user-friendliness of change detection algorithms in point cloud processing software are less developed than other aspects such as fracture delineation and stereonet plotting. The participants in the pooled fund project have indicated that change detection with LIDAR scans could be very useful for a variety of geotechnical applications. The situation should improve in the future as change detection algorithms are improved.

LIDAR Scanning Does Not Eliminate the Need for Other Rock Mass Information

This final report shows that LIDAR scanning provides a significant amount of the information needed for highway geotechnical applications. However, there are a few important types of information that are not provided through LIDAR scanning. LIDAR can only provide information where exposed rock faces occur, and depending on the orientation and extent of these rock faces, information about the overall rock mass may not be adequately covered. It does not take the place of a drilling program to provide rock core throughout the rock mass of interest. Even of the exposed rock faces, it does not provide information on intact rock strength, fracture fill and weathering, and base joint friction angle. And of course LIDAR does not provide information on groundwater hydrology or rainfall.

RECOMMENDED FUTURE STUDIES

Based on the results of the LIDAR pooled fund study, some future studies are recommended, as described below.

Follow-Up Studies at Some of the Pooled Fund Sites

It is recommended that additional studies and analysis be conducted at some of the pooled fund field sites, if there is an interest and resources are available. This could include additional LIDAR scanning for change detection, integrating airborne or mobile LIDAR data, and using the sites for benchmark studies to compare other new technologies and traditional methods of site characterization and monitoring.

Mobile LIDAR

The technology of mobile scanning from moving vehicles is improving, and many states are scanning highways and highway slopes using mobile LIDAR technologies. The data from these mobile units, however, are not being used for geotechnical applications. Mobile scanning

provides the opportunity to scan quickly, economically, and periodically for change detection. It is recommended that a study like the pooled fund study be conducted to look at the possibilities of using mobile scanning for the geotechnical analysis of highway slopes, including rock mass characterization, rockfall, slope stability, and change detection.

Techniques Manual

Based on comments by some of the Technical Advisory Committee members involved in this project, it is recommended that a manual/tutorial be written to go along with this final report, if there is an interest and resources are available. The manual would describe details of how the results in this final report were obtained using point cloud processing software. This document would support the training workshop that took place at the end of the pooled fund workshop in November 2011.

REFERENCES

CFLH. 2012. CRSP-3D, Colorado Rockfall Simulation Program, U.S. Department of Transportation Federal Highway Administration, Central Federal Lands Highway Division, Lakewood, CO.

Combs, John H. and John Kemeny. 2011. "DOT Study of LIDAR Geotechnical Applications in Eight States." *45th U.S. Rock Mechanics / Geomechanics Symposium.* San Francisco, CA: American Rock Mechanics Association. June 26–29. Paper ARMA 11-429, 7 pp.

Cornet, Bruce. 2008. Franklin Mountains Virtual Fieldtrip, http://www.sunstar-solutions.com/sunstar/geology/Franklin/FranklinMt.htm.

Federal Highway Administration (FHWA). 1989. "Rock Slopes: Design, Excavation, Stabilization." USDOT, FHA Pub. No. FHWA-TS-89-045, September.

Goodman, Richard E. 1993. *Engineering Geology: Rock in Engineering Construction*. New York: John Wiley and Sons.

Goodman, Richard E. and D. Scott Kieffer. 2000. "Behavior of rock in slopes." *J. Geotech. Geoenv. Eng.*, 126(8): 675-684.

Hoek, Evert. 2007. Practical Rock Engineering, http://www.rocscience.com/hoek/corner/Practical_Rock_Engineering.pdf. Rocscience site accessed for this study June 17, 2011.

Hudson, John and John Harrison. 2000. Engineering Rock Mechanics. Pergamon Press.

Itasca. 2012. 3DEC. Software for hydrogeological, geomechanics, and microseismological problems in mining, civil, petroleum, waste isolation, and environmental industries. http://www.itascacg.com

Jaeger, John Conrad, and N.G.W. Cook, R.W. Zimmerman. 1979. *Fundamentals of Rock Mechanics*, 3rd Edition, Chapman and Hall, London.

Jones, C.L., J.D. Higgins, and R.D. Andrew. 2000. Colorado Rockfall Simulation Program, Version 4.0. http://store.coloradogeologicalsurvey.org/product/colorado-rockfall-simulation-program-version-4-0/

Kemeny, John, John Combs, Vanessa Bateman, Christ Dimitroplos, Brad Foltz, Doug Hadjin, Mark McClelland, Ty Ortiz, Krystle Pelham, Nick Priznar, Keith Turner, Bill Webster. 2011. "Transportation Pooled Fund Project of Highway Geotechnical Applications of Ground-Based Lidar," *62nd Highway Geology Symposium*, Lexington, KY, July.

Kemeny, John and Keith Turner. 2008. "Ground-Based LiDAR: Rock Slope Mapping and Assessment," US Dept. Transportation Federal Highways Admin. Central Federal Lands Highway Division, Publication No. FHWACFL/TD-08-006, 2008.

Mansfield, Clayton H. and John Kemeny. 2009. "The Use of Terrestrial LIDAR in Determining Directional Joint Dilation Angle Values," Proceedings of the *43rd US Rock Mechanics Symposium and 4th U.S.-Canada Rock Mechanics Symposium*, Asheville, NC, June 28–July 1, 2009.

Mauldon, Matthew, Eric Drumm, William M. Dunne, Vanessa Bateman, Brett Rose, and Marcus Kim. 2007. *Rockfall Management System for Tennessee*. Nashville: Tennessee Department of Transportation (TDOT).

McCarter, B. 2004. Rockfall Hazard Rating: File No 58I0024001137.10LRF. Nashville: Tennessee Department of Transportation (TDOT), Geotechnical Engineering Section, Rockfall Management System. (TDOT internal report, unpublished)

National Technical Information Service (NTIS). 1994. "Rockfall Hazard Mitigation Methods." NHI Course No. 13219, National Highway Inst., U.S. Department of Commerce, National Technical Information Service, Alexandria, Virginia.

Peel, M., B. Finlayson, and T. McMahon. 2007. Updated world map of the Koppen-Geiger climate classification, *Hydrology and Earth System Sciences*, 11, p. 1633–1644, doi:10.5194/hess-11-1633-2007.

Pomerleau, François, Francis Colas, Roland Siegwart, and Stéphane Magnenat. 2013. "Comparing ICP Variants on Real-World Data Sets." In *Autonomous Robots*, 34(3): 133–148, DOI: 10.1007/s10514-013-9327-2, April.

RockWare, 2012. RockPack: Earth science and GIS software, http://www.rockware.com.

Rocscience. 2010. 2D and 3D analysis and design programs for civil engineering and mining applications

Rocscience. 2012. 2D and 3D analysis and design programs for civil engineering and mining applications, including RocFall Version 5.0 for the statistical analysis of rockfalls, and Swedge Version 5.0, a 3D Surface Wedge Analysis for Slopes, http://www.rocscience.com.

Southern Regional Climate Center (SRCC). 2011. Southern Climate, Station Search and Data, Observation Stations, Monteagle: 406162, Climate Normals, http://www.srcc.lsu.edu/stations/index.php?action=metadata&network_station_id=406162.

Split Engineering. 2010. Split-FX Version 2.0 Point Cloud Processing Software, http://www.spliteng.com/split-fx/.

Tennessee Division of Geology (TDG). 2011. Generalized Geologic Map of Tennessee, http://www.tn.gov/environment/tdg/images/geolog_l.jpg.

Western Regional Climate Center (WRCC). 2011. Western U.S. Climate Historical Summaries, Climatological Data Summaries, Northern California, Big Bar and Weaverville sites, http://www.wrcc.dri.edu/summary/Climsmnca.html.